

# Evaluation of energy efficiency in mobile cellular networks using a fluid modeling framework

## Thèse de doctorat de l'université Paris-Saclay

École doctorale n°580 : Sciences et Technologies de l'Information et de la Communication (STIC)

Spécialité de doctorat : Réseaux, Information et Communications  
Unité de recherche : Université Paris-Saclay, CNRS, CentraleSupélec,  
Laboratoire des signaux et systèmes, 91190, Gif-sur-Yvette, France  
Référent : Faculté des sciences d'Orsay

**Thèse présentée et soutenue en visioconférence totale, le  
26 novembre 2020, par**

**Yanqiao HOU**

## Composition du Jury

### **Hind CASTEL-TALEB**

Professeur, Télécom SudParis, IPP

Présidente

### **Marceau COUPECHOUX**

Professeur, Télécom Paris, IPP

Rapporteur & Examinateur

### **Tadeusz CZACHORSKI**

Professeur, IITIS PAN Poland

Rapporteur & Examinateur

### **André-Luc BEYLOT**

Professeur, ENSEEIHT, Université de Toulouse

Examinateur

### **Joanna TOMASIK**

Professeur, CentraleSupélec, Université Paris-Saclay

Examinateuse

### **Véronique VÈQUE**

Professeur, Université Paris-Saclay

Directrice de thèse

### **Lynda ZITOUNE**

Maître de Conférences, ESIEE Paris

Co-encadrante

### **Jean-Marc KELIF**

Ingénieur de recherche, Orange Labs

Invité



## Acknowledgements

I wish to express my sincere appreciation to my supervisor Dr. Véronique Vèque, a full professor in the Electrical Engineering Department of University Paris-Sud, and the head of Telecommunications and Networking group at the Laboratory of Signal and Systems (L2S–UMR 8506), for leading me to the telecommunication area. My research view gets widely broadened during the PhD years which should thanks to communication opportunities strongly supported by Dr. Vèque. This appreciation is also for many helps and cares on my private life.

I also would like to give my many thanks to my co-supervisor Dr. Lynda Zitoune, an associate professor in École Supérieure d'Ingénieurs en Électrotechnique et Électronique (ESIEE), Paris, for smart suggestion and deep discussion on the research direction, technical details and paper manuscripts.

I would further like to thank all my colleagues at the Lab, where they provide me great advices on my work and share their great minds with me. In particular, I would like to thank Dr. Djibrilla Adamou Incha, Mr Melek Charfi and Dr. João Alberto Ferreira, who saved me a lot from language problems and took care of me a lot during my pregnancy. I thank them a lot for the precious friendships.

Special thanks to my Chinese friends, namely Peipei Ran, Xiaoxia Zhang, Jian Song, Chen Kang, Li Wang, Yanpei Liu, Zhan Wang, Chao Zhang and Caifang Cai. They have accompanied me and brought me happiness and help in these three years.

I wish to express my gratitude to Dr Dominique Lesselier, for his assistance during my PhD.

I would like to thank Dr. CASTEL-TALEB Hind, Dr. BEYLOT André-Luc and Dr. TOMASIK Joanna as my jury members, Dr. COUPECHOUX Marceau and Professor CZACHORSKI Tadeusz as referees, Dr. KELIF Jean-Marc as invited member.

I also would like to show my sincere gratitude and deep thanks to my husband and my daughter. Their support, encouragement, smile, and countless sacrifice are the basis of my continuing personal development.

Last but not least, I am grateful to my parents, my brother and my sisters, who are always loving and supporting me all through my PhD.



# Abstract

## English:

The design target of energy efficiency for 5G networks is at least 1000-fold than the currently available 4G system, while offering higher data transmission rate and very low latency. To evaluate the performance of large representative cellular networks and capture the main factors involved in the energy consumption process, representative and accurate models must be developed.

To develop tractable and efficient models, we use the spatial fluid modeling framework and compute the energy efficiency metric. Our model consists of a downlink transmission of an OFDMA cellular network, composed of several base stations and multiple user equipments randomly distributed over the area. An analytical expression of energy efficiency is then derived to study the impact of the major factors involved in the energy consumption process such as fading and shadowing attenuation, cellular coverage type and quality. Extensive numerical simulations were run to compare the results obtained by Monte Carlo simulations and demonstrate the effectiveness and accuracy of the fluid modeling for large cellular networks. The numerical results indicate that user density does not affect energy efficiency. Besides, energy efficiency is more important in suburban environments than in urban environments where the shadowing effect is great, regardless of the cellular coverage type. However, and more generally, micro-cellular networks' deployment offers better energy efficiency than the conventional macro-cellular ones.

Besides, we evaluated the effect of the promising Joint Transmission Coordinated MultiPoint (JT-CoMP) technique on energy efficiency, which is significantly improved as the number of coordinated BSs increases. On the other hand, coordination between base stations is only effective for user equipment that is remote from their base station.

To resume, our numerical results illustrate the effectiveness and accuracy of fluid modeling, which can be considered as a mathematical tool by operators to benchmark cellular networks' energy efficiency.

**Keywords:** energy efficiency, mobile networks, JT-CoMP, performance evaluation, fluid modeling

**Français:**

La conception des systèmes de communication dits 5G cible une efficacité énergétique ambitieuse, au moins 1000 fois supérieure à celle du système 4G actuellement disponible, tout en offrant un débit de transmission de données supérieur et un temps de latence très faible. Il est donc nécessaire de développer des modèles représentatifs et précis des grands réseaux cellulaires afin d'évaluer leur performance et d'identifier les principaux facteurs impliqués dans la consommation d'énergie comme l'atténuation de signal, le type et la qualité de la couverture cellulaire radio.

Nous avons utilisé la modélisation fluide spatiale pour développer des modèles représentatifs et calculables afin de calculer la métrique d'efficacité énergétique. Notre modèle considère un réseau composé de plusieurs cellules opérant en OFDMA sur les liens descendants, et de multiples équipements utilisateurs répartis aléatoirement. Une expression analytique de l'efficacité énergétique a été dérivée pour prendre en compte les principaux facteurs liés à la communication : coefficient d'atténuation de signal, probabilité de couverture, type du réseau. Des simulations numériques ont permis de comparer les résultats avec ceux obtenus par les simulations Monte Carlo et ainsi, montrer l'efficacité et la précision de la modélisation fluide pour de grands réseaux cellulaires. Les résultats numériques montrent que l'efficacité énergétique est indépendante de la densité des équipements utilisateurs. Par ailleurs, l'efficacité énergétique est plus importante dans les environnements suburbains que dans les milieux urbains où l'effet de shadowing est grand et ce, quel que soit le type de réseaux (macro, micro ou femto). Cependant, et d'une façon plus générale, le déploiement de petits réseaux (small cells) offre une meilleure efficacité énergétique comparée au réseau macro classique.

En outre, nous avons évalué l'effet de la technique de transmission conjointe multipoint (JT-CoMP) sur l'efficacité énergétique, qui est considérablement améliorée lorsque le nombre de stations de base coordonnées augmente. En revanche, la coordination entre les stations de base n'est efficace que pour les équipements utilisateurs éloignés de leur station de base.

En résumé, nos résultats numériques mettent en évidence l'efficacité et la précision de la modélisation fluide qui peut être considérée comme un outil mathématique par les opérateurs pour évaluer l'efficacité énergétique des réseaux cellulaires.

**Mots clés:** efficacité énergétique, réseaux mobiles, JT-CoMP, évaluation des performances, modélisation fluide

# Overview of the manuscript

The 5G network design aims to offer more capacities and less latency and fulfill the increasing data traffic, leading to higher energy consumption. From the view point of environmental responsibility, radio communication is a large proportion of information and communications technologies (ICT) related to carbon dioxide ( $CO_2$ ) emissions. During the last decades, Energy Efficiency (EE) has received a lot of attention in wireless communications and is very important, from the viewpoints of both economic benefits and environmental responsibility. The investigation of EE, in wireless networks, is driven using either system-level simulations or stochastic geometry to consider the spatial distribution of nodes (base stations and user terminals) when describing the topological model of the networks. However, since today's wireless communication networks are denser and denser due to the increasing number of base stations (BSs) and user terminals, simulation-based approaches have become a painful task and resource-intensive. On the other hand, stochastic geometry-based studies assume, in most cases, a Poisson point process to describe the locations of nodes, which allows us to derive a closed-form formula of the energy efficiency metrics. Nevertheless, when non-Poisson point processes are considered, eg., perturbed lattice,  $\beta$ -Ginibre point process, and Matérn point process, the performance models are not analytically tractable due to the non-independent nature of points. Therefore, either approximations or simulations are conducted to prove the model accuracy.

Spatial fluid modeling has recently been developed to evaluate network performance, like the signal-to-interference-plus-noise ratio (SINR) and outage probability through analytical expressions. However, an investigation of EE based on fluid modeling in wireless networks is still missing. Additionally, the advanced technique of Joint Transmission Coordinated MultiPoint (JT-CoMP) has been designed to improve such parameters as SINR, capacity, and quality of service. Nevertheless, this technology brings additional energy power consumption for transmitting backhauling information. Hence, while utilizing the JT-CoMP scheme, how to compute EE based on fluid modeling is still an open issue. Performance of JT-CoMP has been studied by simulations or with stochastic geometry but not using fluid modeling. Therefore, our objective is to evaluate EE for the cellular networks

based on the fluid modeling, while considering JT-CoMP and non JT-CoMP schemes, in order to develop an accurate and tractable model and to show the efficiency of fluid modeling.

The PhD thesis is divided into six chapters and it is organized as follows:

In chapter 1, we first outline the background information on energy efficiency (EE) in the information and communications technologies. Then the cellular network concept and its energy consumption are presented. Furthermore, advanced technologies developed to increase spectral efficiency in 4G systems are introduced, as they have the potential to improve EE. Finally, we discuss some survey papers focusing on EE by taking advantage of the advanced technologies.

In chapter 2, we first list some EE models from the perspective of its definition. Then, as the critical components of the EE model, the power consumption models and the throughput models are introduced. Finally, we classify some literature papers on EE from the perspectives of both EE-evaluation and EE-optimization, according to some advanced technologies to illustrate the impact of these technologies on EE.

The chapter 3 is an introduction to the model common to the whole thesis. We first survey main scientific papers published on fluid modeling. Then, we present the cellular system we use in our work. Afterward, the concept of fluid modeling is introduced and the mathematical expressions of SINR and interference factor based on this model are presented. Finally, some numerical results of SINR are shown to validate the accuracy of fluid modeling.

Chapter 4 illustrates a tractable model of EE without considering the impact of shadowing and analyzes the joint effect of shadowing and path-loss exponent on EE based on the spatial fluid modeling in the macro- and femto- cellular networks, respectively. After having developed the associated EE model, the data rate computation is discussed without and with considering the impact of shadowing. In the case of non-shadowing, we develop three data rate models for three scenarios, depending on the network's size. Whereas, in the case of shadowing, we make a brief recall of the signal quality, the mean and standard deviation of interference factor using fluid modeling, and then present a closed-form expression of the signal quality threshold, which is depending on the user equipments' location while considering a fixed coverage probability. Finally, based on the above work, we assess the EE for both macro- and femto- cellular networks in non-shadowing and shadowing cases through simulation results.

In chapter 5, we develop a tractable and efficient EE model based on the spatial fluid modeling framework when JT-CoMP is applied. After reviewing the literature on JT-CoMP technology, we introduce the corresponding system model, including the refined power consumption model and energy efficiency metrics. Then, the data rate computation

and the backhauling traffic computation are presented. Moreover, we investigate the EE enhancement in both macro- (MCN) and femto- (FCN) cellular networks, compared to the baseline case where no coordination is applied. Finally, we show that the EE metrics computed for a femto-cellular system increase depending on some parameters, such as path-loss exponent, network area, and the number of coordinated base stations, when varying the backhauling power cost depending on the data rate requirement. We further reveal the impact of the distance threshold, which corresponds to the predefined threshold of SIR, on EE per cell, thus verifying the effectiveness of JT-CoMP.

Finally, chapter 6 summarizes the thesis and sets some perspectives for the future work. Appendices provides supplementary materials, including the published/submitted contributions.



# Vue d'ensemble du manuscrit

La conception du réseau 5G vise à offrir plus de capacités et moins de latence et à répondre à l'augmentation du trafic de données, entraînant une consommation d'énergie plus élevée. Du point de vue de la responsabilité environnementale, les radiocommunications constituent une part importante des technologies de l'information et des communications (TIC) liées aux émissions de gaz carbonique ( $CO_2$ ). Au cours des dernières décennies, l'efficacité énergétique (EE) a été l'objet de beaucoup d'attention dans les communications sans fil et est très importante, tant du point de vue des avantages économiques que de la responsabilité environnementale. L'étude de l'EE, dans les réseaux sans fil, est conduite à l'aide de simulations au niveau du système ou de géométrie stochastique pour prendre en compte la distribution spatiale des nœuds (stations de base et terminaux d'utilisateurs) lors de la description du modèle topologique des réseaux. Cependant, comme les réseaux de communication sans fil d'aujourd'hui sont de plus en plus denses en raison du nombre croissant de stations de base (BS) et de terminaux utilisateurs, les approches basées sur la simulation sont devenues une tâche pénible et gourmande en ressources. D'autre part, les études basées sur la géométrie stochastique supposent, dans la plupart des cas, un processus ponctuel de Poisson pour décrire les emplacements des nœuds, ce qui nous permet de dériver une formule en forme fermée des métriques d'efficacité énergétique. Néanmoins, lorsque des processus ponctuels non-Poisson sont considérés, par exemple, un réseau perturbé, un processus ponctuel  $\beta$ -Ginibre et un processus ponctuel de Matérn, les modèles de performance ne sont pas analysables en raison de la nature non indépendante des points. Par conséquent, des approximations ou des simulations sont effectuées afin de prouver la précision du modèle.

La modélisation des fluides spatiaux a récemment été développée dans le but d'évaluer les performances du réseau, comme le rapport signal/brouillage et bruit (SINR) et la probabilité de panne au moyen d'expressions analytiques. Cependant, une enquête sur l'EE basée sur la modélisation des fluides dans les réseaux sans fil fait toujours défaut. De plus, la technique avancée dite « Joint Transmission Coordinated MultiPoint » (JT-CoMP) a été conçue pour améliorer des paramètres tels que le SINR, la capacité et la qualité de service.

Néanmoins, cette technologie conduit à une consommation d'énergie supplémentaire pour la transmission des informations de « back-hauling ». Par conséquent, tout en utilisant le schéma JT-CoMP, comment calculer l'EE basée sur la modélisation des fluides reste un problème en suspens. Les performances de JT-CoMP ont été étudiées par des simulations ou avec une géométrie stochastique mais pas en utilisant la modélisation des fluides. Par conséquent, notre objectif est d'évaluer l'EE pour les réseaux cellulaires sur la base de la modélisation des fluides, tout en considérant les schémas JT-CoMP et non JT-CoMP, afin de développer un modèle précis et traitable et de montrer l'efficacité de la modélisation des fluides.

La thèse de doctorat est divisée en six chapitres et est organisée comme suit:

Au chapitre 1, nous présentons d'abord les informations générales sur l'efficacité énergétique (EE) dans les technologies de l'information et de la communication. Ensuite, le concept de réseau cellulaire et sa consommation d'énergie sont introduits. En outre, des technologies avancées développées dans le but d'augmenter l'efficacité spectrale des systèmes 4G sont considérées, car elles ont le potentiel d'améliorer l'EE. Enfin, nous discutons de certains articles de revue axés sur l'EE en tirant parti des technologies de pointe.

Au chapitre 2, nous énumérons d'abord quelques modèles d'EE du point de vue de leur définition. Ensuite, en tant que composants critiques du modèle EE, les modèles de consommation d'énergie et les modèles de débit sont introduits. Enfin, nous classons certains articles de la littérature sur l'EE du point de vue à la fois de l'évaluation de l'EE et de l'optimisation de l'EE, selon certaines technologies avancées pour illustrer l'impact de ces technologies sur l'EE.

Le chapitre 3 est une introduction au modèle commun à l'ensemble de la thèse. Nous examinons d'abord les principaux articles scientifiques publiés sur la modélisation des fluides. Ensuite, nous présentons le système cellulaire que nous utilisons dans notre travail. Puis le concept de modélisation des fluides est introduit et les expressions mathématiques du SINR et du facteur d'interférence basées sur ce modèle sont présentées. Enfin, certains résultats numériques du SINR sont donnés pour valider la précision de la modélisation des fluides.

Le chapitre 4 illustre un modèle traitable d'EE sans tenir compte de l'impact de l'ombrage et analyse l'effet conjoint de l'ombrage et de l'exposant de perte de chemin sur l'EE basé sur la modélisation des fluides spatiaux dans les réseaux macro et femto-cellulaires, respectivement. Après avoir développé le modèle EE associé, le calcul du débit est discuté sans et avec la prise en compte de l'impact de l'observation. Dans un cas de non-ombrage, nous développons trois modèles de débit de données pour trois scénarios, en fonction de la taille du réseau. Dans le cas de l'ombrage, nous faisons un bref rappel de la qualité du signal, la

moyenne et l'écart type du facteur d'interférence en utilisant la modélisation de fluide, puis nous présentons une expression de forme fermée du seuil de qualité du signal, qui dépend de l'emplacement des équipements de l'utilisateur, tout en considérant une probabilité de couverture fixe. Enfin, sur la base des travaux ci-dessus, nous évaluons l'EE pour les deux réseaux macro-cellulaires et femto-cellulaires dans les cas de non-ombrage et d'ombrage grâce aux résultats de simulation.

Dans le chapitre 5, nous développons un modèle d'EE traitable et efficace basé sur le cadre de modélisation des fluides spatiaux lorsque JT-CoMP est appliqué. Après avoir examiné la littérature sur la technologie JT-CoMP, nous présentons le modèle de système correspondant, y compris le modèle de consommation d'énergie raffiné et les mesures d'efficacité énergétique. Ensuite, le calcul du débit de données et le calcul du trafic de backhauling sont présentés. En sus, nous étudions l'amélioration de l'EE dans les réseaux cellulaires macro- (MCN) et femto- (FCN), par rapport au cas de base où aucune coordination n'est appliquée. Enfin, nous montrons que les métriques d'EE calculées pour un système femto-cellulaire augmentent en fonction de certains paramètres, tels que l'exposant de perte de chemin, la zone de réseau et le nombre de stations de base coordonnées, en faisant varier le coût de la puissance de retour en fonction du débit de données exigé. Nous révélons en outre l'impact du seuil de distance, qui correspond au seuil prédéfini de SIR, sur l'EE par cellule, vérifiant ainsi l'efficacité du JT-CoMP.

Le chapitre 6 résume la thèse et présente quelques perspectives de travaux futurs. Les annexes fournissent des documents supplémentaires, y compris les contributions publiées ou soumises.



# Table of contents

<b>Abstract</b>	<b>v</b>
<b>Overview of the manuscript</b>	<b>vii</b>
<b>Vue d'ensemble du manuscrit</b>	<b>xi</b>
<b>List of figures</b>	<b>xix</b>
<b>List of tables</b>	<b>xxiii</b>
<b>1 Related work on advanced techniques in 5G</b>	<b>1</b>
1.1 Introduction . . . . .	2
1.2 Energy efficiency (EE) in ICT . . . . .	3
1.2.1 Environmental and 5G usage aspects . . . . .	3
1.2.2 Operators and users viewpoints . . . . .	4
1.3 Cellular network concept . . . . .	5
1.4 SE-EE relationship . . . . .	6
1.4.1 Spectral efficiency (SE) . . . . .	6
1.4.2 Energy efficiency (EE) . . . . .	7
1.4.3 SE-EE relationship . . . . .	7
1.5 Promising key 5G technologies . . . . .	8
1.5.1 Multiple-Input Multiple-Output (MIMO) . . . . .	8
1.5.2 Coordination Multipoint (CoMP) . . . . .	10
1.5.3 Heterogeneous cellular network (HetNet) . . . . .	11
1.5.4 Relay transmission . . . . .	12
1.5.5 BS on/off strategy . . . . .	13
1.5.6 Cloud radio access network (Cloud-RAN) . . . . .	14
1.6 EE-related surveys . . . . .	15
1.7 Conclusion . . . . .	18

<b>2 Models for EE</b>	<b>19</b>
2.1 Introduction . . . . .	20
2.2 EE models . . . . .	20
2.2.1 Input/output power related EE model . . . . .	21
2.2.2 Cell power consumption and cell area related EE model . . . . .	22
2.2.3 Transmitting power and data rate related EE model . . . . .	23
2.2.4 SE and power cost related EE model . . . . .	23
2.2.5 Overall data rate and power cost related EE model . . . . .	24
2.3 Power consumption models (PCM) . . . . .	24
2.3.1 Ideal load dependent PCM . . . . .	25
2.3.2 Linear PCM . . . . .	25
2.3.3 PCM with sleep mode . . . . .	26
2.3.4 PCM with backhauling cost . . . . .	26
2.3.5 PCM considering non-empty buffer . . . . .	27
2.3.6 PCM with transmitting antennas . . . . .	27
2.3.7 A refined double linear PCM . . . . .	28
2.4 Throughput models . . . . .	28
2.5 Classification of EE models . . . . .	30
2.5.1 Evaluation-based related work . . . . .	30
2.5.2 Optimization-based related work . . . . .	36
2.6 Conclusion . . . . .	44
<b>3 System model</b>	<b>47</b>
3.1 Introduction . . . . .	47
3.2 System model for the thesis . . . . .	48
3.2.1 Energy efficiency definition . . . . .	49
3.2.2 Power consumption model . . . . .	50
3.2.3 Data rate ( $D_{area}$ ) over a network area . . . . .	50
3.3 Overview of fluid modeling . . . . .	51
3.3.1 Notations . . . . .	51
3.3.2 SINR in the hexagonal network . . . . .	52
3.3.3 SINR in fluid network model . . . . .	53
3.4 Accuracy of fluid model . . . . .	54
3.4.1 Simulation process . . . . .	54
3.4.2 Discussion of results . . . . .	55
3.4.3 CDF results . . . . .	57
3.4.4 SIR vs network range . . . . .	58

3.5 Conclusion . . . . .	59
<b>4 Fluid modeling of EE and effect of shadowing on EE</b>	<b>61</b>
4.1 Introduction . . . . .	62
4.2 Energy efficiency definition . . . . .	63
4.3 Data rate computation . . . . .	64
4.3.1 Data rate within the central hexagon . . . . .	65
4.3.2 Data rate over a first ring . . . . .	65
4.3.3 Data rate over a large network . . . . .	66
4.4 Data rate with shadowing consideration . . . . .	70
4.4.1 Signal quality . . . . .	71
4.4.2 Data rate . . . . .	72
4.4.3 Coverage probability . . . . .	73
4.5 Model evaluation: non-shadowing case . . . . .	74
4.5.1 Simulation setup . . . . .	74
4.5.2 Model accuracy . . . . .	75
4.5.3 EE variation vs cell network types . . . . .	76
4.5.4 Impacts of user's density on EE . . . . .	78
4.5.5 EE vs path-loss exponent . . . . .	78
4.5.6 EE variation over a first ring . . . . .	79
4.5.7 EE variation over a large network . . . . .	80
4.6 Model evaluation: shadowing case . . . . .	82
4.6.1 Simulation setup . . . . .	83
4.6.2 Relationship between $\Gamma_{th}$ and $r$ . . . . .	84
4.6.3 Energy efficiency discussion . . . . .	86
4.6.4 EE model accuracy . . . . .	88
4.7 Conclusion . . . . .	89
<b>5 EE analysis of JT-CoMP scheme in macro/femto cellular networks</b>	<b>91</b>
5.1 Introduction . . . . .	92
5.2 JT-CoMP scheme . . . . .	93
5.3 JT-CoMP performance evaluation . . . . .	94
5.4 System model . . . . .	96
5.4.1 Energy efficiency model with JT-CoMP scheme . . . . .	97
5.4.2 Power consumption model with JT-CoMP scheme . . . . .	97
5.4.3 SINR calculation: case of JT-CoMP . . . . .	98
5.5 Data rate computation . . . . .	100

5.5.1	Non-CoMP scenario . . . . .	102
5.5.2	AllUEs-CoMP scenario . . . . .	103
5.5.3	CoMP scenario . . . . .	103
5.6	Backhauling traffic computation: $C_{bh}$ . . . . .	104
5.7	Simulation and results . . . . .	104
5.7.1	Date rate vs the network radius . . . . .	105
5.7.2	EE vs radius $R_a$ in scenario AllUEs-CoMP . . . . .	107
5.7.3	Impact of distance threshold $d_{th}$ on cell EE $EE_{cell}$ in CoMP scenario .	111
5.7.4	EE gain vs BSs number . . . . .	112
5.7.5	Backhauling power cost vs BSs number . . . . .	114
5.8	Conclusion . . . . .	116
<b>6</b>	<b>Conclusion and Perspective</b>	<b>119</b>
6.1	Conclusion . . . . .	119
6.2	Future work . . . . .	121
6.2.1	Other bandwidth scheduling approach . . . . .	122
6.2.2	EE in heterogeneous networks . . . . .	122
6.2.3	EE-evaluation for uplink system . . . . .	123
6.2.4	EE mobility model . . . . .	123
<b>Appendix A</b>	<b>Computation of data rate in remaining part</b>	<b>125</b>
A.1	Basic functions and application on example 1 . . . . .	125
A.2	Data rate for the remaining part for a disc area with any size . . . . .	127
<b>References</b>		<b>131</b>

# List of figures

1.1	An example of cellular network . . . . .	5
1.2	Breakdown of energy consumption in cellular network . . . . .	6
1.3	Sketch of EE-SE tradeoff: (a) in ideal case (b) under practical concerns . . . . .	8
1.4	Diagrams of MIMO schemes . . . . .	9
1.5	CoMP schemes: (a) CB/CS (b) JP/JT . . . . .	10
1.6	A scenario of heterogeneous wireless network (HetNet) . . . . .	11
1.7	Two scenarios of relay systems . . . . .	12
1.8	The average daily traffic demand a residential area . . . . .	13
1.9	Cloud-RAN architecture for mobile networks . . . . .	14
2.1	Percentage of power consumption by different components of a large-cell BS	25
3.1	Cellular network with an integer frequency reuse (IFR) 1 scheme . . . . .	49
3.2	Network area of radius $R_a$ ( $0 < R_a \leq R_e$ ). . . . .	51
3.3	Network model in hexagonal case and main parameters . . . . .	52
3.4	Network model in fluid case and some parameters . . . . .	53
3.5	SINR vs the distance to the BS in a macro cellular network. . . . .	55
3.6	SINR vs the distance to the BS in a femto cellular network. . . . .	56
3.7	CDF of SIR values in a macro cellular network . . . . .	57
3.8	CDF of SIR values in a femto cellular network . . . . .	57
3.9	SIR vs the number of network rings in a macro cellular network . . . . .	58
3.10	SIR vs the number of network rings in a femto cellular network . . . . .	59
4.1	Scenario 1: network area with radius $R_a$ ( $0 < R_a \leq R_e$ ) . . . . .	65
4.2	Scenario 2: network area with radius $R_a$ ( $R_e < R_a \leq 2R_c$ ) . . . . .	66
4.3	Scenario 3: network area with radius $R_a$ ( $0 < R_a \leq R_{nw}$ ) . . . . .	67
4.4	Homogeneous network with a various radius $R_a/a$ . . . . .	68
4.5	Two examples for the decomposition of the network area. . . . .	69
4.6	EE difference vs network radius $R_a$ . . . . .	76

---

4.7	EE variation vs network radius $R_a$ for different network types. . . . .	77
4.8	EE variation vs network radius, $R_a$ , with $R = 1Km$ , $N_u = 500$ . . . . .	78
4.9	EE vs path loss exponent in macro and femto cellular network . . . . .	79
4.10	EE variation vs network radius in a first ring . . . . .	80
4.11	EE vs network radius $R_a$ . . . . .	81
4.12	EE error vs network radius $R_a$ . . . . .	81
4.13	Average EE vs network radius $R_a$ . . . . .	82
4.14	Coverage probability vs SINR threshold for fixed UEs . . . . .	84
4.15	SINR threshold $\Gamma_{th}$ vs UE distance to the BS; Between fluid model and polynomial curve fitting (PCF) . . . . .	85
4.16	EE variation vs network radius $R_a$ in femto cellular network . . . . .	87
4.17	EE variation vs network radius $R_a$ in macro cellular network . . . . .	88
4.18	EE error vs network radius $R_a$ in cellular networks . . . . .	89
5.1	JT-CoMP scheme . . . . .	93
5.2	Hexagonal network and main parameters. . . . .	97
5.3	JT-CoMP in hexagonal model . . . . .	99
5.4	JT-CoMP in fluid model with $n (= 1)$ coordinated BSs . . . . .	99
5.5	Area of interest with various radius $R_a$ ( $0 < R_a \leq R_e$ ) . . . . .	100
5.6	JT-CoMP strategy defined by distance threshold $d_{th}$ . . . . .	101
5.7	$D_{area}$ vs radius of the MCN, $R = 1000m$ , $K_{CoMP} = 50W$ , $n = 1$ , <b>AllUEs-CoMP scenario</b> . . . . .	106
5.8	$D_{area}$ vs radius of the FCN, $R = 50m$ , $K_{CoMP} = 30mW$ , $n = 1$ , <b>AllUEs-CoMP scenario</b> . . . . .	106
5.9	EE vs radius of the network area in a FCN, $K_{CoMP} = 30mW$ , <b>AllUEs-CoMP scenario</b> , $n = 1$ . . . . .	107
5.10	EE vs radius of the network area in a FCN, $K_{CoMP} = 30mW$ , <b>AllUEs-CoMP scenario</b> , $n = 3$ . . . . .	108
5.11	EE vs radius of the network area in a MCN, $R = 1000m$ , $K_{CoMP} = 50W$ , <b>AllUEs-CoMP scenario</b> , $n = 1$ . . . . .	108
5.12	EE vs radius of the network area in a MCN, $R = 1000m$ , $K_{CoMP} = 50W$ , <b>AllUEs-CoMP scenario</b> , $n = 3$ . . . . .	109
5.13	EE per cell vs $d_{th}$ , various $K_{CoMP}$ , $\eta = 2.6$ and $n = 1$ in a FCN . . . . .	111
5.14	SIR versus distance to the BS in Non-CoMP mode, simulated by fluid model with $\eta = 2.6$ in a FCN . . . . .	112
5.15	EE improvement in a MCN, $R = 1000m$ , $\eta = 2.6$ , $K_{CoMP} = 50W$ for <b>AllUEs-CoMP scenario</b> . . . . .	113

5.16 EE improvement in a FCN, $R = 50m$ , $\eta = 2.6$ , $K_{CoMP} = 30mW$ for <i>AllUEs-CoMP scenario</i> . . . . .	113
5.17 $K_{CoMP}$ vs the number of coordinated BSs $n$ in a MCN, <i>AllUEs-CoMP scenario</i> . . . . .	114
5.18 $K_{CoMP}$ vs the number of coordinated BSs $n$ in a FCN, <i>AllUEs-CoMP scenario</i> . . . . .	115
A.1 Decomposition of the remaining region for example 1. . . . .	125
A.2 Fluid model: small integral triangular region (shaded area) and main parameters . . . . .	126
A.3 Fluid model: integral basin region (shaded area) and main parameters . . . . .	126
A.4 Decomposition of the interested area with any size for the computation of data rate. . . . .	127
A.5 Four types of subregions in the decomposition of interested area. . . . .	128



# List of tables

2.1	Main symbols on EE model . . . . .	22
2.2	Classification of evaluation-based related work . . . . .	35
2.3	Classification of optimization-based related work . . . . .	43
3.1	Values of double linear PCM . . . . .	50
3.2	Simulation parameter value . . . . .	55
4.1	Common parameters in a large network . . . . .	68
4.2	Simulation Parameter Value . . . . .	75
4.3	Simulation Parameter Value . . . . .	83
4.4	$\Gamma_{th}$ fitting error between fluid and PCF, with $\mathbb{P}_{cov}^r = 90\%$ , $R = 50m$ , $\eta = 3$ .	86
5.1	Simulation Parameter Value . . . . .	105
5.2	EE results ( $K\text{bits}/\text{Joule}$ ) of a FCN in different scenarios: <i>Non-CoMP</i> and <i>AllUEs-CoMP</i> . . . . .	110
5.3	Numerical results of $EE_{cell}$ and $EE_{25}$ measured by $K\text{bits}/\text{Joule}$ . . . . .	114
5.4	Numerical Results of $EE_{cell}$ measured by $K\text{bits}/\text{Joule}$ in the FCN for fixed $K_{CoMP}$ and various $K_{CoMP}$ with $\eta = 2.6$ . . . . .	115
5.5	Numerical Results of $EE_{cell}$ measured by $bits/\text{Joule}$ in the MCN for fixed $K_{CoMP}$ and various $K_{CoMP}$ with $\eta = 2.6$ . . . . .	115



# Chapter 1

## Related work on advanced techniques in 5G

### Contents

1.1	Introduction . . . . .	2
1.2	Energy efficiency (EE) in ICT . . . . .	3
1.2.1	Environmental and 5G usage aspects . . . . .	3
1.2.2	Operators and users viewpoints . . . . .	4
1.3	Cellular network concept . . . . .	5
1.4	SE-EE relationship . . . . .	6
1.4.1	Spectral efficiency (SE) . . . . .	6
1.4.2	Energy efficiency (EE) . . . . .	7
1.4.3	SE-EE relationship . . . . .	7
1.5	Promising key 5G technologies . . . . .	8
1.5.1	Multiple-Input Multiple-Output (MIMO) . . . . .	8
1.5.2	Coordination Multipoint (CoMP) . . . . .	10
1.5.3	Heterogeneous cellular network (HetNet) . . . . .	11
1.5.4	Relay transmission . . . . .	12
1.5.5	BS on/off strategy . . . . .	13
1.5.6	Cloud radio access network (Cloud-RAN) . . . . .	14
1.6	EE-related surveys . . . . .	15
1.7	Conclusion . . . . .	18

---

## 1.1 Introduction

As far as we know, the fourth generation of the wireless communication systems has been evaluated in terms of spectral efficiency (SE), defined as the throughput per unit of bandwidth. It is an indication of how much traffic a limited frequency spectrum can carry. However, SE can not offer any insight on how efficient the energy consumption is, i.e., the energy required to handle the traffic. Therefore, energy efficiency (EE) has attracted much interest in recent years as one of the key performance indicators to design the energy-efficient 5G wireless networks. A most widely-applied definition of EE is the ratio between SE and the total power consumption [1]. According to the above definition, it is obvious that EE has a close relationship with SE. Hence, many studies have now been conducted to improve EE through improving SE.

From the perspectives of both increasing bandwidth and improving the signal-to-interference-plus-noise ratio at the users, several key and advanced technologies have been developed to improve the SE of advanced 4G wireless networks, like: multiple-input multiple-output (MIMO), base stations (BSs) cooperation, small cells, relay transmission, on-off switching policy of BSs [2], cloud radio access networks (Cloud-RAN), carrier aggregation and millimeter-wave (mmWave) communications. Given the above definition of EE, denoted by SE, these technologies can be considered as promising candidates for 5G mobile cellular systems to improve EE. Additionally, we have found that most of the studied work on the investigation of the energy efficiency (EE) in wireless networks, are conducted with the purpose either to evaluate the impact of some advanced techniques on EE, or to define/design the technical parameters in order to optimize the EE factor. Accordingly, introducing these advanced technologies is very necessary for the reader's better understanding how they enable the dramatic increase of SE and EE.

This chapter aims to identify several technologies, which are crucial and can improve capacity, coverage, or energy efficiency (EE) in the 5G wireless radio networks. Additionally, this thesis is focusing on EE model design for the 5G cellular networks and specifically investigates the effect of coordinated BSs and shadowing on the performance of EE. Therefore, presenting these advanced technologies is helpful to understand our thesis work. Mention that the carrier aggregation and millimeter-wave (mmWave) communications mainly focus on the efficient utilization of spectrum bandwidth, which is beyond the scope of discussion of this thesis. Hence, the two technologies will not be discussed in this chapter.

In this chapter, we first outline the background information on energy efficiency in the information and communications technologies (ICT). Then the concept of cellular network and its energy consumption are presented. Furthermore, the advanced technologies are

introduced, which have the potential to improve EE. Finally, we discuss some survey papers which are focusing on EE through taking advantage of the advanced technologies so as to illustrate the impact of these techniques on EE.

## 1.2 Energy efficiency (EE) in ICT

With the advent of the fifth generation of wireless networks, with millions more base stations (BSs) and billions of connected devices, energy efficiency (EE) has been proposed as one of key performance indicators for the design of energy-efficient wireless networks. The EE of a communication link can be defined as a ratio of the achievable sum rate to the total power consumed and is given in bits/Joule [3]. Energy consumption for wireless systems has become a more and more important issue in the world due to its impact on the environment and the operation cost. For example, carbon emissions of energy sources have great negative impact on the environment, and the price of energy is increasing day by day. Hence, it is very important to study EE in information and communications technologies (ICT).

### 1.2.1 Environmental and 5G usage aspects

Information and communications technologies (ICT), powered by traditional carbon-based energy sources, are playing a more and more substantial role in global greenhouse gas emissions since the amount of energy for ICT increases dramatically with the rapidly growth of the number of connected devices. Presently, the  $CO_2$  generated by ICT accounts for 5% of the global emission [2, 4] and the percentage is increasing briskly due to the explosive growth of service requirements in the near future. Meanwhile, as some parts of ICT systems, infrastructures of cellular mobile networks, wired communication networks and Internet consume more than 14% of the worldwide electric energy nowadays [5, 6]. It is anticipated that 75% of the ICT district will be the radio access communication by 2020 [7]. The truth hints that wireless communications should be highly concerned considering its key role in diminishing ICT-related  $CO_2$  emissions.

However, reducing ICT-related energy consumption and  $CO_2$  emissions is challenging considering the tremendous deployment of telecommunication devices and the requirement of high communication quality. Currently, people foresee the mobile traffic to grow by a factor of 1000 by the year of 2020, and 10 to 100-fold for the number of connected users.

In 5G networks, billions of devices (50 billion by the year of 2020) [8], are served to provide ubiquitous connectivity and innovative and rate-demanding services. For example,

multiple devices (including smartphone, laptop, PC, tablets) would be owned by each person along with human communications and machine correspondence. One of the advantages of 5G is its ability to build a universal and connected communication environment where cars, robots, drones, smart city devices, medical devices, sensors and wearable devices use radio access networks to associate with each other, interacting with users to provide a series of innovative services such as smart grids, smart homes, smart cities, smart cars, telesurgery, and advanced security [9]. Apparently, for the sake of serving such an extensive amount of terminals and comparing to current standards, the provided capacity will have to exponentially increase in the prospect networks. It is estimated that the traffic volume in 5G networks is demanded to reach tens of Exabytes ( $10^{18}$  Bytes) per month. Correspondingly, the capacity provided in 5G networks is required to be 1000 times higher than that in 4G networks. Additionally, some applications require a lower latency. For example, the latency of 5G networks is expected to be lower than  $1ms$  in autonomous vehicles [10].

It is impossible to achieve the above ambitious goals based on the architecture and infrastructure of current 4G networks by scaling up the transmitting powers considering factors like the limited energy resources on the earth, greenhouse gas emissions, electromagnetic pollution, and the slow progress of battery technology and application. According to the energy crunch, the design of 5G wireless communication systems thus necessarily have to consider the energy efficiency (EE) as one of the objectives from the perspective of operators and users.

### 1.2.2 Operators and users viewpoints

From the operators' point of view, the energy consumption in the wireless access network mainly comes from the base station (BS) [11], accounting for more than 57% of the total energy consumption [11–13]. In total, 4.5 GWatt of power is consumed by approximately 3 million BSs in the world [14]. Meanwhile, the financial cost for energy consumption occupies a great proportion of annual operating expenses for service provider [15, 16]. From literatures, one finds the electricity bills cost about 18% (in mature markets of Europe) and 32% (in India) of their operational expenditure (OPEX) [17–19]. The percentage can increase up to 50% for the radio access networks [20, 21]. Thus energy efficiency is of high interest and urgent to be considered for operators since the financial benefits can be expected for a well designed cellular networks.

Energy-efficient wireless communication is also crucial from users' perspective. Around 3 billion mobile terminals (MTs) are in use in the world with power consumption ranging from 0.2 to 0.4 GWatt [22]. The high energy expenditure of wireless access networks has drawn concerns from mobile users in terms of economy and quality-of-experience (QoE).

According to J. D. Power and Associates Reports [23] on the study of wireless smartphone customer satisfaction, superior comments are given to iPhone except for the battery life. In the report of [24], the same problem was found. About 60% of mobile users suffer from the limited battery capacity [25] and the time cost for charging battery in a MT has become a significant factor to value the quality-of-service (QoS) [26]. What's worse, the gap between energy demand and battery capacity offered by MTs is exponentially enlarging [27]. Hence, without a breakthrough in battery technology, the battery life of terminal sets will be the main limitation for the development of energy-hungry applications (e.g., video games, mobile P2P, interactive video, video monitors, streaming multimedia, mobile TV, 3D services, and video sharing) [18].

In the next section, we will show the concept of a cellular network and introduce the power consumption in radio communication system.

### 1.3 Cellular network concept

A wireless cellular network is a mobile network, where a large number of base stations (BSs) with limited power are deployed and provide services. Each BS covers a limited area, called a cell. These cells together provide network coverage over larger geographical areas, where the voice, data, and other types of content can be transmitted via BSs. Even, mobile users are able to communicate with each other while they are moving through cells during transmission. A BS typically uses a different set of frequencies from neighboring BSs, to avoid interference and provide guaranteed service quality within each cell. A simple example of cellular network is shown in Fig. 1.1.

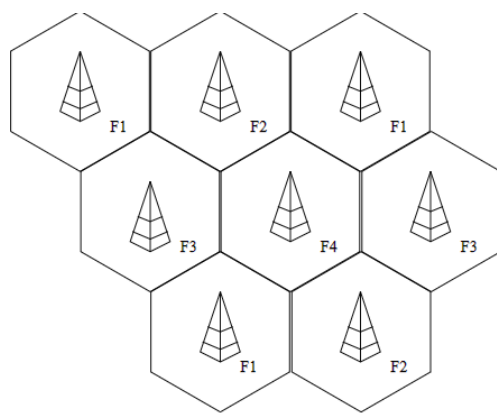


Fig. 1.1 An example of cellular network

The design objectives for cellular networks are to maximize the throughput, spectral efficiency (SE), defined as the throughput per unit of bandwidth while meeting quality-

of-service (QoS) requirements. However, the energy consumption was not be considered at the initial design of the cellular network. The typical power consumption of different elements of a current wireless network [12] is shown in Fig. 1.2. It is clearly shown that

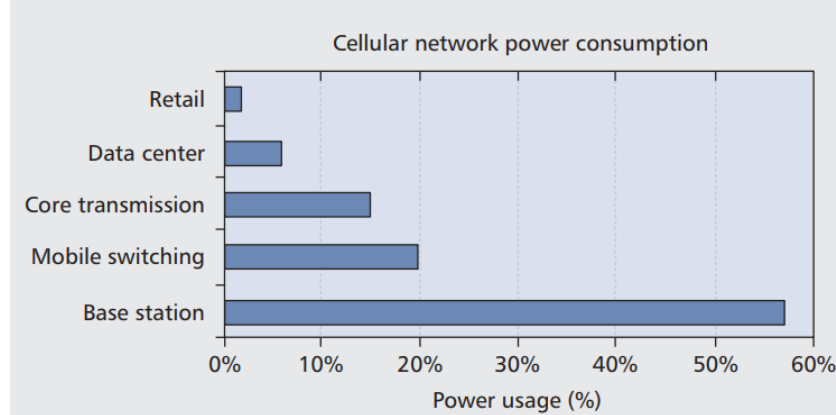


Fig. 1.2 Breakdown of energy consumption in cellular network [12]

BSs consume the highest proportion of energy in cellular networks. Typically, the increase of the number of BSs inevitably leads to the raise of the overall energy consumption in the network. Therefore, from BSs' perspective, one can deploy efficient BSs to decrease the energy consumption in the cellular network and then to obtain a energy-efficient cellular network.

## 1.4 SE-EE relationship

### 1.4.1 Spectral efficiency (SE)

The efficiency of a communication system has traditionally been measured in terms of spectral efficiency (SE) for a point-to-point transmission, where both the transmitter and receiver are equipped with only one antenna. SE refers to the ability of a given channel encoding method to utilize bandwidth efficiently. It is defined as the transmission rate per unit of bandwidth [1, 13, 28]. SE is measured in bits per second per hertz. Let  $BW$  be the system bandwidth,  $P_{use}$  as the given useful transmitting power,  $N_0$  as the power spectral density of additional white Gaussian noise (AWGN). Correspondingly, the signal-to-noise ratio (SNR) at the receiver can be defined as in [13], displayed by,

$$SNR = \frac{P_{use}}{N_0 \cdot BW}. \quad (1.1)$$

Via Shannon's formula, then SE can be denoted as

$$SE = \log_2(1 + SNR) \quad (1.2)$$

The SE metric indicates how efficiently a limited frequency spectrum is utilized.

### 1.4.2 Energy efficiency (EE)

Energy efficiency (EE) has been proposed as a metric to evaluate the energy consumption for the network framework. Various EE metrics have been defined in the literatures [29]. Except the widely used bit-per-Joule capacity [30, 31], the energy-per-bit to noise power spectral density ratio [30, 32–34], the rate per energy [35] or the Joule-per-bit [36] also can be used as an EE metric. The detailed formulas of these EE metrics will be discussed in the next chapter. Bit-per-Joule is expected as the popular EE metric for 4G cellular systems and beyond. Since it not only considers the features and properties of capacity, but also the energy consumption of the whole networks. Taking advantage of the popular EE metric of bit-per-Joule, EE is defined as a ratio of the total transferred bits to the total power consumption. Let  $P_{exp,total}$  be the total consumed power for transmitting data rate in a point-to-point transmission system, the EE can be expressed as

$$\begin{aligned} EE &= BW \cdot (\log_2(1 + \frac{P_{use}}{N_0 \cdot BW})) / P_{exp,total} \\ &= BW \cdot SE / P_{exp,total}. \end{aligned} \quad (1.3)$$

### 1.4.3 SE-EE relationship

For simplification, in most of the theoretical work related to the EE-SE trade-off,  $P_{exp,total} = P_{use}$  for a point-to-point transmission system. According to Eq. (1.2), we derive  $\frac{BW}{P_{use}} = \frac{1}{N_0(2^{SE}-1)}$ . Through combining Eq. (1.2) and Eq. (1.3), we can obtain the relationship between SE and EE, as in [13],

$$EE = \frac{BW \cdot SE}{P_{use}} = \frac{SE}{N_0(2^{SE}-1)} \quad (1.4)$$

From the above expression, EE converges to a constant,  $1/(N_0 \cdot \ln 2)$  when SE approaches zero. On the contrary, EE approaches zero when SE tends to infinity. The fundamental tradeoff between EE and SE is shown in Fig. 1.3 (a). This EE-SE relationship is for point-to-point communication not for network. However, in the practical systems, the EE-SE relation is not as simple as the above formula and this relationship has been influenced by

several hardware constraints, such as circuit power, power amplifier [27]. More precisely, if circuit power is considered, the relationship curve will turn to a bell shape, as illustrated in Fig. 1.3 (b).

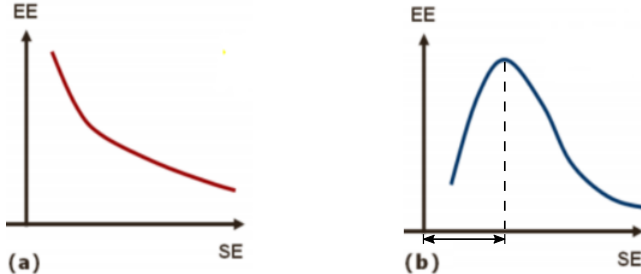


Fig. 1.3 Sketch of EE-SE tradeoff: (a) in ideal case (b) under practical concerns [13]

According to the relationship between EE and SE in Fig. 1.3 (b), we observe that EE can be improved with the increase of SE in the low-SE regime. Since in the low-SE regime, the circuit and transmitting power of the BS site will not increase obviously with the increase of SE, which leads to an increase in EE. Therefore, for the purpose of improvement of EE, some advanced technologies have been widely and popularly used to improve SE, as we list in the following section.

## 1.5 Promising key 5G technologies

In the last ten years, many studies have investigated the spectral efficiency for different types of networks using some advanced radio communication technologies, e.g., multiple-input multiple-output (MIMO), coordination multipoint (CoMP) scheme, heterogeneous cellular networks, relay transmission, the on-off switching policy of base station (BS), and cloud radio access network (cloud-RAN). A brief introduction is given to these technologies in the below part, which helps the understanding of the underlying EE models.

### 1.5.1 Multiple-Input Multiple-Output (MIMO)

MIMO technique has been widely adopted in wireless networks nowadays to transfer and receive more data at the same time by equipping BS or user equipments (UEs) with multiple antennas [6]. A diagram of MIMO is given as in Fig. 1.4. Single-input single-output (SISO), single-input multiple-output (SIMO), and multiple-input single-output (MISO) are regarded as special cases of MIMO. In detail, SISO is a conventional radio system where the transmitter and the receiver have only a single antenna, respectively. SIMO is the special

case when the transmitter has a single antenna and the receiver has multiple antennas. MISO is the contrary. MIMO can also be used with single user or multiple users to form single-user MIMO (SU-MIMO) and multi-user MIMO (MU-MIMO), as shown in the figure.

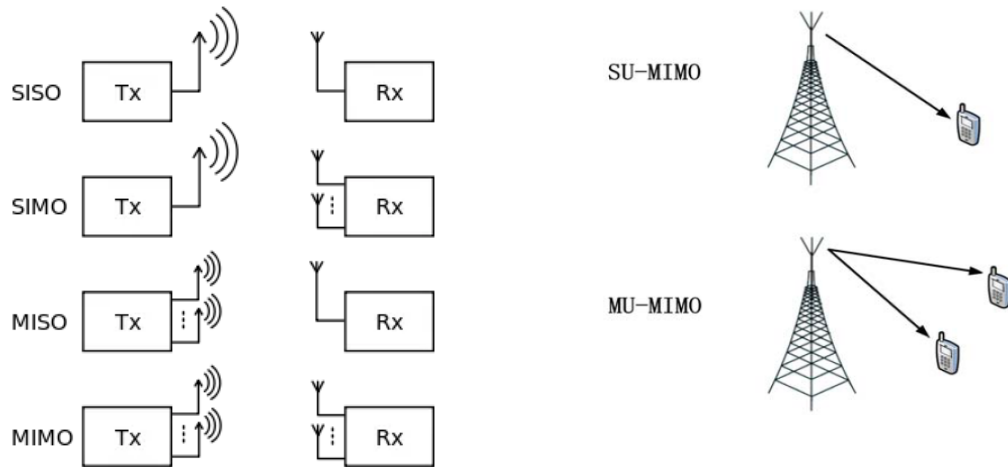


Fig. 1.4 Diagrams of MIMO schemes [6]

MIMO increases the spatial diversity. The array gain is achieved by sending signals that carry the same information through different paths between transmitting antennas and receiver antennas. The variety of paths available in MIMO system can be used to provide additional robustness to the radio link by improving the signal to noise ratio, or by increasing the link data capacity. As a result of the use multiple antennas, MIMO wireless technology is able to considerably increase the SE while still obeying Shannon's law. The transmission using multiple antennas also leads to higher network throughput. Due to the configuration of multiple antennas, MIMO is shown as an effective technology to improve the network capacity, spectral efficiency (SE). Based on the relationship between SE and EE, thereby MIMO is regarded as a method to improve the network energy efficiency. Recently, massive MIMO technology, one of the key enablers for 5G, is emerged where BSs are equipped with a number of antennas to achieve multiple orders of spectral and energy efficiency gains over current LTE networks [37, 38]. However, more antenna devices will consume more circuit power as wells as more signaling overhead in MIMO systems. For example, in order to obtain good performance, channel state information (CSI) is required at the receiver or at both the transmitter and the receiver. Some symbols need to be sent before the data transmission with the purpose of estimating the CSI, which leads to additional signaling overhead. Therefore, the energy efficiency (EE) of MIMO systems is still an open issue if the circuit power consumption and the signal overhead are considered.

### 1.5.2 Coordination Multipoint (CoMP)

CoMP technique has been proposed in 3GPP LTE-Advanced as a tool to improve coverage, cell-edge throughput and system efficiency [39]. In CoMP transmission, several BSs are cooperated to transmit and receive data from multiple UEs based on the shared information between BSs [40]. The cooperation techniques aim to avoid or exploit interference in order to improve the data rates and spectral efficiency of cell edge UEs [41].

CoMP in radio access networks can be applied either in the downlink of the radio systems, namely a transmission coordination, or in the uplink, namely a reception coordination [42]. In general, CoMP includes two main families coordination methods, joint processing/transmission (JP/JT) and coordinated beamforming/coordinated scheduling (CB/CS). JP/JT scheme means that a single UE receives multiple copies of the useful data from different BSs in the coordinated set (the set of BSs that are coordinated). This scheme of JP/JT is aimed at improving the received signal quality of the target UE and/or cancel the interference from the BSs outside the coordinated set. The BSs in coordinated set share the required data via high-speed wired link since the amount of control data to be exchanged is large, e.g., channel knowledge and computed transmission weights. JP/JT in a downlink system is illustrated in Fig. 1.5 (b). However, CB/CS scheme means that data to a single UE is instantaneously transmitted from one of BSs in the CoMP set, and that scheduling decisions and/or generated beams are coordinated transmitted between BSs in order to control the created interference. CB/CS is illustrated in Fig. 1.5 (a).

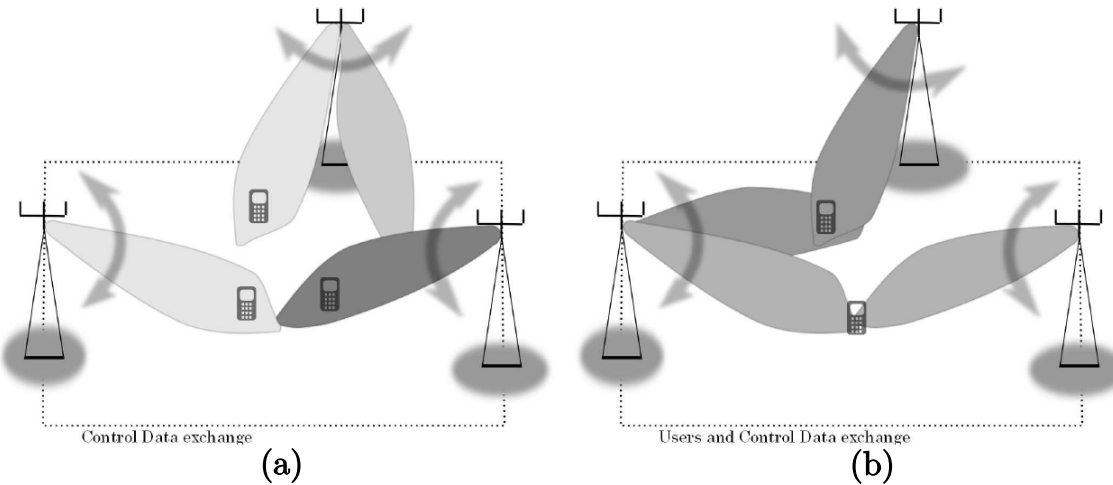


Fig. 1.5 CoMP schemes: (a) CB/CS (b) JP/JT [42]

A JT-CoMP scheme in the downlink system is shown in Fig. 1.5 (b). Each of the UEs are associated with the two closed BSs and receives the useful information from them. Since the transmission power resources of multiple BSs can be used through coherent

transmissions, the maximum received signal powers for the cell-edge UEs are obtained, and the interference from neighboring BSs is significantly mitigated. Thereby, the SINR and SE of the cell-edge UEs are improved significantly [40]. Due to JT-CoMP, cell edge UEs experience lower interference, higher receiving SE and throughput, hence requiring less transmission power from both BSs. Given that the EE is related to throughput and power consumption, thus, JT-CoMP can be regarded as a promising technology to improve the EE for 5G wireless networks.

CoMP technology has been already included in LTE-A standard [43] and it plays an important role in 5G networks due to the advantages of reducing interference and improving SE. Motivated by these advantages, some studies have been investigated on JT-CoMP for the energy efficiency in wireless networks. However, most of the current work is based on intractable models, which needs a lot of time and huge resources to conduct simulations. Therefore, how to develop an accurate and tractable model for EE-evaluation is still an interesting issue while considering the JT-CoMP approach, which provides a research direction for our thesis work.

### 1.5.3 Heterogeneous cellular network (HetNet)

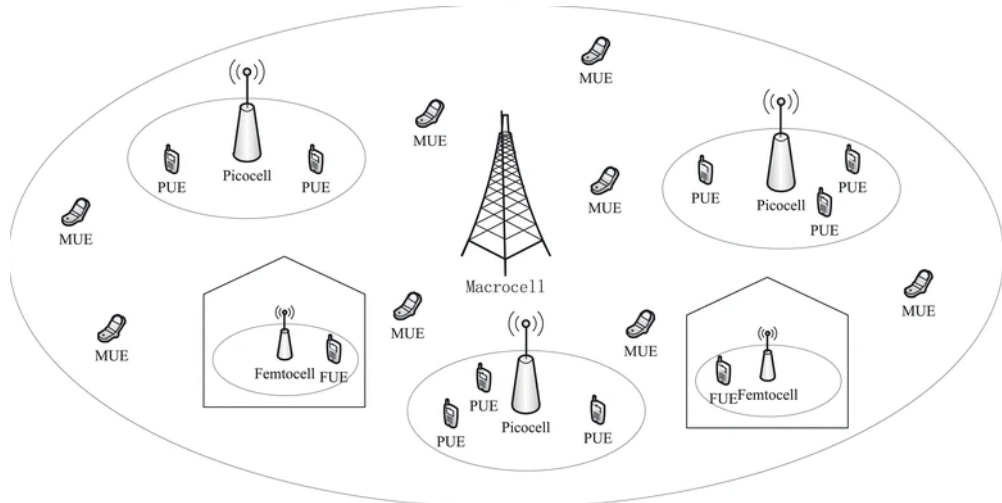


Fig. 1.6 A scenario of heterogeneous wireless network (HetNet) [44]

Heterogeneous networks have been introduced in the LTE-Advanced standardization [45]. A heterogeneous network (HetNet) is one kind of wireless network composed by a mixture types of BSs (macro-, micro-, pico-, and femto- BSs) with different transmission powers and coverage, as shown in Fig. 1.6. In recent years, HetNets are widely deployed in 5G wireless networks so as to enhance the capacity/coverage and to save energy con-

sumption [46]. Through the deployment of multi-tier BSs, the area spectral efficiency (SE) is increased, while transmitting power is reduced due to the decreased propagation loss between nodes [47]. Although the coverage and throughput can be enhanced by deploying dense small cells, a tremendous escalation of energy consumption cannot be avoided, due to the massive small connections in pico cell than the macro cell. The dense and random deployment of small cells and their uncoordinated operation raise important questions about the implication of energy efficiency (EE) in such multi-tier networks [16]. Improving EE can help the operators reduce the operational expenditure as energy constitutes a significant part of their expenditure. As a result, energy efficiency has been evolved as one of the major concerns for network operators to design the HetNet.

#### 1.5.4 Relay transmission

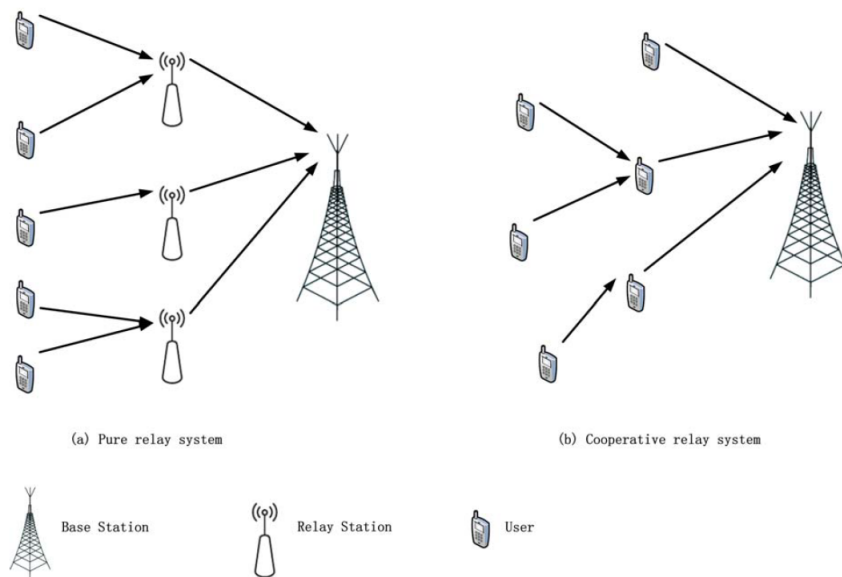


Fig. 1.7 Two scenarios of relay systems [6]

Relaying is an important technology for increasing the coverage and capacity of the network. Relay node (RN) is a kind of BS which covers smaller area than a macro cell and used to collect signals from a BS and resend an amplified or revised version to the target UE. Two kinds of relay systems are taken into account in [6, 48], pure relay systems and cooperative relay systems, as shown in Fig. 1.7. The function of the relay nodes in the pure relay system is only to help the source node to transmit data. However, all the nodes act as information sources as well as relays in the cooperative relay systems. Specially, a micro/femto/pico BS can be regarded as a RN in a HetNet. If a BS is used as a RN, it is not

only a source node to send its own signal, but it can also be as a received node to resend the collected information.

Typically, relaying splits the transmission into smaller hops and better channel quality is provided between base stations and relay nodes, compared to the direct transmission from the base station to users. Therefore, the spectral efficiency can be increased. Furthermore, since the distance between transmitter and receivers is decreased compared with the direct transmission, the transmitting power can be reduced, which lead to the improvement of energy efficiency. Therefore, RN is more efficient in communication due to the lower energy consumption and different fading channels/links. As a consequence, RN is considered as a promising solution to increase the energy efficiency in 5G network.

### 1.5.5 BS on/off strategy

Generally speaking, the network operators deploy and operate base stations (BSs) based on the peak traffic volume and the BSs are kept switched-on, regardless of the traffic load. For example, the traffic load can reach the peak during the daytime. Nevertheless, the traffic load declines sharply after the office hours [2]. Based on internal surveys on operator traffic data within the EARTH project and the Sandvine report [49], the average daily traffic demand of a residential area is illustrated in Fig. 1.8. Therefore, dynamic switching on/off the BS depending on the traffic demand maybe lead to saving the energy.

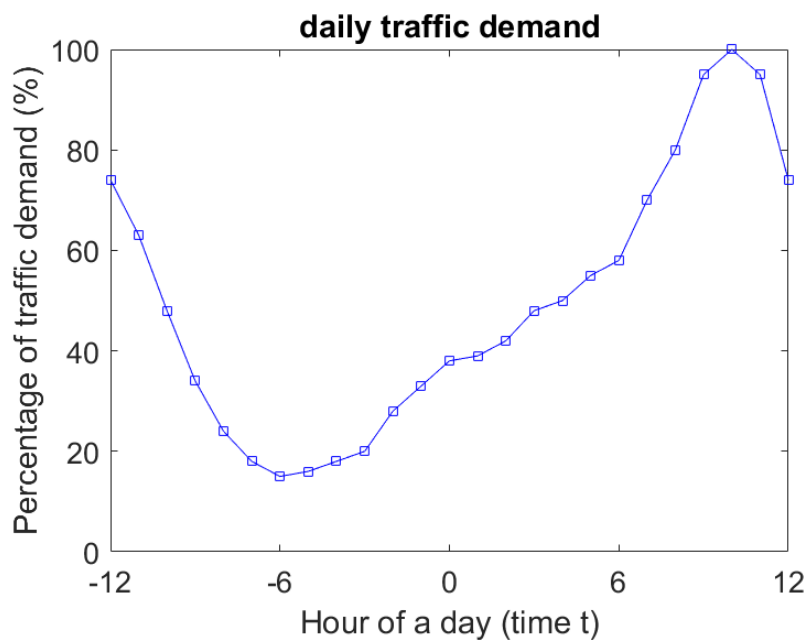


Fig. 1.8 The average daily traffic demand a residential area

BS switching on/off is proposed as a technique to save operating energy through adjusting the transmission strategy of network according to the traffic demand. Operators switch off unnecessary infrastructure nodes or elements while satisfying constraints such as coverage and data rate requirements [9]. In detail, the users in switching-off BS coverage can be served by neighboring active BSs in order to maintain the user throughput and the reliability performance. Given that EE is defined as a ratio of throughput over the power consumption, EE increases with the decrease of the power consumption while the throughput remains the same. Therefore, this technique is expected to be utilized to meet the energy saving requirement for dense and ultra-dense deployments in future 5G networks.

### 1.5.6 Cloud radio access network (Cloud-RAN)

Spurred by the impressive spread of cloud computing, cloud radio access network (Cloud-RAN) is a network architecture where baseband resources are pooled to a remote data-center, named baseband units (BBU) pool, so that they can be shared between BSs. This can be implemented via software [50]. Fig. 1.9 gives an overview of the overall Cloud-RAN architecture (RRH: remote radio head, BBU: baseband units). In more detail, only the radio frequency (RF) chain and the baseband-to-RF conversion stages are presented by the BSs and the BSs are connected through high-capacity links to the data-center, where all the baseband processing and the resource allocation algorithms are run [9].

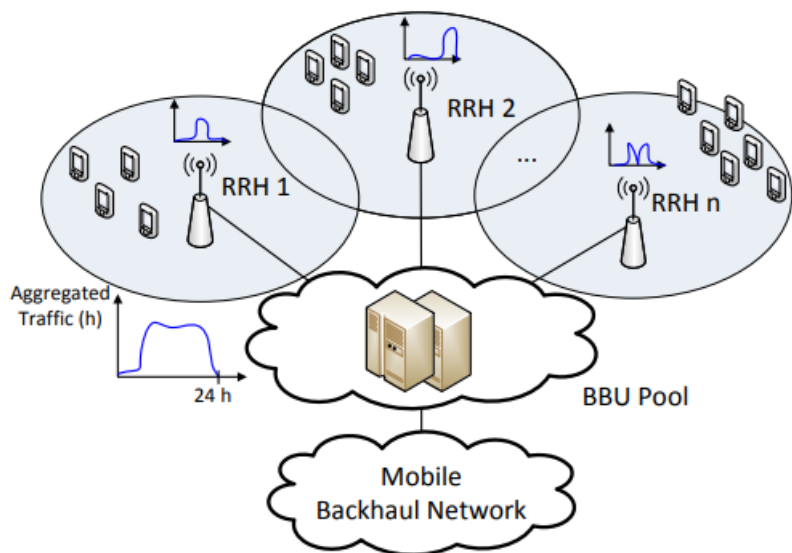


Fig. 1.9 Cloud-RAN architecture for mobile networks [50]

Cloud-RAN is a network architecture that shows significant promises in improving both the spectrum efficiency and the energy efficiency of wireless networks [51]. It brings these benefits based on the below four folds [52, 53]. Firstly, a centralized BBU pool allows for the joint precoding of user messages for interference mitigation. Therefore, the transmitting power of BSs can be reduced with the less interference generated. Secondly, the cooperative BS with distributed antenna equipped by radio remote head (RRH) provides higher spectrum efficiency [51]. Thirdly, most of the baseband signal are proceed by the BBU pool under the Cloud-RAN architecture. Then, the conventional highcost high-power BSs can be replaced by low-cost low-power radio remote heads (RRHs). Fourthly, the central processor can perform joint resource allocation among the BSs to allocate resources according to the users' traffic demand, and put idle BSs into sleep mode during non-peak time for energy saving. Based on the advantages of reduction deployment costs in Cloud-RAN, Cloud-RAN is another key technology instrumental to making 5G networks more energy-efficient.

## 1.6 EE-related surveys

The tremendous growth of wireless communication systems leads to challenges in efficiently utilizing limited network resources to meet the high QoS requirements. Higher capacity wireless links are expected but suffer from increasing power consumption and associated financial cost. Meanwhile, the battery capacity of the smartphones limits the improvement of QoS. Additionally, the slow development of related technologies in battery also enlarges the gap between energy demand and battery capacity offered by mobile terminals. Therefore, energy efficiency is becoming more and more important for wireless system design.

Most of the surveys available in the literature theoretically discussed the energy efficiency in 5G wireless networks from the perspective of the state-of-the-art technologies. Some surveys of current literature on energy efficiency will be presented in the following part.

Surveys in [6, 46, 54, 55] discussed how to design the EE wireless communication from the technical methods. For example, the work in [6] summarizes the advanced techniques of MIMO and relay transmission, resource allocation between signaling and data symbols in order to design EE networks. Those advanced technologies are only analyzed to improve the SE from the view point of information-theoretic analysis. Moreover, the authors in [46] mainly discussed the trade-off between EE and SE, QoS for 5G wireless communication, based on a system framework of green HetNets along with some techniques, such as network dynamic cooperative transmission and dynamic resource allocation. However, they studied EE from the network architecture and cross-layer design perspectives, which mainly focus

on the design principle. The detailed and precise equation of EE is not discussed in that literature.

Alternatively, the enabling technologies (massive MIMO, millimeter waves and small cells) for 5G green networks are investigated in [54]. Specially, the authors identified the achievable capacity/throughput gains from both theoretical and practical perspectives according to some references, for example, the system capacity of a massive MIMO system can be increased by factors of 3 to 6.7 for a base station with 64 antennas serving 15 clients simultaneously. Moreover, an overview description of mobile access and several new concepts for 5G networks are demonstrated in [55], where some key performance indicators, the trends of EE and the evolutionary technologies of Massive MIMO, relay transmission, cloud-RAN and small cell are illustrated for 5G networks.

The four mentioned surveys only focused on the discussion of the advanced technologies so as to improve SE, whereas none of them are studied the EE and limited to quantify the improvement of EE.

On the other hand, the papers in [9, 18, 19] discussed the energy saving from the perspective of the radio resource management. For example, the survey in [9] provides an investigation on the energy-efficient design and operation of 5G networks from the domains of resource allocation and network planning and deployment. Different other surveys focusing on the traditional electrical energy, the energy harvesting and transfer and hardware solutions for energy efficient 5G networks are first proposed in that literature. Some open issues are also addressed in [9], such as how to combine all energy-efficient techniques to optimize EE, how to use random matrix theory, stochastic geometry and learning techniques in order to deal with randomness of the deployed devices and user equipments and thereby to maximize EE.

Moreover, from the perspectives of radio resource management and network deployment strategies, the authors in [18] overview the energy-efficient technologies of various relay and cooperative communications in wireless networks. Specially, the most popular EE metric of bit-per-Joule is discussed there, which is defined as the system throughput for unit-energy consumption. Considering that daily traffic loads at BSs vary widely over time and space as shown in Fig. 1.8, thus, a lot of energy is wasted when the traffic load is low. Accordingly, these energy-efficient technologies proposed in [18] are mainly discussed under low-traffic loads.

Alternatively, from the perspectives of network operators and mobile users, the literature in [19] elaborates a brief survey on energy-efficient techniques and solutions in order to design and improve the efficiency usage of energy. A unified-treatment way of energy efficient solutions is adopted for network operators and mobile users. For instance, the

green solutions of switching on-off radio devices and radio resource scheduling are mainly emphasized according to the low/high call traffic load conditions. However, it mainly focuses on direct communications (i.e., no multi-hop or relaying techniques) for licensed networks and users.

Specially, some work highlight the energy efficient 5G wireless network based on outstanding technology, like Massive MIMO in [37] and switching on-off BSs in [56]. The work in [37] discusses an overview of massive MIMO technology, a realistic power consumption models in MIMO systems and some outstanding techniques for EE-maximization. The survey pointed out that EE-maximization of a Massive MIMO system can be achieved using the Massive MIMO technique through minimizing power amplifier (PA) power loss, scaling the number of BS antennas and reducing radio frequency requirements at BS. The simulation results show that the sum EE of all users can be improved by increasing the number of BS antennas and it exists a maximum achievable sum EE. Furthermore, the results also reveal that the optimal number of antennas increases from 63 to 92 and the peak EE increases from 3.6 to 9.2 *Mbits/Joule* with the raise of the number of users from 6 to 50 in the system.

Authors in [56] emphasize that the switching on/off BSs technology in order to improve the EE in 5G dense and ultra-dense networks. They present that switching-off unnecessary network elements can be as one of tools for decoupling the scaling of networks from the growth of operating power, which is aimed at adjusting the network capacity according to the demand in order to save operating energy. They mainly emphasize and devise an energy-saving algorithm based on a majorization-minimization approach for turning-off some unnecessary BSs. However, the quantitative improvement of EE is missing from discussion.

Unlike most of the surveys that discussed the EE in the physical layer while some advanced technologies are exploited, the survey in [28] presents an overview of different EE trade-off mechanisms of green communications with respect to each protocol layer, such as physical, media access control (MAC), network, transport and application layer, respectively. Specially, the technologies of sleeping mode, cell breathing, cell zooming are investigated in terms of the EE trade-offs. However, the quantitative improvement of EE are limited in their investigation.

All survey papers discussed above illustrate that a energy-efficient wireless network can be designed through taking advantage of the 5G technologies candidates. Moreover, they also indicated that the 5G technologies candidates can be used to evaluate EE or to study the problem of EE optimization. Nevertheless, these conclusions are drawn from the

perspectives of theoretical and design principle. In the next chapter, we will present some literatures to show the advanced technologies on EE through some simulation results.

## 1.7 Conclusion

This chapter provides the background information and some related work on advanced techniques, beneficial to improve EE for 5G wireless networks. We first introduce research motivation on EE in ICT and the cellular network concept. Then the relationship between SE and EE is presented, which is helpful to understand our thesis work. Moreover, the typical approaches and techniques to reduce the system energy consumption and to improve the SE are presented, such as MIMO technique, coordination multipoint transmission, heterogeneous cellular network, relay transmission, BS switching off and Cloud-RAN, which are promising to be exploited in 5G networks. Finally, we discussed some surveys which are focusing on the green communication.

To investigate the impact of the network parameters on EE, and to capture the major factors involved in the energy consumption process, representative and accurate models are needed. Therefore, in the next chapter, we will present the EE models which have been utilized in some literatures.

# Chapter 2

## Models for EE

### Contents

2.1	Introduction . . . . .	20
2.2	EE models . . . . .	20
2.2.1	Input/output power related EE model . . . . .	21
2.2.2	Cell power consumption and cell area related EE model . . . . .	22
2.2.3	Transmitting power and data rate related EE model . . . . .	23
2.2.4	SE and power cost related EE model . . . . .	23
2.2.5	Overall data rate and power cost related EE model . . . . .	24
2.3	Power consumption models (PCM) . . . . .	24
2.3.1	Ideal load dependent PCM . . . . .	25
2.3.2	Linear PCM . . . . .	25
2.3.3	PCM with sleep mode . . . . .	26
2.3.4	PCM with backhauling cost . . . . .	26
2.3.5	PCM considering non-empty buffer . . . . .	27
2.3.6	PCM with transmitting antennas . . . . .	27
2.3.7	A refined double linear PCM . . . . .	28
2.4	Throughput models . . . . .	28
2.5	Classification of EE models . . . . .	30
2.5.1	Evaluation-based related work . . . . .	30
2.5.2	Optimization-based related work . . . . .	36
2.6	Conclusion . . . . .	44

---

## 2.1 Introduction

As illustrated in the previous chapter, energy efficiency (EE), as one of key performance indicators, becomes an important concern while designing a 5G wireless network, not only because of the increasing energy price but also because of the environmental requirement of a lower  $CO_2$  emission of communication networks. Hence, EE has received much attention by both academia and industry through utilizing the different network model tools, such as system-level simulations and stochastic geometry. Much efforts have been done to investigate the problems of EE evaluation and EE optimization through using some advanced technologies, such as multiple-input multiple-output (MIMO), coordination multipoint (CoMP) scheme, heterogeneous cellular networks (HetNets), relay transmission and the on-off switching policy of base station (BS). However, an appropriate definition of EE is the fundamental to study the EE performance for the network.

Various EE models have been proposed in both academia and industry from the measurement level of power amplifier, antenna, base stations (BSs), user equipments (UEs) and the network. Among these models, some are proposed for simplicity, and the others are proposed while considering the network performance such as spectral efficiency, throughput and capacity. One can choose the EE model according to the measurement level as well as the network performance. In this regards, it is very important to understand the detailed definitions of EE metric in different literatures.

Throughout this chapter, we aim to present some EE models according to the different EE definitions, and to classify the literatures on EE according to these promising technologies so as to investigate the impact of these technologies on EE, which will be useful to understand our thesis work.

In this chapter, we first list some EE models from the view point of EE definition. As the important components of the EE model, then the power consumption models and the throughput models are introduced. Furthermore, we classify some literatures on EE from view points of both EE evaluation and EE optimization. The further classification of the categories are based on the advanced technologies, since they have great impact on EE. Afterwards, we summarize the impact of these techniques on EE through comparing the simulation results in the literatures.

## 2.2 EE models

Various models have been proposed by both academia and industry to evaluate the EE performance. In general, from the perspective of measurement level, most of the proposed

EE models are on three different levels in mobile cellular networks so as to obtain the network performance. The three different levels are as follows:

- Hardware component level (for wireless equipment subsystems e.g. power amplifier, antenna, etc.)
- Node level (e.g. BSs and user terminals)
- System or network level (for a group of equipments that form a network).

Additionally, we also found that there are two ways of defining energy efficiency metrics. First, EE is defined as the ratio between the energy output and the energy input, which is the oldest model on EE. Secondly, considering the network performance of QoS parameters such as throughput and capacity, EE is defined as the ratio between a given network performance and the energy consumed [57].

Therefore, according to the measurement level and the various definitions of EE, a review of the EE models used in wireless communication networks is carried out. Table 2.1 summarized the related variables and symbols of EE, capacity and throughput used throughout our discussion.

### 2.2.1 Input/output power related EE model

At the system level, a simple definition of the energy efficiency is defined by the operators is the ratio between the network output power (energy) and the total input power (energy) [21]. This model is the oldest model. Denoting the network output power (i.e., the power of the radio frequency (RF) transmitted signal) and the input power (consumed), as  $P_o$  and  $P_i$ , respectively, the energy efficiency  $EE_{sys}$  for the network is given by

$$EE_{sys} = \frac{P_o}{P_i} \quad (2.1)$$

According to the above definition, we observe  $EE_{sys}$  has no unit. Generally, the deployment of cellular networks is typically optimized for ubiquitous radio access of mobile users. This implies that a significant portion of base stations (BSs) are primarily providing coverage. Eq. (2.1) shows that it is not necessary to achieve the full traffic load for the network, since the users ask for the low service during the off-peak traffic hours. Therefore, this equation can be used when the coverage of a cellular network is required to be greater than a given value, i.e., to reach an acceptable coverage probability.

Table 2.1 Main symbols on EE model

Notation	Definition
$EE_{sys}$	system or network EE
$APC$	area power consumption (ratio of cell power consumption to cell area)
$ECI$	energy consumption index (ratio of power cost and data rate)
$EE$	energy efficiency
$EE_u$	EE of a user $u$
$P_o$	network output power
$P_i$	network input power
$P_{exp,cell}$	total power consumption in a cell
$A_{area}$	cell area
$E_{exp}$	the network energy consumption during the observation period
$N_{bit}$	the number of correctly delivered bits during the observation period
$P_{exp,ave}$	the average network power
$R_{ave}$	the average data rate
$SE_{area}$	the area spectral efficiency
$P_{exp,u}$	the total transmitting power of user $u$
$R_u$	the achievable data rate of user $u$
$C_n$	the maximum data rate of the network
$Th_{total}$	the sum achievable data rate of the network
$PC_{total}$	the total power consumption of the network

### 2.2.2 Cell power consumption and cell area related EE model

To assess the EE for networks having different coverage areas, the area power consumption is introduced, defined as the ratio between the average power consumption per cell and the corresponding cell area [58]. Denoting  $P_{exp,cell}$  as the total power consumption in the cell and  $A_{area}$  as the cell area, the area power consumption  $APC$  is given as

$$APC = \frac{P_{exp,cell}}{A_{area}} [W/Km^2] \quad (2.2)$$

measured in  $W/Km^2$ . This EE model can be used at the node level (e.g. BSs) and the system level, respectively. Since the cell area can not only refer to the coverage of a certain BS but also the coverage of the whole network. Accordingly,  $P_{exp,cell}$  can be the total power consumption of a certain BS or the total power consumption of the whole network, from the perspectives of both the node level and the system level, respectively. Moreover, the coverage area can reflect the area power consumption from a deployment perspective. Additionally, this equation can be used to compare the power consumption in HetNets while varying the number of micro BSs in one cell so as to investigate the impact of deployment

strategies on the power consumption. However, this model needs to be used in conjunction with other performance metrics as it cannot be used to successfully access the EE of two networks having different capacity or throughput.

### 2.2.3 Transmitting power and data rate related EE model

Another EE model on the node level is the energy consumption index (ECI) or energy per bit, proposed in the "Energy Aware Radio and neTworking tecHnologies (EARTH)" project [59]. The energy per bit is measured in J/bit. The energy per bit metric is defined as a ratio of the network energy consumption (EC) during the observation period ( $T$ ) to the total number of bits ( $B$ ) that were correctly delivered in the network during the same time period. Since the network energy consumption is simply the (average) power multiplied by the observation period, this metric could be equivalently described as the ratio between (average) network power ( $P_{exp,ave}$ ) and the (average) data rate ( $R_{ave}$ ) and expressed in W/bps. Denoting  $E_{exp}$  as the network energy consumption and  $N_{bit}$  as the amount of data correctly delivered in the network, the definition of ECI is given by

$$ECI = \frac{E_{exp}}{N_{bit}} = \frac{P_{exp,ave}}{R_{ave}} [\text{J/bit or W/bps}]. \quad (2.3)$$

The ECI focuses on the amount of energy spent per delivered bit and hence is an indicator of network bit delivery EE. This may be especially important in the scenario of high traffic loads. Furthermore, ECI approaches infinity with traffic load close to zero, since the network energy consumption  $E_{exp}$  does not typically go to zero for low traffic loads. ECI is commonly used in the literature, especially for theoretical studies and single link evaluations. Nevertheless, for the low traffic load scenario, the traffic demands of the mobile terminals do not always require BSs at the full power. Specially, the energy cost for the error reception of data is not considered in this model.

### 2.2.4 SE and power cost related EE model

For the sake of reflecting the achieved network coverage, the authors in [16, 60] define the EE as the ratio between the area SE and the average network power consumption. Denoting  $P_{exp,ave}$  as the average network power consumption and  $SE_{area}$  as the area SE, the network EE, denoted  $EE_{sys}$ , can be displayed as

$$EE_{sys} = \frac{SE_{area}}{P_{exp,ave}} (\text{bit/J/Hz}) \quad (2.4)$$

$EE_{sys}$  is measured in  $bit/J/Hz$ . The objective of this definition is to increase the number of transmitted information bits per unit energy, which has been widely used in various publications. This model can be used to evaluate the EE at the component, node and system levels. Moreover, it can also be applicable for the low service demands scenario, where a reasonable network coverage should be guaranteed while considering the strategy of switching off BSs. Specially, the area is a constant for evaluating the system EE.

### 2.2.5 Overall data rate and power cost related EE model

A classical and most widely-applied model to evaluate the EE for the telecommunication networks is the Bit-per-Joule metric. It is defined as a ratio of total volume of data transferred to the energy consumed within a given time interval, expressed by

$$EE = \frac{\text{overall date rate}}{\text{total power comsumption}} \text{ (bits/J or bits/s/watt)} \quad (2.5)$$

The system capacity,  $C_n$ , is the maximum total number of bits that the network can deliver per Joule of energy by one/multiple BSs. The overall network throughput,  $Th_{total}$ , is the sum of the data rates that are successfully delivered to all the terminals in a network, composed by one/multiple cells. Denoting  $PC_{total}$  as the total power consumption, EE also can be expressed as  $EE = C_n/PC_{total}$  or  $EE = Th_{total}/PC_{total}$ .

Depending on the specific area of interest, this EE model can be covered on component, node and system levels in wireless cellular networks. For example,  $EE$  becomes  $EE_u$  (the energy efficiency of one user) at the user's level and  $EE_{sys}$  at the network or system level, respectively. Considering the simplicity of this EE model, it has been applied in many literatures for 4G networks and beyond.

Given that the most used definition of energy efficiency is related to the throughput or capacity and to the power consumption, here we will briefly present some power consumption models (PCMs) and throughput models, which are popular and most used in literatures.

## 2.3 Power consumption models (PCM)

In [12, 14, 21, 61], the percentage of power consumption by different components of a large-cell base station (BS) is reported, as shown in Fig. 2.1. We observe that the power amplifier and feeder cost about 65.6% of the total power. Moreover, the power cost by signal processing overhead, battery backup and power supply loss, cooling loss, power

amplifier loss also can not be ignored. Therefore, a model to quantity the component cost is necessary. Nowadays, various power consumption models have been proposed in literatures for the BS. A summary of different models to calculate power consumption is presented as follows. Here, the power consumption for the BS  $b$  is denoted as  $P_{exp,b}$ .

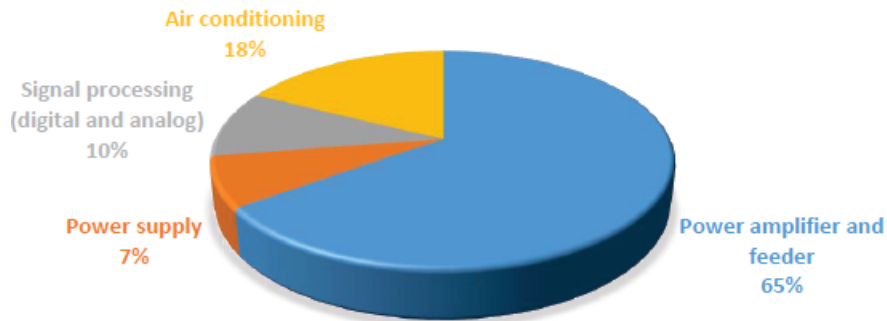


Fig. 2.1 Percentage of power consumption by different components of a large-cell BS [14].

### 2.3.1 Ideal load dependent PCM

The authors in [62] introduce an ideal load dependent power model with the assumption that the power cost by base station (BS) is proportional to the BS utilization (or loads). In other words, when a BS is utilized, it includes power consumption for transmitting antennas, power amplifiers, cooling equipment and so on. However, there is no power consumption for the BS in an idle state. Let  $\varphi_b$  denote the BS utilization and  $P_{tx}$  stands for the BS transmitting power. The equation of power consumption can be displayed as

$$P_{exp,b} = \varphi_b P_{tx}. \quad (2.6)$$

This is a relatively old model to quantify the power consumption of one BS, which assumes  $P_{exp,b}$  depending on the utilization of BS,  $\varphi_b$ . However, such a model is not realistic since the power consumption does not matter with BS utilization, as illustrated in Fig. 2.1.

### 2.3.2 Linear PCM

In [63], a linear/canonical power consumption model is employed as

$$P_{exp,b} = \zeta P_{tx} + P_{circuit}, \quad (2.7)$$

where  $\zeta$  is an inverse of the drain efficiency of transmitting amplifier and  $P_{circuit}$  is the total circuit power expenditure by radio frequency (RF) chain components (filters, mixers, and synthesizers) and baseband operations (digital up/down conversion, precoding, receiver combining, channel coding/decoding and channel estimation). The energy consumption of power amplifier is excluded in  $P_{circuit}$ , which is independent of the transmission state.

However, Eq. (2.7) tends to overestimate the system power consumption because they assume that the transmitting buffer is never empty during the whole transmission frame, which is not true since the transmitter has the idle state. Furthermore, given the consideration of Rayleigh fading scenario, where a signal will randomly vary or fade according to a Rayleigh distribution, it is not possible to have a deterministic estimation when the buffer becomes empty during the frame transmission.

### 2.3.3 PCM with sleep mode

When the traffic requirement of users is zero, it means there is no traffic load for the BS and the BS can be in sleep mode. However, the BS still uses some power. Therefore, [2] proposed a new power consumption model of one BS, expressed as

$$P_{exp,b} = \begin{cases} \rho_{load} P_{tx} + P_{active}, & \text{if } 0 < P_{tx} \leq P_{tx,max} \\ P_{sleep}, & \text{if } P_{tx} = 0 \end{cases} \quad (2.8)$$

where  $\rho_{load}$  denotes a constant coefficient depending on the traffic load,  $P_{tx}$  is the transmitting power of BS,  $P_{active}$  is the minimum power required to support BS with non-zero transmitting power,  $P_{tx,max}$  is the BS transmitting power at the maximum load and  $P_{sleep}$  accounts for the power consumption of the BS in sleep mode. Normally,  $P_{sleep} < P_{active}$  so that this power model is popular to be used while the switching on/off technology is adopted.

### 2.3.4 PCM with backhauling cost

In order to capture backhauling energy needs, the authors in [64] propose a general power consumption model,

$$P_{exp,b} = a \cdot P_{tx} + b \cdot P_{sp} + c \cdot P_{bh} \quad (2.9)$$

where  $P_{exp,b}$ ,  $P_{tx}$ ,  $P_{sp}$  and  $P_{bh}$  denote the average consumed energy per BS, the radiated power per BS, the signal processing power per BS, and the power due to backhauling, respectively. The coefficients  $a$ ,  $b$ , and  $c$  denote the scale with respect to the corresponding

power type amplifier and feeder losses, cooling, or battery backup. The three coefficients can be computed according to the parameters in [65]. This model assumes that all BSs are under full load, i.e., the energy consumption for an idle BS is not considered.

### 2.3.5 PCM considering non-empty buffer

A new average power consumption model is introduced in [66] which fully accounts for the non-empty buffer probability (NBP) and jointly optimizes both the transmitting power and the quality-of-service (QoS) exponent for the data link layer in a wireless point-to-point system, which is damaged by complex additive white Gaussian noise and block fading (the channel state is independent from one to another). The new power consumption model is thus formulated as:

$$P_{exp,b}(P_{tx}) = \zeta \cdot P_{rob} \cdot P_{tx} + P_{circuit} = \underbrace{\frac{R_{max,arri}}{\mathbb{E}_\gamma[\log(1 + P_{tx}\gamma)]}}_{P_{rob}} \cdot \zeta \cdot P_{tx} + P_{circuit} \quad (2.10)$$

where  $P_{rob}$  is the probability of non-empty buffer,  $\zeta$  is an inverse of the drain efficiency of transmitting amplifier,  $R_{max,arri}$  is the maximum constant arrival data at the physical layer of the transmitter,  $P_{tx}$  is the transmitting power and  $\gamma$  is the exponential random variable modeling the Rayleigh fading channel. This model is applicable for Rayleigh fading channel and data link layer regardless of the noise impact.

### 2.3.6 PCM with transmitting antennas

When considering the effect of the number of transmitting antennas, a novel linear model is presented in [65] as

$$P_{exp,b} = N_{ant} \cdot (\zeta P_{tx,PA} + L_{SP}) \cdot (1 + L_C) \cdot (1 + L_{PSBB}), \quad (2.11)$$

where  $N_{ant}$  denotes the number of antennas in the system,  $P_{tx,PA}$  refers to the transmitting power per power amplifier (PA),  $\zeta$  is an inverse of the power amplifier efficiency,  $L_{SP}$ ,  $L_C$ ,  $L_{PSBB}$  are the signal processing overhead, cooling loss, and battery backup and power supply loss, respectively. While the power consumption for direct current to analog current converters is neglected, this model gives an upper bound on the power consumption of a BS equipped with transmitting antennas.

In [59, 67], this model has been refined so that the power consumption of the other BS components, e.g., direct current (DC) and analog current (AC) converters, are also

included. Denoting  $N_{ant}$  as the number of antennas per BS,  $P_{tx}$  as the transmitting power per BS,  $\zeta$  as an inverse of the power amplifier efficiency,  $P_{fixed}$  as the non-transmission power consumption including baseband processing, battery backup, cooling, etc, the power consumption model is given as

$$P_{exp,b} = \zeta P_{tx} + N_{ant} P_{circuit} + P_{fixed}. \quad (2.12)$$

Even though this model takes into account the non-linearity of the power amplifier (PA), it has been illustrated that the relation between the relative radio frequency (RF) output power and the BS power consumption is nearly-linear. The given results show that the power consumption of components like DC-DC/AC-DC converter and cooling unit will not grow linearly with the number of antennas.

### 2.3.7 A refined double linear PCM

The refined double linear power consumption model (PCM) [68] is given by:

$$P_{exp,b} = N_{ant} \cdot (\Delta_P \cdot P_{tx,PA} + P_0) + P_1 \quad (2.13)$$

where  $\Delta_P = (1 + L_C) \cdot (1 + L_{PSBB}) / \mu_{PA}$ ,  $\mu_{PA}$  being power amplifier efficiency,  $P_0 = L_{SP} \cdot (1 + L_C) \cdot (1 + L_{PSBB})$ , and  $P_1$  is a fixed part accounting for the direct current (DC) and analog current (AC) converters.

## 2.4 Throughput models

In the below part, we will present some concepts like the network capacity  $C_n$ , the overall network throughput  $Th_{total}$ , area spectral efficiency  $SE_{area}$ , and the user achieved data rate  $R_u$ .

The network capacity,  $C_n$ , is defined as the maximum amount of data that may be transferred by one or multiple BSs. Additionally, the overall network throughput,  $Th_{total}$ , is defined as the sum of the data rates that are successfully delivered to all the terminals in a network. Particularly,  $Th_{total}$  equals  $C_n$  while Shannon formula is used, since Shannon formula is applied to compute the highest number of binary digits per second during the transmission.

In a MIMO uplink system, the authors in [69] define system network capacity  $C_n$  (measured by bits per second) based on Shannon capacity, which is related to the total

bandwidth of the network  $BW_n$  and network channel information, as given by

$$C_n = BW_n \log_2 \det(I + P H H^\dagger), \quad (2.14)$$

where  $H$  stands for the channel matrix between BSs and user terminals,  $I$  is the identity matrix and  $P$  represents the transmission power of each user terminal, and  $\dagger$  is the transposition operation. The matrix  $H$  characterizes the MIMO channel, where the fast fading, noise and interference are considered in the wireless communication. Specially, in the classical network without MIMO technology, the channel matrix  $H$  is a  $1 \times 1$  matrix.

The area spectral efficiency  $SE_{area}$  (measured over a unit area) is popularly used for the energy efficiency expression [16] in a low traffic demand case, as displayed by

$$SE_{area} = \lambda_n \mathbb{P}_n(\Gamma_{th}) \log_2(1 + \Gamma_{th}), \quad (2.15)$$

where  $\lambda_n$  denotes the BS density,  $\Gamma_{th}$  is a certain signal quality-of-service (QoS) threshold and  $\mathbb{P}_n$  stands for the coverage probability. The area spectral efficiency,  $SE_{area}$ , actually measures the network throughput,  $Th_{total}$ , while considering the coverage probability. The coverage probability  $\mathbb{P}_n$  can be computed by averaging the success probability over the distance to the nearest node. Specially, success probability is defined as  $\mathbb{P}(\gamma_{x \rightarrow u} > \Gamma_{th})$  when the signal-to-noise ratio (SNR)  $\gamma$  of the transmitting signal from the BS at  $x$  to the mobile terminal at  $u$  is above the threshold  $\Gamma_{th}$ .

Based on the knowledge of the instantaneous channel state information (CSI) [70, 71], the achieved data rate  $R_u$  by the user  $u$  is related to the allocated bandwidth  $B_u$  and to the received SNR,  $SNR_u$  at user  $u$ , displayed as

$$R_u = B_u \log_2\left(1 + \frac{SNR_u}{\Gamma}\right) \quad (2.16)$$

where  $\Gamma$  is the SNR gap between the channel capacity and a practical coding and modulation scheme. Specially,  $\Gamma$  equals 1 in Shannon formula.

Given that the feedback of the instantaneous CSI between each user and its serving base station is needed, a lot of expenses have to be paid by the operators and users. For this case, the statistical CSI is utilized and the achieved data rate  $R_u$  is rewritten in a statistical average sense [72], as

$$R_u = E_H[B_u \log_2\left(1 + \frac{SNR_u}{\Gamma}\right)], \quad (2.17)$$

where  $E_H$  stands for the expectation over the channel matrix  $H$ .  $R_u$  in Eq. (2.16) and Eq. (2.17) is measured in bits per second.

Based on the models of energy efficiency (EE), power consumption and throughput discussed before, much work have been studied on the EE performance in some literatures. According to the published papers, we found that most of the work on the energy efficiency (EE) investigation in wireless networks are conducted with the purpose either to evaluate the impact of some advanced techniques on the EE, or to define/design the parameters of these advanced techniques in order to optimize the EE. Therefore, a classification of the literatures on EE performance will be presented in the following section, according to these two objectives: EE evaluation and EE optimization.

## 2.5 Classification of EE models

As discussed in chapter 1, these advanced technologies are promising to be utilized so as to improve the network EE for the future radio communication networks, such as multiple-input multiple-output (MIMO), coordination multipoint (CoMP) scheme, heterogeneous cellular networks (HetNets), relay transmission and the on-off switching policy of base station (BS). Hence, we further categorize the evaluation-based related work and the optimization-based related work of EE according to these advanced technologies, in order to investigate the impact of these technologies on EE.

### 2.5.1 Evaluation-based related work

In this subsection, we further investigate the impact of these technologies, e.g., MIMO, CoMP, HetNets, Relay and BS switching on/off, on EE through the simulation results in some evaluation-based related work. Moreover, considering that most of the EE models are proposed at the hardware component level, the node level and the system or network level, we also discuss the evaluation-based related work according to the measurement levels.

#### – MIMO system

Many literatures focus on the investigation of the impact of MIMO technique on EE owing to the improvement of spectral efficiency brought by this technique. As an example, Ngo *et al.* [3] investigated the trade-off between EE and SE for a very large single-cell/multi-cell multiuser MIMO uplink system, where EE is defined as a ratio of the sum of data rates transmitted per user terminal over the transmitting power consumption of each user. The system EE,  $EE_{sys}$ , can be expressed as  $EE_{sys} = \frac{\sum_u R_u}{P_{exp,u}}$  bits/J, where  $R_u$  denotes the achieved data rate of user  $u$  equipped with single antenna, computed by Eq. (2.17), and  $P_{exp,u}$  is the total transmitting power consumption of user  $u$ , computed by Eq. (2.6). The

numerical results reveal the EE and SE can be improved through taking advantage of large antenna arrays with lower transmitting power regime, compared to a single-antenna system. However, the circuit power consumption in the power consumption model (PCM) is not taken into account. Additionally, when a realistic PCM is considered, Fabien Heliot *et al.* [68] presented a novel and generic closed-form approximation of the trade-off between EE and SE over a MIMO Rayleigh fading channel, where EE-SE trade-off can be regarded as a problem of expressing EE by SE. Based on the energy consumption index (ECI), as defined in Eq. (2.3), and a more realistic PCM, as defined in Eq. (2.13), the approximation accuracy is assessed. Through a comparison of EE gain between in MIMO and SISO systems over Rayleigh fading channel, the simulation results show that EE is not always improved with the increase of SE and the number of antennas. Indeed, MIMO system will consume more circuit power and more signaling overhead with numerous antenna configurations, resulting that the practical EE gain decreases with the number of transmitting antennas.

In a nutshell, for the purpose of increasing EE, it is very important to choose an appropriate number of antennas in the future MIMO system.

#### – CoMP system

Fabien Heliot *et al.* [73] analyzed the EE of both uplink and downlink in a idealistic CoMP communication system, through assuming perfect backhaul links between each BS and an idealistic cooperative processing. EE is defined as a ratio of the channel capacity, as defined in Eq. (2.14), to the system consumed power, defined in Eq. (2.11). Numerical results demonstrate that multi-BS cooperation can improve the EE when the link quality between the BSs and MSs is weak, e.g., cell-edge communication, and that the backhauling and cooperative processing power should be kept low in order to provide EE gain. However, in that paper, the numerical results are obtained based on the assumption that the power consumption required for backhaulings and cooperative multiple BSs is regarded as a constant, which is not realistic.

In contrast, considering the realistic backhauling power consumption model, the work in [74] investigated the EE for a Beyond-LTE cellular network through taking advantage of the cell switch-off scheme and JT-CoMP transmission technology. EE is defined as the ratio between the received capacity of one user, defined in Eq. (2.14), and the total access network power consumption, defined in Eq. (2.9). Through simulations with realistic parameters, the results show that the CoMP scheme used jointly with the cell switch off schemes is more energy efficient in the access networks. Specially, setting a proper number of coordinated BSs, namely CoMP set degree, is very important in terms of energy efficiency. A higher CoMP set degree may cause a decrease in energy efficiency performance due to

signaling and backhauling overhead in the network. Meanwhile, taking advantage of the CoMP scheme, the authors in [64] also evaluated the EE for a cellular network and the numerical results indicate that CoMP technique can not bring benefit to the energy efficiency when CoMP set degree is above three, due to the additionally required backhauling power for the cooperative set.

Unlike the conventional cellular networks powered by on-grid energy, Abu Jahid *et al.* [75] proposed a novel network model to evaluate EE for a downlink LTE-A cellular hybrid system, powered by both on-grid energy and solar energy. The EE is defined as the ratio of aggregate throughput of the network, defined in Eq. (2.16), to the total power required for running the network, defined in Eq. (2.12). This model is utilized in two scenarios: 1) SINR-based JT-CoMP and 2) distance-based JT-CoMP. In SINR-based JT-CoMP technique, the best two BSs offering maximum SINR are serving a user and in distance-based JT-CoMP one, two closest BSs are intended to serve a user. Simulation results illustrate that the proposed SINR-based JT-CoMP scheme achieves a superior EE performance compared to the distance based JT-CoMP hybrid model.

Overall, CoMP technology can be used to improve the EE for the future wireless communication networks, through setting an appropriate number of coordinated BSs for the cooperative set.

#### – HetNet

From the BS deployment point of view, the EE evaluation is investigated in a cellular network [58], in an interference-limited heterogeneous cellular mobile radio networks [76], in a 5G wireless network [77] and in an ultra dense HetNets [78], respectively, so as to illustrate the impact of different types of BSs deployment on EE.

The authors in [58] studied the impact of deployment strategies on the area power consumption, through deploying varying numbers of micro BSs in a macro cell. The area power consumption (APC) is defined as the ratio between the average power consumption per cell, formulated in Eq. (2.7), and the corresponding cell area. The definition of area spectral efficiency, as the achievable data rate in a network per unit bandwidth per unit area, measured in bit per second per Hertz per square kilometer, is also demonstrated so as to find the minimum area power consumption. The numerical results reveal that the area spectral efficiency can be increased through improvement of the density of micro BSs, whereas the area power consumption is moderate with the raise of the number of micro BSs in the full traffic load scenario. Since the deployment of additional micro BSs per cell increases the average power consumption per cell, resulting the increase of the area power consumption.

Additionally, with random micro BSs deployment and ‘bits/J’ as the EE metric, Henrik Klessig *et al.* [76] investigated the EE of a heterogeneous OFDM-based mobile network while taking into account the co-channel interference by varying traffic demand per area. The EE is defined as the ratio between the actual throughput of the reference area, defined in Eq. (2.16), and the total power consumption, defined in Eq. (2.7). The simulation results indicate that a EE gain of about 20% can be achieved through increasing deployment density of micro BSs, since the area spectral efficiency is enhanced and the transmitting power of macro BSs is reduced with the micro BSs deployment, while still providing coverage. Comparing to the work in [58] for the full traffic load scenario, this network EE model can be applied in both non-full load scenario and hot spot scenario.

Unlike the work in [58, 76] with micro BSs deployment in macro, Safdar Rizvi *et al.* [77] investigated the EE of a 5G HetNet when small BSs (pico, femto) are deployed in the macro cells. The EE is defined as a ratio of the maximum data rate of the network, defined in Eq. (2.16), over the total power consumption, defined in Eq. (2.7). The numerical analysis have confirmed that EE is enhanced in 5G HetNet when the number of small BSs, i.e., pico and femto, is increased in a rational manner. Additionally, [78] investigates the impact of BS deployment on EE using the stochastic geometry theory and derives a closed-form EE with respect to the BS deployment in an ultra dense HetNet where the pico BSs are deployed in the macro cells. The network EE is defined as the ratio between the minimum achievable throughput, defined in (2.15), and the total power consumption of the whole network, defined in Eq. (2.6). Numerical results show that with the increasing number of pico BSs, EE first increases and then decreases due to the rise of power consumption caused by the increment of pico BSs.

Overall, in the HetNets, the density of small cell BSs should be designed carefully in order to obtain the maximum network EE.

### – Relay system

The energy consumption in relay systems is also investigated. Roberto Fantini *et al.* [79] presented an analysis of the energy efficiency (EE) from the view points of two relay schemes: two hop scheme and the multicast cooperative scheme. The division of the two schemes is based on whether the relay node (RN) creates cell of its own or not. According to the observed numerical results in terms of energy consumption index, energy can be saved up to 15.6% in the two-hop relay scheme. RN can be as an effective tool to reduce the energy consumption in telecommunication networks and achieve a great improvement on the capacity.

### – BS on/off

Taking into account the BS on/off strategy, Chang Li *et al.* [67] investigated the effect of the BS density and number of transmitting antennas on the network throughput and energy efficiency in a random cellular network where all BSs are micro-BSSs equipped with multiple antennas. According to whether the BSs have users to serve, the BSs can be divided into active BSs and inactive BSs. The inactive BSs do not transmit any signals. The network EE, measured in  $\text{bit}/\text{J}/\text{Hz}$ , is defined as the the network throughput to the power consumption per unit area, defined in Eq. (2.12). Specially, the power consumption per unit area includes the power consumption from both the active and inactive BSs, constituted by the transmitting power, the circuit power of the corresponding radio frequency chain and the non-transmission power consumption, including baseband processing, battery backup, cooling, etc. The simulation results show that 1). EE first increases and then decreases with the increase of BS density when the ratio of non-transmission power cost to the total BS power consumption is smaller than a given value. Otherwise, EE decreases as BS density increases. 2). EE first increases and then decreases with the increase of the number of BS antennas, when the non-transmission power consumption is smaller than a given threshold value. Otherwise, EE of a single-antenna system is better that of a multi-antenna system.

Therefore, the different components of BS power consumption play a critical role in the EE when the technology of BS switching on/off is applied.

### – MIMO + CoMP

However, with increasingly demanding of EE, only utilizing an advanced technology is not enough to satisfy the energy-efficient design. Therefore, some existing publications have investigated the EE through taking advantage of multiple advanced technologies.

The work in [80] derived a closed-form approximation (CFA) of the EE-SE trade-off for the uplink of a CoMP system with MIMO Rayleigh fading channel. The network EE,  $EE_{sys}$ , is defined as a ratio of the sum rate of all UEs, defined in Eq. (2.17), over the total power consumption, defined in Eq. (2.9), given as  $EE_{sys} = \frac{\sum_u R_u}{\sum_u P_{exp,u}}$  bits/J.  $R_u$  and  $P_{exp,u}$  denote the achieved data rate and the total transmitting power consumption of user  $u$ , equipped with multiple antennas. The simulation results show that in a realistic PCM, CoMP system is more energy efficient than a non-cooperative system due to the improvement in SE and mainly for cell-edge communication. However, EE decreases with the increase of the number of cooperating BSs, since the backhauling and processing power consumption brought by CoMP technique is increased.

All the literatures discussed above validate that the advanced technologies can increase the network capacity and improving system EE for the wireless network through theoretical analysis and simulation results. Table 2.2 summarizes the classification discussed above according to the advanced technologies. More general and comprehensive information can be found in that table.

Table 2.2 Classification of evaluation-based related work

Tech.	Model	Measure. level	Up/ Down-link	Comments
MIMO	Bit-per-Joule [3], Energy consumption index (ECI) [68]	Node	up, down	MIMO can improve EE without considering circuit power consumption by antennas [3]; MIMO can not improve EE with ultra-multiple antenna configurations and a realistic PCM [68]
CoMP	Bit-per-Joule [64, 73–75]	System, system, node, system	both, both, down, down	All work indicate the improvement of EE with CoMP. However, a constant backhauling power cost is assumed [73]; the power consumption of solar energy is included [75]; [64, 74] illustrates the size of cooperative set above three can't improve EE
HetNet	Area power consumption (APC) [58], Bit-per-Joule [76–78]	System	down	All work illustrate that HetNet deployment can improve EE. However, deployment of micro, macro BSs [58, 76]; pico, femto and macro BSs [77]; pico, macro BSs [78]
Relay	ECI [79]	Node	down	Rely can reduce energy consumption and a two-hop scheme is more efficient
BS on/off	Bit-per-Joule-Hz [67]	System	down	EE increases with the raise of BS density and the number of BS antennas when the power consumption of BS component satisfy certain conditions
MIMO + CoMP	Bit-per-Joule [80]	System	up	Discussed EE-SE trade-off problem and appropriate number of cooperating BSs can lead EE improvement

### 2.5.2 Optimization-based related work

Appropriate performance EE models are of primary importance for the design of green wireless communication networks, because they are directly related to the choice of the optimization objectives and the constraints of the corresponding optimization problems.

Based on the throughput models, power consumption models (PCMs) and the EE models discussed before, we found the existing literatures investigate the optimization of EE either from a power minimization perspective or data rate maximization perspective. Therefore, an overview of EE maximization is presented below regarding these two perspectives. Considering that all EE-optimization problems are proposed based on some advanced technologies, such as HetNet, BS switching on/off strategy, CoMP, MIMO, and relay, in this subsection, we further classify the optimization-based related work on EE according to these advanced technologies.

#### – Power optimization

From the power perspective, the EE maximization problem can be transferred to minimize the total power cost, expressed as

$$\begin{aligned} \min \quad & P_{total} \\ \text{s.t.} \quad & \gamma_k \geq \gamma_D, \quad P_{tx} \leq P_{tx,max} \end{aligned} \tag{2.18}$$

where  $P_{total}$ ,  $P_{tx}$ ,  $P_{tx,max}$  represent the overall power consumption, the transmitting power per BS and the maximum transmitting power per BS, respectively,  $\gamma_k$ ,  $\gamma_D$  is respectively the achievable data rate of the  $k$ th UE and the fixed quality-of-service (QoS) target for every user. Taking advantage of these advanced technologies and based on the Eq. (2.18), we present some related work of EE optimization in the below part and introduce the specific concepts of the total power consumption in different literatures.

##### i). HetNet

An investigation of the impact of BS's density and the transmitting power on the network energy consumption is presented in [81] for both homogeneous and heterogeneous networks. The total power consumption  $P_{total}$  is computed as  $\lambda_n^{macro}P_{exp,b}^{macro} + \lambda_n^{micro}P_{exp,b}^{micro}$ , where  $\lambda_n^{macro}$  and  $\lambda_n^{micro}$  account for the density of macro and micro BSs, respectively,  $P_{exp,b}^{macro}$  and  $P_{exp,b}^{micro}$  are the total power consumption of macro and micro BSs, as defined in Eq. (2.7). The numerical results show that the heterogeneous deployment is one of advanced technology to improve the network EE.

### ii). HetNet + BS on/off

Taking advantage of some dynamic sleeping strategies of BSs and the tool of stochastic geometry, the optimization problem of network EE is investigated for dense cellular networks [82] and for a 5G HetNet [83]. Unlike the conventional HetNets, the HetNet architecture in the two literatures is separated into the control and data planes, where a macro BS manages control signal and low data rate traffic and small BSs, e.g., pico, micro and femto BSs, manage only the high data rate traffic. The optimization objective  $P_{total}$ , in the two literatures are given as  $P_{total} = \sum P_{exp,b} \lambda_n$  and  $P_{total} = P_{exp,b}^{macro} + P_{exp,b}^{small} + P_{switching}$ , respectively, where  $\lambda_n$  denotes the spatial density of BSs,  $P_{exp,b}^{small}$  is total power cost by small cell BSs,  $P_{switching}$  is the power cost owing to switching states of BSs and  $P_{exp,b}$  is computed by Eq. (2.8). The numerical results in [82] and [83] reveal that the separated network architecture is a better energy-efficient solution compared to the conventional HetNet architecture. However, the difference between [82] and [83] is that the former only considered the constraints of power control and quality-of-service (QoS) at UEs, while the latter also covers the delay constraint.

### iii). MIMO + HetNet

In [84], a combination of two densification approaches, massive MIMO BS and small-cell access points (SCAs), is considered to minimize the total power consumption, including dynamic emitted power and static hardware power, while satisfying quality-of-service (QoS) constraints for the users and power constraints for the BS and SCAs. The power consumption model is calculated by Eq. (2.7). Nevertheless, the beamforming vectors is regarded as optimization variables in that work. The simulation results show that the network EE can be improved by employing massive MIMO at the BSs or deploying some small cells. However, EE can reach a saturation point by combining massive MIMO and small cells due to the additional power consumption coming from the extra hardware.

### iv). CoMP + BS on/off

The study in [85] designed energy-aware cooperation strategies for green cellular networks in order to ensure the system energy-saving while satisfying UE traffic demands. Specially, a heuristic algorithm is proposed to cope with sleep-mode of BSs and cooperate among active BSs. The power consumption is computed by Eq. (2.12), which includes the dynamic serving power consumption of a BS, corresponding to the number of downlink channel resource blocks allocated to each UE served by this BS. Compared to the conventional system where all BSs are on, the simulation results

demonstrate that the heuristic algorithm is outperformed under any kinds of traffic loads, for instance, energy can be saved about 60% in low-load scenario and about 30% in high-load scenario.

In fact, Eq. (2.18) only reflects the minimization of power consumption in the system and the total volume of data transferred by this power is not presented apparently. Therefore, in what follows, we present some literatures which investigate the EE maximization problem from the perspective of data rate.

### – Data rate optimization

Regardless of the technology used in the wireless network, the most widely-used EE model for the optimization problem is Bit-per-Joule. While satisfying the constraints of power control and data rate, the general formula for the energy optimization problem is expressed as

$$\begin{aligned} \max \quad & EE_{sys} = \frac{R_{total}}{P_{total}} \\ \text{s.t.} \quad & 0 \leq P_{tx} \leq P_{tx,max}, R_{total} \geq R_{th} \end{aligned} \quad (2.19)$$

where  $P_{total}$  denotes the overall power consumption in the system,  $P_{tx}$ ,  $P_{tx,max}$  represent the transmitting power per BS and the maximum transmitting power per BS, respectively,  $R_{total}$  is the maximum amount of data,  $R_{th}$  accounts for the data rate requirement. Through taking advantage of the common optimization formula of Eq. (2.19), in the following part, an overview of the optimization-based related work is present according to some advanced technologies in order to investigate their impact on EE. We also explain the different concepts of the optimization goal in literatures.

#### i). MIMO

The EE maximization problem is investigated for a uplink multi-user MIMO system [70], for a downlink multicell multiuser multiple-input single-output (MU-MISO) system [86] and for a uplink and downlink of single-cell multi-user MIMO system [38], respectively. In [70], the total data rate and the power cost are computed by Eqs. (2.16) and (2.7), respectively. Based on the knowledge of instantaneous CSI, the EE maximization can be achieved through a low-complexity optimal power allocation algorithm. The numerical results demonstrate that EE of MU-MIMO can be improved with a circuit management strategy where users can choose to turn off electronic circuit operations when some antennas are not utilized. In particular, both electronic circuit and radio frequency (RF) transmission power consumption are taken into account in the single cell environment. However, the priority of UEs is

not considered. Through introducing a weight coefficient characterized the priority of UEs in [86], the EE is defined as the ratio between the weighted sum data rate of all users, defined in Eq. (2.14), and the system overall power consumption, defined in Eq. (2.12). A two-layer optimization scheme is proposed to solve the non-convex fractional problem of EE optimization. Numerical results illustrate that the proposed scheme has a fast convergence and can achieve near-optimal EE.

However, the total EE for the uplink and downlink system in [38] is defined as a ratio of the average sum rate, defined in Eq. (2.14), to the average overall power consumption of the system, defined in Eq. (2.7). The optimal solution of EE is obtained through selecting the appropriate optimization variables, e.g., the number of BS antennas, the number of active user equipments, and the achievable rate per user in a single-cell scenario with perfect channel state information (CSI). The numerical results show that massive MIMO technology (deploying large number of low-power antennas at BSs) is an effective method to achieve the EE maximization. Typically, different from the normal linear PCM, the circuit power cost includes the power consumption of the channel estimation process, power consumption of the channel coding and decoding unit, and power consumption of the linear processing by one BS. Unlike the previous work, the authors also analyzed the EE optimization in the single-cell scenario with imperfect CSI and in the multi-cell scenario with perfect CSI.

### ii). MIMO + HetNet

Taking advantage of the tool of stochastic geometry, the work in [60] discussed the uplink EE maximization problem for a dense heterogeneous MIMO cellular network, where BSs configured with massive antennas are distributed according to a homogeneous Poisson point processes (PPP) and UEs equipped with single antenna are uniformly distributed. The EE model of Bit-per-Joule-Hz, as defined in Eq. (2.4), is utilized to replace Bit-per-Joule metric in Eq. (2.19). The Eqs. (2.14) and (2.12) are used to compute the data rate and the system power consumption, respectively. The numerical results show that the maximum of EE can be achieved through adding extra BS antennas, such as a massive MIMO setup with 91 antennas per BS and 10 UEs. Typically, the area power consumption includes the power cost of radiated amplifier antenna, of BS transceiver chains, of the signal processing, coding and decoding of UEs.

### iii). MIMO + CoMP + Relay

Unlike most previous related works, in [87], a unified framework of power allocation

policies is proposed to maximize the global energy efficiency (GEE), defined as the ratio between the sum achievable rate and the total consumed power, as well as to minimize the weighted EE for users in a 5G uplink wireless network while taking advantage of the emerging techniques of OFDMA, MIMO, CoMP and relay transmission. The total data rate and the power cost are computed by Eqs. (2.16) and (2.7), respectively. The numerical results analyze the impact of minimum-rate constraints on the algorithm, which is proposed to guarantee GEE convergence. However, they assume that one or more resource blocks are exploited for data transmission.

#### iv). CoMP

Based on the tool of Poisson point process (PPP), EE maximization is investigated for a downlink coherent JT-CoMP network [88] while considering the circuit power and non-ideal power amplifiers (PAs), and for a downlink CoMP network [89] while exploiting the power efficient cache hardware at BSs. Specially, in [88], EE is defined as the ratio between the number of overall data bits transmitted, defined in Eq. (2.16), and the total energy consumed by all nodes, defined in Eq. (2.12). The numerical results show that EE can be promoted by the application of power allocation. Unlike other PCM where the power consumption is only devoted to the BSs, the total power consumption in [88] comes from both of BSs and UEs.

Moreover, the network EE in [89] is defined as the ratio between the average network throughput  $R_{ave}$ , defined in Eq. (2.16), and the average total power consumption  $P_{exp,ave}$ , defined in Eq. (2.9). The numerical results show EE maximum can be obtained through optimizing cache capacity of each BS. In particular, the total power consumption includes the power cost at BS for transmitting, for operating the baseband and radio frequency circuits, for caching and backhauling, and for cooling and power supply.

Additionally, a distributed power optimization scheme based on max-min weighted EE in [90] is proposed with quality-of-service (QoS) constraint in a downlink CoMP system, which is based on limited intercell coordination. The authors convert the optimization problem to a standard form of max-min fractional problem and Eq. (2.16) is used to compute data rate. Simulation results show that the proposed scheme can significantly improve the minimum EE. Typically, unlike the common PCM of Eq. (2.9), the power cost is computed by  $P_{tx} + P_{circuit} + P_{bh}$ , where the additional backhauling power cost  $P_{bh}$  for supporting CoMP is regarded as a constant.

v). CoMP + HetNet

In [91, 92], authors investigate the problem of EE optimization in an OFDMA downlink HetNet using CoMP transmission while applying a realistic power consumption model and considering the quality-of-service (QoS) constraint. The network EE is defined as a ratio of total system throughput, defined in Eq. (2.16), to the total power consumption, defined in Eq. (2.12). Unlike the general HetNet, the authors define a novel HetNet CoMP system, which is composed of many HetNet cell. Each of HetNet cell includes one centralized macro BS, several small BSs and many UEs. The centralized macro BS can cooperates with multiple small BSs in the same HetNet cell as well as other macro BSs located at different HetNet cells. Simulations results illustrate that there is a tradeoff between EE and SE. Typically, the power consumption of backhaul links is considered.

Moreover, unlike the above HetNet, the authors in [93] design a JT-CoMP precoder for the purpose of EE maximization while guaranteeing the data rate requirement of each UE in a HetNet, where several pico-BSSs are located in the coverage of a macro-BS and the two kinds of BSs jointly serve multiple UEs with the same time frequency resource. The network EE can be defined as a ratio of the total achievable data rate of all UEs, obtained by Eq. (2.16), over the total power consumption of the HetNet, defined in Eq. (2.7). The simulation results show that the optimal EE can be achieved through the proposed JT-CoMP precoder scheme. However, the power consumption for backhauling links between the macro-BS and the pico-BSSs, and the interference among the pico-cells is ignored in that literature.

vi). CoMP + BS on/off

Based on the stochastic geometry, the work in [94] investigated one network performance metric, named energy-spectral efficiency (ESE), for the dense large-scale cellular networks through taking advantage of the advanced technologies of CoMP transmission and BS switching on/off scheme. Additionally, a closed-form expression of ESE is proposed with some network parameters, e.g., CoMP activation factor, BS-density, mobile-traffic intensity, system bandwidth and average data rate requirement. Numerical results show that the maximization of ESE is obtained through jointly optimizing the CoMP activation factor and the BS density while considering the constraint of users' outage probability. Typically, unlike the previous EE model, the network ESE is measured by bit/Hz/Joule, and defined as a ratio of the total throughput of users per unit area to the overall power consumption  $P_{total,b}$  multiplied by the system bandwidth  $BW_n$ , expressed by  $ESE = \frac{\rho_u \times R_u}{P_{total,b} \times BW_n}$ , where  $\rho_u$  is the density of users.

### vii). HetNet + BS on/off

Based on the tool of stochastic geometry, the optimization of EE is proposed in [95] for a HetNet employing two sleep strategies for the small cell BSs, namely random sleeping policy and strategic sleeping policy. In the random sleeping policy, the small cell BSs are divided into four modes with some probability, i.e., on, off, sleep and standby. Instead of randomly operating small cell BSs, BSs are chosen to sleep according to traffic load in the strategic sleeping policy. The EE metric is defined as the ratio between the overall throughput per unit area, defined in Eq. (2.16), and the total power consumption of BSs. Power consumption model (PCM) is given as  $P_{tx} + P_{MP} + P_{RF} + P_{FPGA}$ , where  $P_{tx}$  accounts the transmitting power of BSs,  $P_{RF}$  is the power cost of the amplifier and radio frequency transmitter,  $P_{MP}$  denotes the power cost of a microprocessor for the purpose of managing the standardized radio protocols and associated baseband,  $P_{FPGA}$  is the power consumption of the field-programmable gate array (FPGA) with other integrated circuitry in order to support a range of functions, including data encryption, hardware authentication, and network time protocol. The simulation results show that there are about 30% improvement in EE with random sleeping policy and about 15% improvement with a strategic sleeping policy. Different from the common EE metric in Eq. (2.19), the transmitting power is assumed as a constant proportion of the total power consumption, which neglects the instantaneous transmitting power varying with the instantaneous traffic load.

Moreover, the authors in [16] also investigated the optimization of EE and the power consumption minimization in HetNets through the deployment of different sleeping policies and small cells. The EE is defined as a ratio of the area spectral efficiency, defined in Eq. (2.15), over the average network power consumption,  $P_{ave,exp}$ , computed by  $P_{ave,exp} = \lambda_n P_{exp,b}$ .  $\lambda_n$  is the density of macro BS. The numerical results illustrate that the EE improvement is related to the sleeping strategy used and that the deployment of small cells generally leads to higher EE but this gain saturates as the density of small cells increases.

All these optimization-based related work validated that EE improvement can be achieved through using some advanced technologies. Alternatively, according to these related work, we also find that even if the same technology is used in the wireless networks, different EE model can be chosen while considering some constraints, such as power control, quality-of-service (QoS) of UEs and delay constraint. The key is to develop an effective and low-complexity algorithm or scheme so as to obtain the optimal solution of EE. A classification of EE optimization problem proposed in literatures is presented in Table 2.3, according to these advanced technologies mentioned before.

Table 2.3 Classification of optimization-based related work

Power	Technique	Up/ Down-link	Constraints Power, QoS, delay	Comments
	HetNet [81]	down	Power, QoS	Minimize the APC through joint BS density and BS transmission power optimization strategy [81]
	HetNet+ BS on/off [82, 83]	down	Power, QoS; Power, QoS, delay	Improving EE with a separated Het-Net in [82, 83]. Power cost related to BSs' density [82] and covering power cost for switching states of BSs [83]
	MIMO+ Het-Net [84]	down	Power, QoS	Achieving high EE with beamforming variable [84]
	CoMP+ BS on/off [85]	down	Power	Using a strategy of changing the number of coordinated BSs according to traffic demands
Data rate	MIMO [38, 70, 86]	up, down, both	QoS; Power; Power	Considering power cost of channel coding and decoding unit [38]; Turning-off UEs electronic circuit [70]; Considering priority of serving UEs [86]
	MIMO + Het-Net [60]	up	Power, QoS	Using Bit-per-Joule-Hz model
	MIMO + CoMP + Relay [87]	up	Power, QoS	To maximize the globle EE and minimize individual EE per UE
	CoMP [88–90]	down	Power, QoS; –;Power	Power cost devoted by BSs and UEs [88], by BS caching [89]. Backhauling power cost as a constant [90]
	CoMP + Het-Net [91–93]	down	Qos; Qos; Power, QoS	Considering backhauling power cost [91, 92]. Ignoring pico BSs interference and backhauling power cost [93]
	CoMP + BS on/off [94]	down	QoS	Proposing a novel energy-spectral efficiency (ESE) model
	HetNet + BS on/off [16, 95]	down	QoS,delay; QoS	Total power cost related to density of BSs [16]; Including power cost of FPGA [95]

## 2.6 Conclusion

According to the related work on EE evaluation and EE optimization in the above section, it can be found that different EE models can be used in wireless communication networks. Moreover, different PCM and throughput models can be selected to compute the network EE even if the same network is set up and the same EE metric is used in different literatures. Typically, we found that the Bit-per-Joule metric is the most widely-used EE model, since it reflects the energy required to handle the traffic and it can be applied at the different measurement levels, such as at the component, node and system levels. Therefore, considering its simplicity and popularity of the Bit-per-Joule metric, we will use this metric throughout the PhD thesis.

Alternatively, through comparing the numerical results between these related work, we also find that those 5G technologies candidates of MIMO, CoMP, HetNets, relay and BS switching on/off strategy can enhance the network EE, which is consistent with the theoretical discussion on technologies, as mentioned in chapter 1. Nevertheless, these technologies must satisfy certain conditions so that they can improve the system EE. For instance, 1) MIMO technique can bring EE improvement with using the appropriate number of antenna configuration, since the excessive number of antennas may bring additional circuit power consumption. 2) CoMP technique can improve EE when the number of coordinated BSs does not exceed three, since the additional power consumption for backhauling increases as the raise of the number of coordinated BSs. 3) While utilizing the HetNet technique, it is very important to choose the appropriate density of small cell BSs so as to obtain the maximum of EE. 4) For achieving the optimal EE in the system, it is the key to develop a suitable sleeping policy for BSs and to chose the appropriate density of BSs, while the BS switching on/off technique is applied.

The basic concepts of EE, PCM and throughput models discussed in the related work provide the background and fundamental knowledge of EE, which helps us to propose our own EE model. Additionally, we find that most of the above related work on EE for the CoMP system is based on intractable models, which needs a lot of time and huge resources to conduct simulations. Hence, how to develop an accurate and tractable model for EE evaluation is still an interesting issue with considering the CoMP technique. Furthermore, some works have shown that a tractable network model, namely fluid modeling, can be used to evaluate performance of JT-CoMP. Motivated by that work, how to develop a tractable EE model based on this fluid modeling and Bit-per-Joule metric is also an open issue. In this regards, the main objective of the present thesis is to develop a tractable EE model

based on the fluid modeling and to investigate the joint impact of shadowing and path-loss exponent on EE in a wireless cellular network and in a CoMP system.

Finally, we summarize this chapter. This chapter provides an overview of the EE models which are exploited in most of the literatures. We first listed some EE models based on different EE definitions. Given that the EE models are closely related to the throughput and power consumption models, then we introduced the power consumption models and the throughput models. Moreover, based on EE-evaluation and EE-optimization, a catalog of the EE-related work is presented, which illustrates that different EE models can be used in the various networks and that the 5G promising technologies and their technical parameters have an important impact on EE.

In the next chapter, we will present the system model and our EE model based on the aforementioned PCM and EE metric in order to analyze the network performance.



# Chapter 3

## System model

### Contents

3.1	Introduction	47
3.2	System model for the thesis	48
3.2.1	Energy efficiency definition	49
3.2.2	Power consumption model	50
3.2.3	Data rate ( $D_{area}$ ) over a network area	50
3.3	Overview of fluid modeling	51
3.3.1	Notations	51
3.3.2	SINR in the hexagonal network	52
3.3.3	SINR in fluid network model	53
3.4	Accuracy of fluid model	54
3.4.1	Simulation process	54
3.4.2	Discussion of results	55
3.4.3	CDF results	57
3.4.4	SIR vs network range	58
3.5	Conclusion	59

---

### 3.1 Introduction

With the progress towards 5G wireless network, energy efficiency (EE) has become one of the key design criterion for future wireless communications. As shown in the previous chapter, the EE models are utilized to evaluate and optimize this metric. It is observed that the Bit-per-Joule metric is the most popular model for evaluating EE due to its definition of

a ratio between the throughput or capacity and the power consumption. Therefore, taking advantage of this EE definition, the purpose of our work is to propose a mathematical framework for a downlink transmission network in order to evaluate the network EE based on a so-called fluid modeling.

The spatial fluid modeling is an approximation approach for networks, where the interfering BSs are replaced by a continuum of infinitesimal interferers [96]. Unlike a Poisson network model where the distribution of all BSs is assumed following a Poisson point processes distribution with a BSs density, the fluid modeling is tractable due to the below assumption. Given the inter site distance (ISD) between two BSs, the interfering BSs, consisted by a given finite number of BSs, are regarded as a continuum of transmitters with a BSs density, which can be denoted using ISD. This means that the transmitted interference power is considered as a continuous field over the entire network. Then, the total interference power of a UE with fixed distance to its serving BS can be easily calculated by integrating. Based on this model, Kelif *et al.* proposed analytical formulas for the signal-to-interference-plus-noise ratio (SINR) in HetNets [97] and in a Poisson wireless network [98], and for outage probability in cellular networks [96]. Furthermore, taking advantage of this model, the paper [99] investigated the impact of coordination between BSs in a dense area. In addition, authors in [100] also developed a tractable expression of the total cell data rate and investigated its variations considering various frequency reuse and scheduling schemes in an OFDMA cellular network. All these work highlighted the benefits of this modeling method as it reduces considerably the analysis complexity and provides a macroscopic evaluation of the network performance.

Spurred by the tractable advantages of spatial fluid modeling, the goal in this chapter is to develop a tractable analytical expression of EE-evaluation based on this fluid framework. This expression will be used throughout all the thesis work. First, system model is introduced to provide the main network environment under consideration. In particular, we discuss in detail the EE definition and the power consumption model we used. Further, we illustrate how to compute the SINR in the hexagonal network and in the fluid one, respectively, since SINR is the basic parameter to compute the data rate and EE. Finally, we discuss some simulation results in order to prove the accuracy of fluid modeling.

## 3.2 System model for the thesis

In this thesis, we consider a downlink transmission of an OFDMA cellular network, composed of  $N_{BS}$  base stations (BSs) and  $N_u$  user equipments (UEs) randomly distributed over the network. Since the radio resources of each BS are divided into many parallel and orthogonal

sub-carriers, only inter-cell interference is considered. In the system, the integer frequency reuse (IFR) 1 scheme is used, which means all the subcarriers allocated in one cell can be utilized anywhere regardless of UEs' location. For frequency reuse 1, the cell bandwidth equals the network bandwidth  $BW_n$ , as shown in Fig. 3.1. Here, an equal bandwidth scheduling scheme is taken into account. Thus, all UEs are assigned the same bandwidth whatever the spectral efficiency is available to them. We assume an homogeneous network such that the transmission power  $P_{tx}$  is same for every BS equipped with an omni-directional antenna.

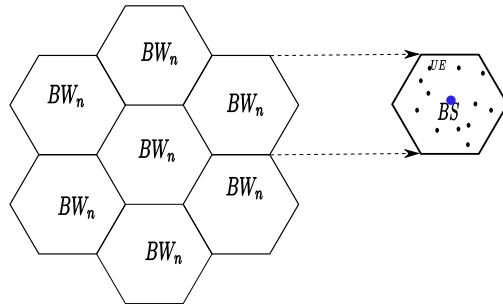


Fig. 3.1 Cellular network with an integer frequency reuse (IFR) 1 scheme

### 3.2.1 Energy efficiency definition

In our thesis, we chose the classical Bit-per-Joule metric as the energy efficiency (EE) model, as illustrated in Eq. (2.5) of chapter 2, since it is the most popular model to evaluate EE in the telecommunication networks. Given that the Bit-per-Joule capacity indicates the amount of energy consumed for transmitting information, here we consider the common definition of EE as the ratio of total data rate  $D_{area}$  over a network area to the total power consumption:

$$EE = \frac{D_{area}}{N_{BS} \times P_{exp}}, \quad (3.1)$$

where  $P_{exp}$  is the total energy expenditure per BS and  $N_{BS}$  denotes the total number of BSs in the system.

According to Eq. (3.1) and as stated in [37, 78, 95], EE is not only related to the data rate but also depends upon the BS power consumption. This EE model served to assess the performance of the heterogeneous networks (HetNets) under different sleeping policies [16], and to review the impact of BS density on EE in [78]. The numerical results in [78] shown that the network EE first increases and then decreases with the increasing number of pico BSs, due to the rise of power consumption. We will introduce how to compute the

power consumption  $P_{exp}$  per BS and the total data rate  $D_{area}$  based on the fluid modeling in the below part.

### 3.2.2 Power consumption model

Here, we consider a realistic double linear power consumption model (PCM) [68], as defined in Eq. (2.13) (already been introduced in the second chapter). Since, this PCM covers the most of the energy consumption in the system, such as the power cost by the transmitting antenna, the baseband processing, the cooling system, the battery backup, the power supply and the direct current (DC)-DC and analog current (AC)-DC converters.

The double linear PCM is defined as

$$P_{exp} = N_{ant}(\Delta_p P_{tx} + P_0) + P_1, \quad (3.2)$$

where  $N_{ant}$  is the number of transmitting antennas per BS,  $P_{tx}$  is the transmitting power per power amplifier (PA),  $P_1$  is the fixed part accounting for the direct current (DC) and alternating current (AC) converters.  $\Delta_p$  and  $P_0$  denote some circuit power consumption which includes the signal processing overhead  $L_{SP}$ , cooling loss  $L_C$  and battery backup and power supply loss  $L_{PSBB}$ , respectively, characterized by  $\Delta_p = (1 + L_C)(1 + L_{PSBB})/\mu_{PA}$  and  $P_0 = L_{SP}(1 + L_C)(1 + L_{PSBB})$ ,  $\mu_{PA}$  being the power amplifier (PA) efficiency.

This model shows that the BS power consumption increases with the number of antennas,  $N_{ant}$ , and the transmitting power,  $P_{tx}$ . However, the power consumption of components like DC-DC/AC-DC converters and cooling unit will not grow linearly with  $N_{ant}$ . The numerical values of  $P_{tx}$ ,  $\Delta_p$ ,  $P_0$ ,  $P_1$  for different types of BSs, like macro, micro and pico/femto BSs, are given in Table 3.1 as in [68].

Table 3.1 Values of double linear PCM [68]

Parameters	$P_{tx}(W)$	$\Delta_p$	$P_0$	$P_1$
macro BSs	80	7.25	244	255
micro BSs	6.31	3.14	35	34
pico or femto BSs	0.25	4.4	6.1	2.6

### 3.2.3 Data rate ( $D_{area}$ ) over a network area

We focus on evaluating the data rate  $D_{area}$  of the network area with radius  $R_a$ . For example, when  $0 < R_a \leq R_e$ , the area of interest is a small part of the central cell, as shown in Fig. 3.2. According to Shannon's formula, we can compute the achievable data rate of one UE

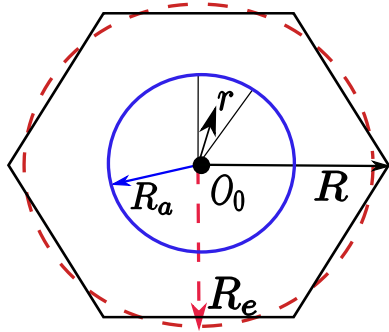


Fig. 3.2 Network area of radius  $R_a$  ( $0 < R_a \leq R_e$ ).

and the total data rate  $D_{area}$  over the network area of interest. Since the EE is computed based on the  $D_{area}$  and  $P_{exp}$ , the detailed information on the computation of the data rate  $D_{area}$  will be presented in the next chapter.

Based on the aforementioned EE model, power consumption model and data rate expression, we can evaluate the network EE. Since the data rate is related to the SINR expression, the basic thing is to explain how to compute SINR based on the fluid modeling. In the following subsection, we shortly recall the fluid network modeling and present the SINR expression and interference factor expression using the spatial fluid modeling.

### 3.3 Overview of fluid modeling

In an OFDMA network, radio resources of a BS are divided into many parallel and orthogonal subcarriers and inner-cell interferences are neglected. The spatial fluid modeling is to approximate a hexagonal network of several rings around a central cell. Here, only downlink communications are considered and the shadowing effects are neglected. The network is homogeneous and all base stations (BSs) have the same transmitting power.

#### 3.3.1 Notations

The sketch of the hexagonal network is given in Fig. 3.3. The network is homogeneous. Every hexagon has the same cell radii  $R$ .  $R_c$  and  $R_{nw}$  denote the half distance between two adjacent BSs and the network range, respectively.  $R_e$  is defined as the equivalent radius of a circle whose area is identical to the hexagonal cell, i.e.,  $R_e = aR_c$  where  $a = \sqrt{2\sqrt{3}/\pi}$ . The network environment consists of  $N_{BS}$  BSs and  $N_u$  UEs per cell. Assuming a uniform distribution for the BSs and the UEs, the density of BSs is  $\rho_{BS} = 1/(2\sqrt{3}R_c^2)$  and the density of UEs is  $\rho_u = N_u/(2\sqrt{3}R_c^2)$ .

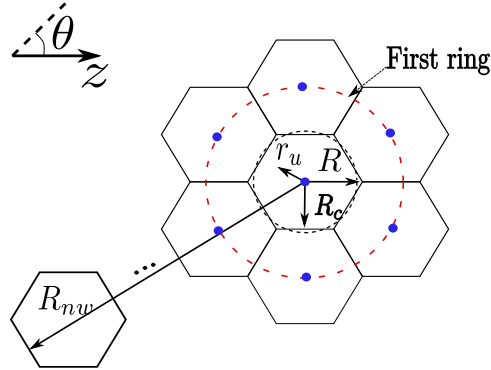


Fig. 3.3 Network model in hexagonal case and main parameters

In the following, we introduce the computation of signal-to-noise-plus-interference ratio (SINR)  $\gamma_u$  for a UE  $u$  in the hexagonal network and in the proposed fluid network modeling, respectively.

### 3.3.2 SINR in the hexagonal network

Regarding the propagation model, the useful power  $p_{b,u}$  received by UE  $u$  from BS  $b$  is written as  $p_{b,u} = P_{tx} K r_u^{-\eta}$ , where  $K$  is a constant,  $\eta$  ( $> 2$ ) is the path-loss exponent,  $r_u$  denotes the distance between the UE and the serving BS. The total external signal power (interference)  $p_{ext,u}$  received at  $u$  equals  $\sum_{j \neq b} P_{tx} K r_{u,j}^{-\eta}$ , where  $r_{u,j}$  is the distance between  $u$  and the BS  $j$ . Given the above notations, the SINR  $\gamma_u$  for a given UE  $u$  is given by

$$\begin{aligned}\gamma_u &= \frac{P_{tx} K r_u^{-\eta}}{\sum_{j \neq b} P_{tx} K r_{u,j}^{-\eta} + N_0} \\ &= \frac{r_u^{-\eta}}{\sum_{j \neq b} r_{u,j}^{-\eta} + \sigma}\end{aligned}\tag{3.3}$$

where  $\sigma = N_0 / (K P_{tx})$  and  $N_0$  denotes the received power from additional white Gaussian noise.

As introduced in [96], the other-cell-interference-factor (OCIF)  $y_f(r, \eta)$ , for a fixed UE at distance  $r$ , is defined as a ratio between the total external interference power from other cells and the useful power, displayed as

$$\begin{aligned}y_f(r, \eta) &= \frac{p_{ext,u}}{p_{b,u}} \\ &= \frac{\sum_{j \neq b} r_{u,j}^{-\eta}}{r_u^{-\eta}}\end{aligned}\tag{3.4}$$

### 3.3.3 SINR in fluid network model

In the spatial fluid model introduced in [96, 98, 99], a network (constituted by a finite number of BSs) is regarded as an equivalent continuum of transmitters which are uniformly distributed in the spatial domain. Considering that the distance between interfering BSs is  $2R_c$ , the set of transmitting power by interfering BSs in the network is also treated as a continuous field over the entire system.

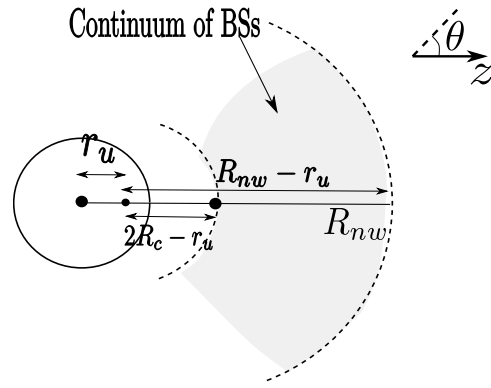


Fig. 3.4 Network model in fluid case and some parameters

For a given UE located in the central cell, we consider a circular shaped network around this central cell with radius  $R_{nw}$ , as shown in Fig. 3.4. The interfering area is the shaded region limited over the rings with radii  $2R_c - r_u$  and  $R_{nw} - r_u$ , respectively, centered at the UE's position. For each elementary surface  $ds = zdz d\theta$  at a distance  $z$  which contains  $\rho_{BS} ds$  BSs, the corresponding interference power equals  $\rho_{BS} z dz d\theta P_{tx} K z^{-\eta}$ . The integration over all the interfering area, gives the total amount of external interference power  $p_{ext,u}$ , approximated as in [96], by

$$\begin{aligned} p_{ext,u} &= \int_0^{2\pi} \int_{2R_c - r_u}^{R_{nw} - r_u} \rho_{BS} P_{tx} K z^{-\eta} z dz d\theta \\ &= \frac{2\pi \rho_{BS} P_{tx} K}{\eta - 2} [(2R_c - r_u)^{2-\eta} - (R_{nw} - r_u)^{2-\eta}]. \end{aligned} \quad (3.5)$$

Therefore, the SINR  $\gamma_u$  in the fluid modeling can be expressed as

$$\gamma_u = \frac{P_{tx} K r_u^{-\eta}}{\frac{2\pi \rho_{BS} P_{tx} K}{\eta - 2} [(2R_c - r_u)^{2-\eta} - (R_{nw} - r_u)^{2-\eta}] + N_0}. \quad (3.6)$$

As a consequence, the other-cell-interference-factor (OCIF),  $y_f(r, \eta)$ , for a UE at distance  $r$ , can be approximated as in [96],

$$y_f(r, \eta) = \frac{2\pi\rho_{BS}r^\eta}{\eta-2}[(2R_c - r)^{2-\eta} - (R_{nw} - r)^{2-\eta}]. \quad (3.7)$$

When  $R_{nw}$  is much larger than  $r_u$  ( $R_{nw} \gg r_u$ ) and neglecting the thermal noise  $\sigma$  (e.g., in urban environments), Eq. (3.6) can be further simplified into

$$\gamma_u = \frac{(\eta-2)r_u^{-\eta}}{2\pi\rho_{BS}(2R_c - r_u)^{2-\eta}}. \quad (3.8)$$

The substitution of  $\rho_{BS} = 1/(2\sqrt{3}R_c^2)$  into Eq. (3.8) and the introduction of the normalized distance  $x = r_u/R_c$ , the above equation can be rewritten into

$$\gamma_u(x) = \frac{\sqrt{3}}{\pi}(\eta-2)x^{-\eta}(2-x)^{2-\eta}, \quad (3.9)$$

from which one finds the  $\gamma_u$  for UE  $u$  only depends upon the relative distance to the serving BS,  $r_u/R_c$ , and the path-loss exponent,  $\eta$ .

The analytically tractable expression of  $\gamma_u$  of Eq. (3.8) can be easily used to compute the data rate over a network area of interest,  $D_{area}$ . In the following section, some numerical results will be presented to validate the accuracy of the fluid modeling.

## 3.4 Accuracy of fluid model

In this section, we show some numerical results of the SINR and its cumulative distribution function (CDF), which are obtained by fluid modeling and Monte Carlo simulations, respectively. Simulations are carried out on MATLAB. For the simplification purpose, the noise, the effect of shadowing and fast fading are ignored in all the simulation process. Therefore, the SINR is equal to the SIR in this section.

### 3.4.1 Simulation process

For Monte Carlo (MC) simulations, we consider 15 rings of hexagonal cells around a central hexagon such that  $R_{nw} = 31R_c$ .  $N_u$  UEs are generated uniformly in the central hexagon and we assume that they are attached to the BS located at the center of a hexagon. We sort all these UEs depending upon the distance to their serving BS, and we average the SINR,  $\gamma_u$ , for all UEs at the same distance. The results presented here are obtained by averaging

over 5000 MC simulations, by using Eq. (3.3). The numerical results of fluid modeling are obtained by simulating Eq. (3.8) for the SINR. The numerical values of transmitting power are set according to Table 3.1 for the macro and femto cellular networks, respectively. The other simulation parameters are set up according to Table 3.2 for the other network parameters.

Table 3.2 Simulation parameter value

Parameters	Value
Cell radius $R$ in macro and femto cellular networks, resp.	{1000, 50}m
Half distance between BSs, $R_c$	$R\sqrt{3}/2$
Range of network $R_{nw}$	$31R_c$
Equivalent radius of one cell, $R_e$	$R_c\sqrt{2\sqrt{3}/\pi}$
Distance of UE to its serving BS, $r$	[ $R/50$ $R$ ]
Number of UEs $N_u$	30
Path loss exponent $\eta$	{2.6, 3, 3.5, 4}
Density of BSs $\rho_{BS}$	$1/(2\sqrt{3}R_c^2)$

### 3.4.2 Discussion of results

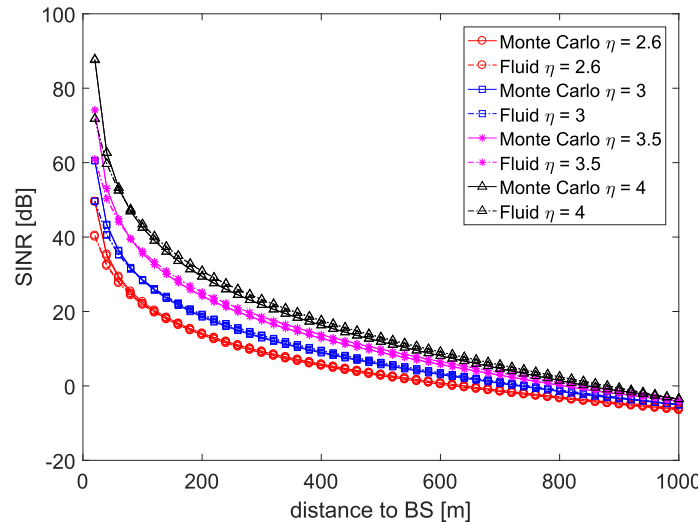


Fig. 3.5 SINR vs the distance to the BS in a macro cellular network.

Fig. 3.5 and Fig. 3.6 depict the SINR  $\gamma_u$  as a function of distance from the serving BS in macro cellular network and femto cellular network, respectively. The curves of the two

figures prove the accuracy of the fluid modeling towards the hexagonal lattice one. We also notice that there is a slight difference between fluid and hexagonal models, mainly for the UEs located closer to the serving BS. The difference is related to the circular shaped form considered in fluid model. Indeed, whatever the position of UEs in the inner circle, the average of the external power of all neighboring BSs is the same. However, in the hexagonal model, this assumption is no longer true, since we consider the real distance from neighboring BSs.

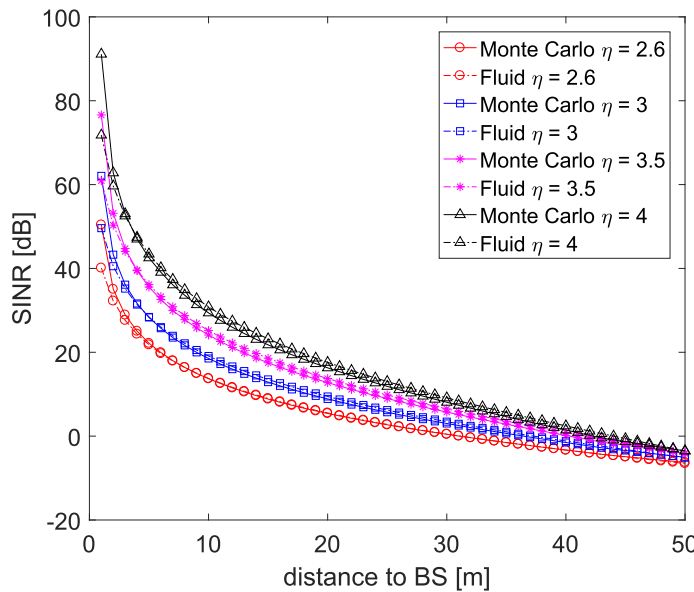


Fig. 3.6 SINR vs the distance to the BS in a femto cellular network.

Furthermore, for the accuracy purpose, we compare the numerical results in Fig. 3.5 with the ones developed in [100] while considering the same system parameters values for a macro cellular network. We observe that for a given distance, the numerical values of SINR obtained by fluid modeling in Fig. 3.5 and the ones in [100] are the same with the identical path-loss exponent  $\eta$ , which illustrates the accuracy of our code. However, focusing on the results obtained by Monte Carlo simulations in Fig. 3.5 and in [100], we also observe that there is a little difference in a short area around the BS, due to the randomness of the locations of UEs.

Moreover, we observe that the SINR of UEs, near the serving BS, is larger than the ones located at the edge. For example, for  $\eta = 3.5$  in Fig. 3.5, the SINR reaches 50.3dB at 40m from the serving BS, and about -3.1dB at 960m further. We also observe that values of the SINR for UEs, which is far from their serving BS, are same obtained by fluid and Monte Carlo simulation. Since for the UEs located at the cell edge, the principal

received power is the interference power coming from other external BSs. The SINR,  $\gamma_u$ , decreases exponentially with the distance whatever the path-loss exponent values,  $\eta$ , and it is proportional to the path-loss exponent value, i.e.,  $\gamma_u$  is higher for a larger path-loss exponent  $\eta = 4$ . We conclude that the values of SINR are larger in suburban area ( $\eta$  in  $\{3.5, 4\}$ ) than the ones in the urban area ( $\eta$  in  $\{2.6, 3\}$ ). Additionally, we can also observe the same conclusion in the femto cellular network, as shown in Fig. 3.6.

### 3.4.3 CDF results

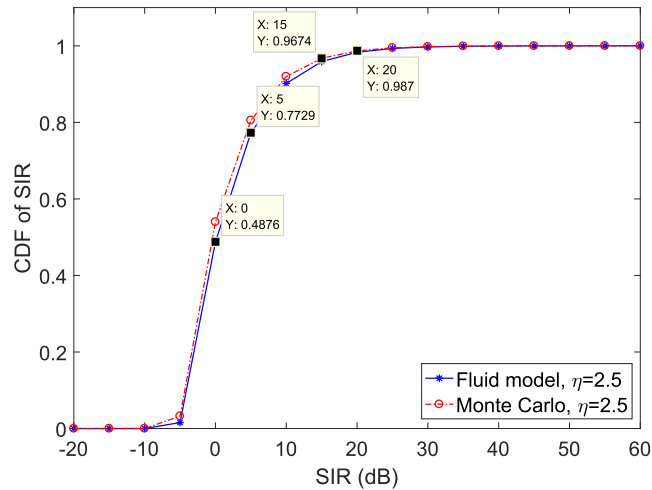


Fig. 3.7 CDF of SIR values in a macro cellular network

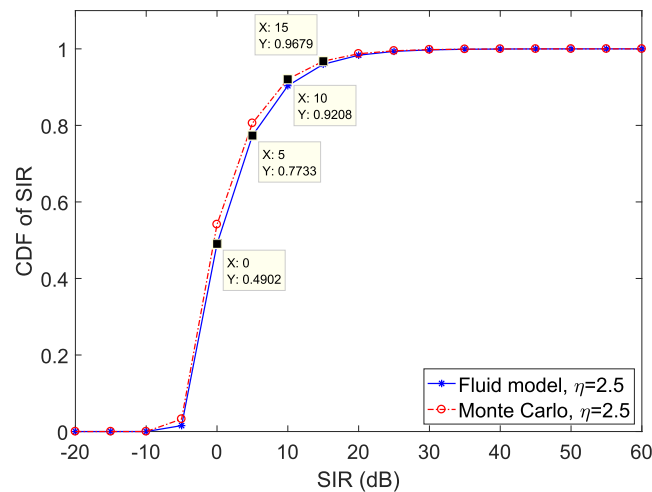


Fig. 3.8 CDF of SIR values in a femto cellular network

For further verification of the accuracy of the spatial fluid modeling, we also investigate the cumulative distribution function (CDF) of SINR. Fig. 3.7 and Fig. 3.8 describe the CDF along with various SINR threshold for  $\eta = 2.5$  in the macro and femto cellular networks, respectively. The numerical values in both two figures show that the analytical results match well with Monte Carlo ones, which reveals the accuracy of the fluid modeling, despite the small difference. For example, the error is about 0.05 in the range [−5 15] dB. In addition, we observe that the mean value of SIR is about 0dB (1bps) in both two figures. In other words, due to the uniform distribution of UEs, the SIR of half of the UEs are greater than 0dB (1bps).

### 3.4.4 SIR vs network range

For illustrating the impact of network range on SIR, we investigate the SIR of fixed UEs varies with the number of network rings. Fig. 3.9 and Fig. 3.10 depict the SIR variation depending on the number of network rings in two types of cellular networks, macro and femto, respectively, for  $\eta = 3$ . The distances,  $r_u$ , of UE are set as {300m, 500m, 800m} and {20m, 25m, 40m} in macro and femto cellular networks, respectively. The numerical results of SIR are obtained based on Eq. (3.6) with considering network range,  $R_{nw}$ , and Eq. (3.8) with neglecting  $R_{nw}$ . Focusing on Fig. 3.9, we observe that the numerical values of SIR are almost the identical when the number of network rings is larger than 15, whatever the values of  $r_u$ . In other words, when the network range  $R_{nw} \geq 31R_c$ , we can use the simplified Eq. (3.8) to compute data rate and EE in a fluid modeling. Thus, we set the network range is  $31R_c$  in the simulation section. The same conclusion can be found in the femto cellular networks.

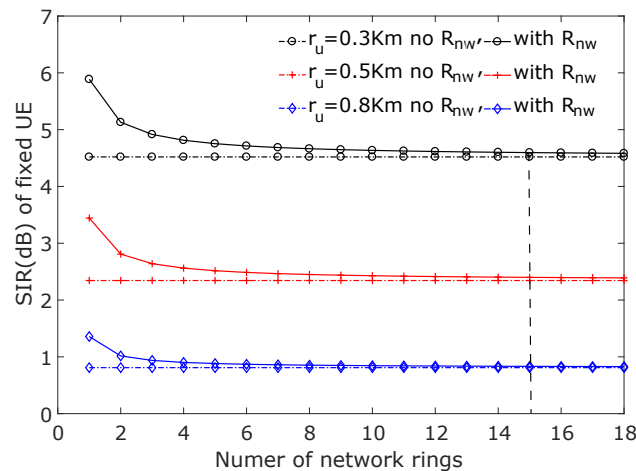


Fig. 3.9 SIR vs the number of network rings in a macro cellular network

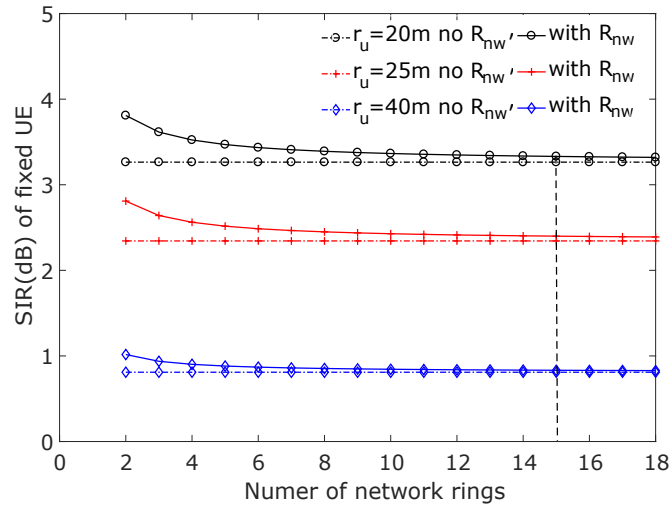


Fig. 3.10 SIR vs the number of network rings in a femto cellular network

### 3.5 Conclusion

In this chapter, we developed a tractable analytical expression of EE-evaluation based on this fluid framework, which will be used in the following chapters. First, we presented the system model for evaluating network energy efficiency, including the expression of EE and power consumption model. Then, we presented the expression of SIR in fluid modeling, which is tractable. Furthermore, we discussed the simulation results of SIR and CDF of SIR. The observations point out that the analytical results obtained by fluid model are similar to the ones established by Monte Carlo simulations, which show the accuracy of fluid modeling.

In the next chapter, we will present the computation of data rate based on this system model in detail and the work using this system model to evaluate EE for the large cellular networks so as to investigate the impact of shadowing on EE.



# Chapter 4

## Fluid modeling of EE and effect of shadowing on EE

### Contents

4.1	Introduction . . . . .	62
4.2	Energy efficiency definition . . . . .	63
4.3	Data rate computation . . . . .	64
4.3.1	Data rate within the central hexagon . . . . .	65
4.3.2	Data rate over a first ring . . . . .	65
4.3.3	Data rate over a large network . . . . .	66
4.4	Data rate with shadowing consideration . . . . .	70
4.4.1	Signal quality . . . . .	71
4.4.2	Data rate . . . . .	72
4.4.3	Coverage probability . . . . .	73
4.5	Model evaluation: non-shadowing case . . . . .	74
4.5.1	Simulation setup . . . . .	74
4.5.2	Model accuracy . . . . .	75
4.5.3	EE variation vs cell network types . . . . .	76
4.5.4	Impacts of user's density on EE . . . . .	78
4.5.5	EE vs path-loss exponent . . . . .	78
4.5.6	EE variation over a first ring . . . . .	79
4.5.7	EE variation over a large network . . . . .	80
4.6	Model evaluation: shadowing case . . . . .	82
4.6.1	Simulation setup . . . . .	83
4.6.2	Relationship between $\Gamma_{th}$ and $r$ . . . . .	84

---

4.6.3	Energy efficiency discussion . . . . .	86
4.6.4	EE model accuracy . . . . .	88
4.7	Conclusion . . . . .	89

---

## 4.1 Introduction

To support the requirement of x1000 traffic increase in 5G networks, the EE has to be improved dramatically x1000 at least in the next 5 years time-frame [10, 101]. However, the goal is not easy to achieve considering so many factors, such as the environmental, economical and operational concerns [102]. In particular, from the operators perspective, EE is urgent to be considered for designing the cellular networks due to that a high EE reduces the commercial expenditure of operators. In addition, several EU-funded research projects have been carried out to develop more energy-efficient wireless communications, e.g., Energy Aware Radio and neTwork tecHnologies (EARTH) [103], Towards Real Energy-efficient Network Design (TREND) [104] and Mobile and wireless communications Enablers for Twenty-twenty (2020) Information Society (METIS) [105]. On the other hand, several collaborative initiatives, such as the GreenTouch consortium [106], and the 5G Infrastructure Public Private Partnership (5G PPP) [107], have also focused on analyzing the energy-efficient wireless networks through utilizing some promising techniques. In these work, the proposed solutions are achieved using system-level simulations, or stochastic geometry to describe network model (mainly the nodes locations and the propagation models) and to derive consequently the EE performance model. Nevertheless, since today's networks are more and more dense due to the increase number of BSs, simulation-based approaches have become a hard task and resource-intensive. Moreover, stochastic geometry-based studies assume in most cases a Poisson point process to describe the nodes locations which allows to derive a closed-form formula of the energy metric. However, when non-Poisson point processes are considered, eg., perturbed lattice,  $\beta$ -Ginibre point process, and Matérn point process, the performance models are not analytically tractable due to the non-independent nature of points [108]. Therefore, representative, tractable and accurate models are needed to evaluate the EE performance of the cellular networks in the energy consumption process, which motivates this work.

In addition, shadowing is used to model random variations of the received power signals on the path loss due to the encountered obstacles like buildings, trees, terrain conditions [109, 110], during the transmission of signal in wireless channel. In detail, the obstacles make the signal change at random, resulting a random variation of the received

signal power for the UEs, with the same distance to the transmitter whereas in different locations. Commonly, shadow fading is modeled using the log-normal distribution in the radio propagation process, thus it is also called as lognormal fading. Some research efforts are made to illustrate the impact of shadowing fading. The authors in [111] derived some closed-form expressions for the interference factor's mean and standard deviation, as well as the outage probability while taking into account the impact of the path-loss exponent and the shadowing. The authors in [112] show that shadowing increases outage probability in cellular radio networks. Additionally, the work of [113] shows that the coverage probability is severely reduced by shadowing in a Poisson small cell network. The above work illustrates that the effect of shadowing is significant and should not be neglected while characterizing the performance of cellular networks, i.e., coverage probability and outage probability. Nevertheless, the influence of shadowing on the EE is still an open issue while the fluid modeling is utilized.

Hence, our objective in this chapter is to develop a tractable EE model for cellular networks based on the spatial fluid modeling without considering the shadowing effect, and to investigate the impact of shadowing on EE. We first present a tractable and effective EE model for an OFDMA cellular network based on the spatial fluid modeling, which reduces the analysis complexity. Then, we present how to compute the data rate while the impact of shadowing is neglected. Furthermore, we develop a closed-form expression of the signal-quality threshold using the Polynomial Curve Fitting (PCF) approach so as to compute the data rate with taking into account the shadowing effect. Finally, we discuss the simulation performance to prove the effectiveness and accuracy of the proposed model through a comparison between fluid modeling and Monte Carlo simulations.

## 4.2 Energy efficiency definition

We consider the common definition of EE as the ratio of total data rate  $D_{area}$  in a network area over the total power consumption, i.e.,  $EE = \frac{D_{area}}{N_{BS} \times P_{exp}}$ , as defined in Eq. (3.1). Metric EE is measured in terms of bits/Joule, which is the maximum amount of bits that can be reliably delivered by the system per Joule of energy.  $N_{BS}$  denotes the overall number of BSs in the system, and  $P_{exp}$  accounts for the total energy expenditure per BS.  $P_{exp}$  can be calculated according to the Eq. (3.2).

Since the definition of EE is not only related to the data rate, but also related to the power consumption of the system, we present how to compute the total data rate  $D_{area}$  without/with considering the effect of shadowing during the transmission of signal in the radio system.

### 4.3 Data rate computation

In a cellular system, both the signal and interference strength decay super-linearly with distance [114]. Therefore, the distance between the BS and mobile users is a key element to quantify the fundamental network performance metrics and to estimate the system capacity and the energy efficiency, which are critical indicators for the network deployment. Much work on EE and data rates has been investigated focusing on the central cell. However, in a practical scenario, the statistical distance of UEs to the origin is changing due to UEs's life activity, either inside or outside the central cell, or any point of the system network. As a result, the data rate and energy consumption exist outside the central cell. Therefore, it is an interesting issue to investigate the data rate over a disc region, not only limited to the central cell.

The objective is to compute the total data rate,  $D_{area}$ , over a disc region with radius of  $R_a$ . Let the center of a central hexagon be the origin. The radius of  $R_a$  is also called the statistical distance. Based on the different size of  $R_a$ , in this chapter, we consider three scenarios, i.e.,  $0 < R_a \leq R_e$ ,  $R_e < R_a \leq 2R_c$  and  $0 < R_a \leq R_{nw}$ .  $R_e$  is the radius of a disk with a surface equivalent to the central hexagonal cell, such that  $R_e = aR_c = \sqrt{2\sqrt{3}/\pi}R_c$  with  $a = \sqrt{2\sqrt{3}/\pi}$ .  $R_c$  is the half distance between two BSs and  $R_{nw}$  is the network range.

According to the Shannon's formula, the spectral efficiency (SE), measured by bps/Hz, for a UE  $u$  is a function of signal quality  $\gamma_u$  as

$$\text{SE}_u(r) = \log_2(1 + \gamma_u(r)). \quad (4.1)$$

The maximum of achievable data rate  $D_u(r)$  for user  $u$  at distance  $r$  is the multiplication of the user's bandwidth  $B_u$  and  $\text{SE}_u$ , i.e.,

$$D_u(r) = B_u \times \text{SE}_u(r). \quad (4.2)$$

Since the user's density  $\rho_u$  is invariant, users are assigned with the same bandwidth, and the total data rate  $D_{area}$  over the area is closely related to the SINR  $\gamma_u(r)$  of users,  $D_{area}$  can be written as the integration of  $D_u$  over the interested area. Mention that  $\gamma_u(r)$  has been given as  $\gamma_u = \frac{(\eta-2)r_u^{-\eta}}{2\pi\rho_{BS}(2R_c-r_u)^{2-\eta}}$ , as defined in Eq. (3.8).

Therefore, in the following subsection we focus on evaluating the data rate  $D_{area}$  of interested area in different scenarios through Eqs. (3.8), (4.1) and (4.2).

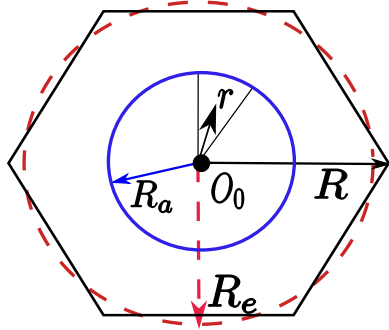


Fig. 4.1 Scenario 1: network area with radius  $R_a$  ( $0 < R_a \leq R_e$ )

### 4.3.1 Data rate within the central hexagon

Fig. 4.1 depicts the scenario when the interested area is one part of the central cell, i.e. ( $0 < R_a \leq R_e$ ). Since the UEs are uniformly distributed in every cell, the density  $\rho_u$  is a constant. Therefore, the number of users  $N'_u$  over the area of interest is given as  $N'_u = (N_u R_a^2) / (a^2 R_c^2)$ , where  $N_u$  is the number of users per cell.

Considering an equal bandwidth sharing among UEs,  $B_u = BW_n / N_u$  where  $BW_n$  is the total bandwidth. Based on Eqs. (3.8), (4.1) and (4.2), replacing  $\rho_u = N_u / (2\sqrt{3}R_c^2)$ , the total data rate  $D_{area}$  can be written as

$$\begin{aligned} D_{area} &= \int_0^{2\pi} \int_0^{R_a} B_u \rho_u \log_2(1 + \gamma_u(r)) r dr d\theta \\ &= \frac{BW_n \pi}{\sqrt{3}R_c^2} \int_0^{R_a} r \log_2(1 + \gamma_u(r)) dr. \end{aligned} \quad (4.3)$$

A worthwhile observation is that the Eq. (4.3) neither depends on the number of UEs deployed per cell nor upon the value of  $\rho_u$ . When  $R_a = R_e$ , the above equation is evolved to compute the total cell data rate,  $D_{cell}$ , as in [100].

### 4.3.2 Data rate over a first ring

Actually, when a user moves from one cell to its adjacent cell, the BS located at the adjacent cell becomes its new serving BS for the user. In this case, the SINR and data rate for the user maybe change due to changes in relative distance between the user and its new serving BS. Thus, to investigate the data rate over a first ring is also an interesting issue.

Beyond the central cell, we explain here how to compute the total data rate. Assume a user  $m$ , located outside the central cell at distances  $r, r_m$  from the central cell BS  $O_0$  and its serving BS  $B$ , respectively, as shown in Fig. 4.2. According to the law of cosines, the

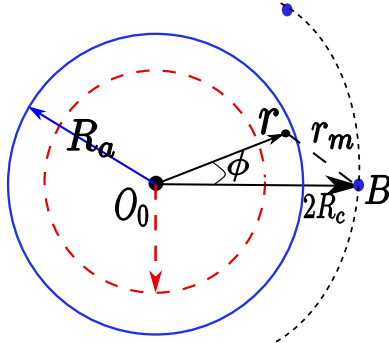


Fig. 4.2 Scenario 2: network area with radius  $R_a$  ( $R_e < R_a \leq 2R_c$ )

distance  $r_m$  of the user  $m$  from its serving BS  $B$  can be expressed as

$$r_m = \sqrt{(2R_c)^2 + r^2 - 4rR_c \cos\phi}. \quad (4.4)$$

The SINR  $\gamma_m$  is computed by

$$\begin{aligned} \gamma_m(r) &= \frac{(\eta-2)r_m^{-\eta}}{2\pi\rho_{BS}(2R_c-r_m)^{2-\eta}} \\ &= \frac{(\eta-2)[4R_c^2+r^2-4rR_c \cos\phi]^{-\eta/2}}{2\pi\rho_{BS}[2R_c-(4R_c^2+r^2-4rR_c \cos\phi)^{1/2}]^{2-\eta}}. \end{aligned} \quad (4.5)$$

Based on Eq. (4.2) and replacing  $\rho_{BS}$  and  $\rho_u$  by their values, the total data rate over a disc with radius  $R_a$  is given as

$$D_{area} = D_{cell} + \frac{6BW_n}{\sqrt{3}R_c^2} \int_0^{\frac{\pi}{6}} \int_{R_e}^{R_a} r \log_2(1 + \gamma_m(r)) dr d\phi. \quad (4.6)$$

### 4.3.3 Data rate over a large network

By minor extension, the application of the spatial fluid framework is used to compute the data rate over an area with any size. Because users may move to any point in the network due to their random activities. As a result, there is signal quality at any point over the network. Hence, in this subsection, we focus on how to compute the data rate over a disc area with radius  $R_a$  ( $0 < R_a \leq R_{nw}$ ). Before presenting the computation of data rate  $D_{area}$  in this case, we introduce some approximation between disc and hexagon.

### Approximation between disc and hexagon

Setting the origin of the global coordinate system at the central BS, as shown in Fig. 4.3, the disc region with radius of  $R_a$  is of interest and denoted by  $S_{disc}$ . The objective here is to compute total data rate  $D_{area}$  over  $S_{disc}$  based on Eq. (3.8).

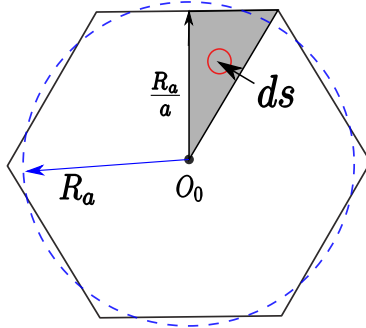


Fig. 4.3 Scenario 3: network area with radius  $R_a$  ( $0 < R_a \leq R_{nw}$ )

For simplicity, some literatures took into account the hexagonal cell as a circular cell with equal area to investigate the network performances, such as other-cell interference [115] and the received power at a BS [116]. These work shown that the circular cell and the hexagonal cell can be transformed into each other where the locations of all UEs are the same. Hence, in this subsection we made the following approximations.

- (1) The interested circular region  $S_{disc}$  has the same area as the equivalent hexagon  $S_{hex}$ , such as  $S_{disc} = S_{hex}$ .
- (2) The date rate over a circular region is equal to the data rate over an equivalent hexagonal region. Because UEs' position remains unchanged whatever in the disc region or in the equivalent hexagonal area.
- (3) Using the symmetric property of a hexagon, the hexagon can be divided into 12 small triangles.

Based on the above approximation, the total data rate  $D_{area}$  over an interested disc region  $S_{disc}$  is equal to the total data rate over an equivalent hexagon area  $S_{hex}$ . As a result,

$$\begin{aligned}
 D_{area} &= \iint_{S_{disc}} \rho_u B_u \log_2(1 + \gamma_u(r)) ds \\
 &= \iint_{S_{hex}} \rho_u B_u \log_2(1 + \gamma_u(r)) ds \\
 &= 12 \times D_{hex}^{tri},
 \end{aligned} \tag{4.7}$$

where  $D_{hex}^{tri}$  is the data rate of the shaded triangular region, as shown in Fig. 4.3. Therefore, we present how to compute the total data rate of the shaded triangular region,  $D_{hex}^{tri}$ , in the following part.

The notations used in this subsection are summarized in Table 4.1.

Table 4.1 Common parameters in a large network

Parameter	Description
$S_{disc}$	surface area of a disc region with radius $R_a$
$D_{area}$	data rate over $S_{disc}$
$S_{hex}$	surface area of an equivalent hexagon
$D_{hex}^{tri}$	data rate over an area, i.e., twelfth of $S_{hex}$
$D_{cell}$	data rate per hexagonal cell
$\Delta_{O_0S_2S_1}$	surface area of a triangle
$D_\Delta$	data rate over the triangle area, $\Delta_{O_0S_2S_1}$ ( $D_\Delta = \frac{3D_{cell}}{4}$ )
$\square_{S_1S_2S_3S_4}$	surface area of a square
$D_\square$	data rate over the square area $\square_{S_1S_2S_3S_4}$ ( $D_\square = D_{cell}$ )
$D_{re}$	data rate over the remaining area
$n_t$	the number of $D_\Delta$
$k$	the number of $D_\square$

### Computation of data rate $D_{hex}^{tri}$

According to the approximation of the disc area by a hexagon, the network area is enclosed by two axes, for example, the x-axis represents the value of  $R_a/a$ , as shown in Fig. 4.4.  $D_{hex}^{tri}$  is decomposed as repeated blocks of the highlighted triangles, rectangle with vertices  $S_1$ ,  $S_2$ ,  $S_3$ ,  $S_4$ , and some remaining part. Two examples are given in the following to explain the law of geometric decomposition.

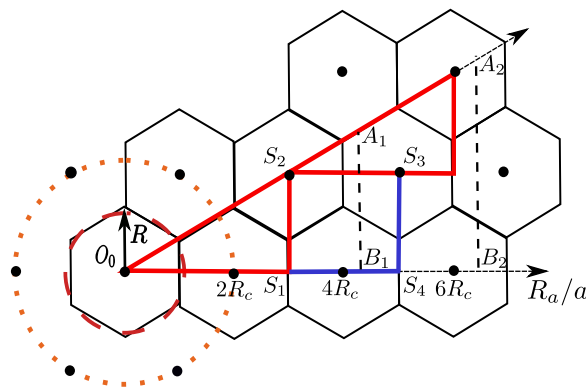


Fig. 4.4 Homogeneous network with a various radius  $R_a/a$

The first example shows the case when  $3R_c < R_a/a < 5R_c$ , so that  $D_{hex}^{tri}$  is the data rate over the triangle with vertices  $O_0, A_1$  and  $B_1$ . The corresponding decomposition scheme is sketched by Fig. 4.5(a). Hence, the data rate  $D_{hex}^{tri}$  is a summation of  $D_\Delta$  (data rate over a triangle) and data rate over the remaining part which is a trapezoid with vertices  $S_1, S_2, A_1$  and  $B_1$ . For the evaluation of data rate,  $D_\Delta$ , with the knowledge that the data rate is only related to the distances from the serving BS and UEs, it is not difficult to derive that  $D_\Delta = 3D_{cell}/4$ . The computation of the data rate over the remaining part is given in Appendix A.

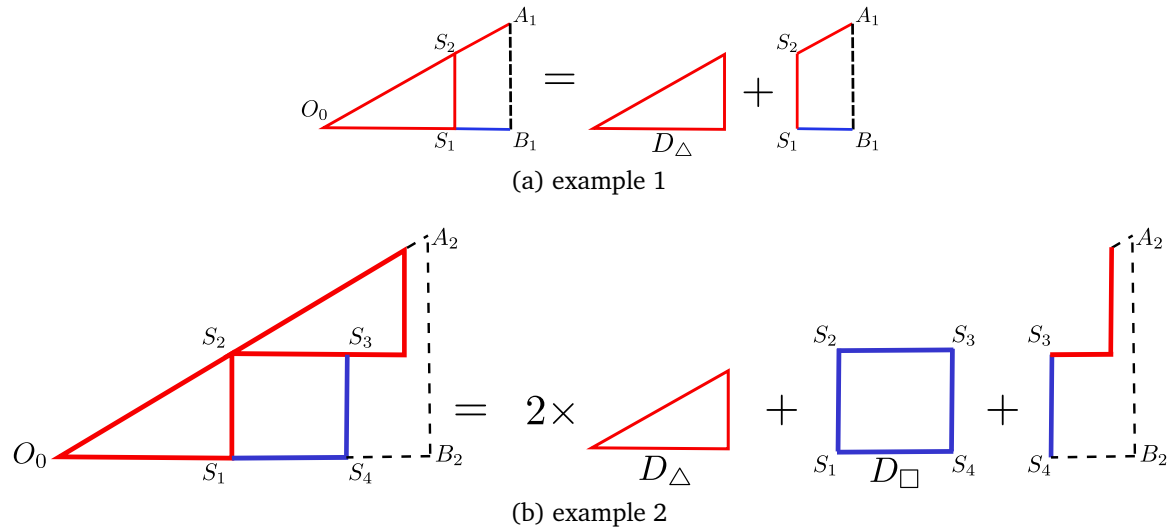


Fig. 4.5 Two examples for the decomposition of the network area.

The second example illustrates the case when  $6R_c < R_a/a < 7R_c$ .  $D_{hex}^{tri}$  is the data rate over the surface area with vertices  $O_0, A_2$  and  $B_2$ , as shown in Fig. 4.5(b). Let  $D_\square$ ,  $D_{cell}$  denote the data rate over the square area  $\square_{S_1S_2S_3S_4}$  and data rate over a hexagonal cell, respectively. Following similar analysis as the first example and based on the geometry property of a hexagon,  $D_{hex}^{tri}$  is decomposed as two  $D_\Delta$ , one  $D_\square$ , and the data rate over the remaining part, where  $D_\square = D_{cell}$ . Appendix A presents the approach to compute the data rate over the remaining region, as for the first example.

As seen from the above two examples, the data rate with any value of  $R_a/a$  is a summation of multiple  $D_\Delta$ ,  $D_\square$ , and the data rate over the remaining part, i.e.,

$$D_{hex}^{tri} = n_t D_\Delta + k D_\square + D_{re}, \quad (4.8)$$

where  $n_t, k$  are non-negative integers and denote the number of repeated parts of  $D_\Delta$  and  $D_\square$ , respectively.  $D_{re}$  denotes the data rate over the remaining area. With any given

value of  $R_a/a$ , the computation of the data rate for the remaining part, i.e.,  $D_{re}$ , follows the approach described in Appendix A. We here present how to compute  $n_t$  and  $k$ .

Taking advantage of the symmetry pattern of a hexagon, we observe that the number of  $\Delta_{O_0S_2S_1}$  appears with a period  $3R_c$  and that the number of  $\square_{S_1S_2S_3S_4}$  appears with a period  $2R_c$  along the  $R_a/a$  axis. Hence, the number of  $D_\Delta$ ,  $n_t$ , can be defined as

$$n_t = \left[ \frac{R_a}{a}, 3R_c \right], \quad (4.9)$$

where  $[\cdot, \cdot]$  is the quotient operator. Additionally, we observe that  $D_\square$  appears at the right (towards to positive direction of the axis of  $R_a/a$ ) and  $\square_{S_1S_2S_3S_4}$  depends on  $R_a/a$  and  $n_t$ . Hence, the number of  $D_\square$ ,  $k$ , is given by

$$k = \sum_{n=1}^{n_t} \max \left\{ 0, \left[ \frac{R_a}{a} - 3nR_c, 2R_c \right] \right\}. \quad (4.10)$$

Eqs. (4.9) and (4.10) are obtained based on the geometric characteristic of a hexagon.

A detailed example is given to better understand the above two equations. Assuming  $6R_c < R_a/a < 7R_c$  as in example 2 and according to Eq. (4.9),  $n_t$  is calculated, i.e.,  $n_t = 2$ , which illustrates that there are two  $D_\Delta$ . With  $n_t = 2$  and following Eq. (4.10), the value of  $k$  is a summation, which yields to the value of 1, i.e.,  $k = 1$ . That shows that there is one  $D_\square$ . In one word, according to Eqs. (4.9) and (4.10), we obtain  $n_t = 2$  and  $k = 1$  for  $6R_c < R_a/a < 7R_c$ , which is in accordance with the truth, as shown in Fig. 4.5(b). That illustrates the accuracy of Eqs. (4.9) and (4.10).

Therefore, for a given value of  $R_a$ , using Eqs. (4.9), (4.10) and the computed  $D_{re}$  in Appendix A,  $D_{hex}^{tri}$  over a triangle area can be easily computed. Then replacing  $D_{hex}^{tri}$  in Eq. (4.7), we can obtain the data rate  $D_{area}$  over a disc region with radius of  $R_a$ .

As a result, we can easily compute the EE metric in Eq. (3.1) by replacing  $P_{exp}$  with Eq. (3.2), replacing  $D_{area}$  with Eq. (4.3) or Eq. (4.6) or Eq. (4.7).

## 4.4 Data rate with shadowing consideration

In this section, we recall first the SINR expression of a user equipment  $u$  located at a distance  $r$  from its serving BS  $b$ , taking the path-loss exponent and the shadowing impact into account. Then, to calculate the data rate over a network area  $D_{area}$ , we rely on the proposed fluid model to present a formula of the coverage probability. Especially, in the case of a fixed coverage probability, we further drive a closed-form expression between SINR

threshold  $\Gamma_{th}(r)$  and UE's distance  $r$  through a polynomial curve fitting method, which is compared with the fluid modeling.

#### 4.4.1 Signal quality

Regarding the propagation model, the received power  $p_b$  at the UE  $u$ , located at a distance  $r$  from its serving BS,  $b$ , can be written as,

$$p_b = P_{tx} K r^{-\eta} A_b, \quad (4.11)$$

where  $A_b = 10^{\frac{\xi_b}{10}}$  denotes the shadowing effect. The lognormal random variable  $A_b$  characterizes the random variations of the received power around a mean value.  $\xi_b$  stands for a normal distributed random variable (RV), with zero mean and standard deviation,  $\sigma$ , which is between 0 and 8 dB.  $P_{tx} K r^{-\eta}$  represents the mean value of received power from BS  $b$ , at UE  $u$ , where  $K$  is a constant and  $\eta (> 2)$  is the path-loss exponent. The interference received power,  $p_{ext}$ , at  $u$  from the external BSs is:

$$p_{ext} = \sum_{j \neq b} P_{tx} K r_j^{-\eta} A_j. \quad (4.12)$$

Given the above notations, the SINR  $\gamma_u$  of a given UE  $u$  is

$$\gamma_u = \frac{P_{tx} K r_b^{-\eta} A_b}{\sum_{j \neq b} P_{tx} K r_j^{-\eta} A_j + N_0}, \quad (4.13)$$

where  $N_0$  is the Gaussian noise. Neglecting the noise power because of the urban area and considering same transmission power of BSs,  $P_{tx}$ , the SINR can be rewritten as

$$\gamma_u = \frac{r^{-\eta} A_b}{\sum_{j \neq b} r_j^{-\eta} A_j}. \quad (4.14)$$

Let  $\gamma_u = 1/A_f$  with

$$A_f = \frac{\sum_{j \neq b} r_j^{-\eta} A_j}{r^{-\eta} A_b}, \quad (4.15)$$

where  $A_f$  can be approximated by a lognormal RV with mean value,  $m_f$ , and standard deviation,  $s_f$  [117–119]. According to the definition of [119], the terms  $m_f$  and  $s_f$  can be

calculated as

$$\begin{aligned}
m_f &= \frac{1}{a} \ln[y_f(r, \eta)H(r, \sigma)] \\
s_f^2 &= 2[\sigma^2 - \frac{1}{a^2} \ln(H(r, \sigma))] \\
y_f(r, \eta) &= \frac{\sum_{j \neq b} r_j^{-\eta}}{r^{-\eta}} \\
H(r, \sigma) &= e^{a^2 \sigma^2 / 2} [G(r, \eta)(e^{a^2 \sigma^2 - 1}) + 1]^{1/2} \\
G(r, \eta) &= \frac{\sum_{j \neq b} r_j^{-2\eta}}{(\sum_{j \neq b} r_j^{-\eta})^2} \\
a &= \frac{\ln 10}{10}
\end{aligned} \tag{4.16}$$

where  $m_f$  is measured in dB. The term  $y_f(r, \eta)$ , considered as the interference factor since it stands for the  $A_f$  factor without shadowing. Specially, in the fluid modeling, the interference factor,  $y_f(r, \eta)$ , for a fixed UE at distance  $r$  can be computed by  $y_f(r, \eta) = \frac{2\pi\rho_{BS}r^\eta}{\eta-2}[(2R_c - r)^{2-\eta} - (R_{nw} - r)^{2-\eta}]$ , as displayed in Eq. (3.7). The factor  $G(r, \eta)$  can also be rewritten as

$$G(r, \eta) = \frac{y_f(r, 2\eta)}{[y_f(r, \eta)]^2}. \tag{4.17}$$

#### 4.4.2 Data rate

The data rate over a network area, as shown in Fig. 4.1, is computed while taking the impact of shadowing into account.

As shown in [16, 19], the spectral efficiency of a given UE can be measured while considering the coverage probability. According to Shannon's formula, the average achievable throughput, for a UE  $u$  at the distance  $r$ , is given as

$$D_u(r) = B_u \mathbb{P}_{cov}^r \log_2(1 + \Gamma_{th}(r)), \tag{4.18}$$

where  $\mathbb{P}_{cov}^r = \mathbb{P}(\gamma_u > \Gamma_{th}(r))$  is the coverage probability [120], and  $B_u$  is the UE's bandwidth. Hence, the total data rate  $D_{area}$  over a network area of radius  $R_a$ , can be computed as

$$D_{area} = \int_0^{2\pi} \int_0^{R_a} B_u \rho_u \mathbb{P}_{cov}^r \log_2(1 + \Gamma_{th}(r)) r dr d\theta, \tag{4.19}$$

where  $\rho_u$  is the UE's density.

Therefore, to compute the data rate,  $D_{area}$ , we first define the coverage probability based on the other-cell-interference-factor (OCIF),  $y_f(r, \eta) = \frac{2\pi\rho_{BS}r^\eta}{\eta-2}[(2R_c - r)^{2-\eta} - (R_{nw} - r)^{2-\eta}]$ , as shown in Eq. (3.7), Eqs. (4.14), (4.16) and (4.17). Then, we derive a closed-form formula of the SINR threshold,  $\Gamma_{th}$ , in the case of a fixed coverage probability using the Polynomial Curve Fitting (PCF) method.

#### 4.4.3 Coverage probability

In the propagation channels, often coverage probability is used as a metric to assess the performance of the communication system [121]. The coverage probability,  $\mathbb{P}_{cov}^r$ , is defined in [121, 122] as the probability for the signal quality SINR,  $\gamma_u$ , of a UE  $u$  to be larger than a threshold value  $\Gamma_{th}$  and can be expressed as,

$$\mathbb{P}_{cov}^r = \mathbb{P}(\gamma_u > \Gamma_{th}). \quad (4.20)$$

Based on Eqs. (4.14), (4.15), (4.16), as in [111, 119], we have,

$$\begin{aligned} \mathbb{P}_{cov}^r &= \mathbb{P}(\gamma_u > \Gamma_{th}) \\ &= \mathbb{P}\left(\frac{1}{\Gamma_{th}} > \frac{1}{\gamma_u}\right) \\ &= \mathbb{P}\left(\frac{1}{\Gamma_{th}} > A_f(m_f, s_f)\right) \\ &= \mathbb{P}\left(10\log_{10}\left(\frac{1}{\Gamma_{th}}\right) > 10\log_{10}(A_f)\right) \\ &= 1 - Q\left[\frac{10\log_{10}\left(\frac{1}{\Gamma_{th}}\right) - m_f}{s_f}\right], \end{aligned} \quad (4.21)$$

where  $Q$  is the error function, denoted as  $Q(x) = \frac{1}{2\pi} \int_x^{+\infty} e^{-\frac{t^2}{2}} dt$ . For a given  $r$ , we can compute the corresponding  $\Gamma_{th}$  according to Eqs. (3.7), (4.16), (4.17) and (4.21) in the case of a known  $\mathbb{P}_{cov}^r$  and a fixed path-loss exponent  $\eta$ . Furthermore, we can plot the variation of  $\Gamma_{th}$  depending on the UE's distance  $r$  based on the fluid framework. Then, using the Polynomial Curve Fitting (PCF), we can set up an accurate fitting of an analytical function relying  $\Gamma_{th}$  to  $r$ .  $\Gamma_{th}$  can be expressed by a third degree polynomial of  $r$ , as,

$$\Gamma_{th}(r) = w_0 + w_1 r + w_2 r^2 + w_3 r^3, \quad (4.22)$$

where the coefficients  $w_0$ ,  $w_1$ ,  $w_2$  and  $w_3$  can be obtained through the least-square fitting. For example,  $w_0 = 25.6483$ ,  $w_1 = -1.3220$ ,  $w_2 = 0.0222$  and  $w_3 = -0.0002$  for  $\eta = 2.6$

and  $\sigma = 3dB$ . The coverage probability should be high enough to overcome the rapid degradation of signal quality caused by the obstacles effect. Normally,  $\mathbb{P}_{cov}^r$  should follow the relationship  $\mathbb{P}_{cov}^r \geq C_0$ ,  $70\% \leq C_0 \leq 95\%$ , as shown in [123]. Here, we set  $\mathbb{P}_{cov}^r = 0.9$  whatever the distance  $r$  for all UEs [111], in order to guarantee the signal quality for all UEs and to achieve a high coverage probability.

Replacing  $\Gamma_{th}(r)$  of Eq. (4.22) and  $\rho_u = N_u/(2\sqrt{3}R_c^2)$  in Eq. (4.19), the total data rate  $D_{area}$  is expressed as

$$D_{area} = \frac{BW_n \pi \mathbb{P}_{cov}^r}{\sqrt{3}R_c^2} \int_0^{R_a} r \log_2(1 + w_0 + w_1 r + w_2 r^2 + w_3 r^3) dr. \quad (4.23)$$

For simplify purposes, an equal bandwidth sharing among UEs is considered here  $B_u = BW_n/N_u$  ( $BW_n$  is the total bandwidth), as well as a constant coverage probability  $\mathbb{P}_{cov}^r$ .

To compare with the case of a network without shadowing effect  $\sigma = 0$ , the data rate is computed by Eq. (4.3) with  $\gamma_u(r) = \frac{(\eta-2)r_u^{-\eta}}{2\pi\rho_{BS}[(2R_c-r_u)^{2-\eta}-(R_{nw}-r_u)^{2-\eta}]}$ .

Simulations are performed to assess the performance of the proposed fluid modeling in two cases: non-shadowing and shadowing impact in the network.

## 4.5 Model evaluation: non-shadowing case

In this section, the differences of the data rate per cell obtained by fluid modeling and Monte Carlo simulations are first presented. Then, we estimate the EE of a small area constrained by  $0 < R_a \leq R_e$  and with different kinds of cellular networks. After, the investigation on the impact of the user density and the path-loss exponent on the cell EE for various cellular networks is studied. At the end, we evaluate the performance of EE over the first ring ( $R_e < R_a \leq 2R_c$ ) and the large cellular networks ( $0 < R_a \leq R_{nw}$ ), in order to validate the corresponding fluid models.

### 4.5.1 Simulation setup

Three values of the cell radius are considered as  $R \in \{1000, 200, 50\}$ m and stand for the macro, micro and femto cellular networks, respectively. We consider 15 rings of hexagonal cells around a central hexagon such that  $R_{nw} = 31R_c$ .  $N_u$  users are generated uniformly in the central hexagon and we assume that they are attached to the BS located at the center of the hexagon. To indicate the effect of pathloss, Erceg model [124] is utilized with  $A = (4\pi\zeta f)^2/(c\zeta^{\eta/2})^2$ ,  $\zeta = 100$  m,  $f = 2.5$  GHz,  $\eta = \{2.6, 2.8\}$  and  $c$  is the speed of light in air. Here, thermal noise density =  $-174$  dBm/Hz.

For Monte Carlo (MC) simulations, the results presented here are obtained by averaging over 3000 MC simulations. The main idea of Monte Carlo trails is as follows. First, we initial the number of iterations and the number of UEs. Then, we create the location of all BSs and UEs, and compute the  $\gamma_u$  for every UE in every iteration. Based on the  $\gamma_u$ , we compute the total data rate of all UEs located at a disc region with radius  $R_a$ . Next, we update the iteration and repeat the above process until finishing all the iterations. After that, we average the total data rate over the number of iterations and obtain the averaged data rate. We also compute the total power consumption for the networks. Finally, using the definition of EE in Eq. (3.1), we compute EE with the average data rate and the total power cost.

The numerical results of fluid modeling are obtained by simulating  $D_{area}$  using Eq.(4.3) for the first scenario, Eq. (4.6) for the second scenario and Eq. (4.7) for the third scenario, after replacing them in EE definition, as shown in Eq. (3.1). The other simulation parameters are set up according to Table 3.1 for the power consumption model as defined in [68], and Table 4.2 for the other network parameters.

Table 4.2 Simulation Parameter Value

Parameters	Value
System bandwidth $BW_n$	10MHz
Carrier frequency	2GHz
Cell radius $R$	{1000, 200, 50}m for macro, micro and femto resp.
Half distance between BSs, $R_c$	$R\sqrt{3}/2$
Range of network $R_{nw}$	$31R_c$
Radius of interested area $R_a$	$[R/20 \quad 2R_c]$
Equivalent radius of one cell, $R_e$	$R_c\sqrt{2\sqrt{3}/\pi}$
Number of antennas $N_{ant}$	1
Number of users $N_u$	{100, 500}
Path loss exponent $\eta$	{2.6, 2.8}
Density of BSs $\rho_{BS}$	$1/(2\sqrt{3}R_c^2)$
Density of users $\rho_u$	$N_u/(2\sqrt{3}R_c^2)$

### 4.5.2 Model accuracy

In order to validate the accuracy of our model, we compute the difference of EE obtained by fluid modeling and Monte Carlo simulations, considering the same  $R_a$ ,  $\eta$ ,  $BW_n$ ,  $N_u = \{100, 500\}$  in a macro cellular network. The difference is plotted in Fig. 4.6 and computed

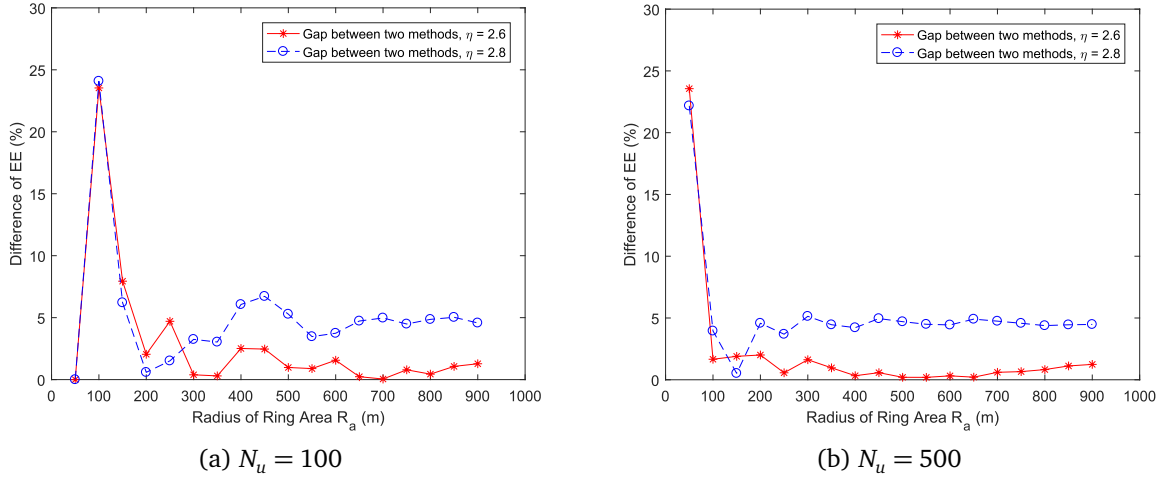


Fig. 4.6 EE difference vs network radius  $R_a$

by

$$Difference = \frac{|EE \text{ by Fluid} - EE \text{ by Monte Carlo}|}{EE \text{ by Fluid}} \times 100\% \quad (4.24)$$

As seen, the relative error is smaller than 7% when  $R_a > 150\text{m}$ ,  $N_u = 100$  in Fig. 4.6(a). This illustrates that fluid modeling can be considered as an effective tool to evaluate EE. When the number of users per cell is increased to 500, a similar phenomenon is observed in Fig. 4.6(b). Specially, the curves in Fig. 4.6 show significant differences when  $R_a < 150\text{m}$ , e.g., about 24% with  $\eta = 2.6$ ,  $R_a = 100\text{m}$  in Fig. 4.6(a) and 23% with  $\eta = 2.6$ ,  $R_a = 80\text{m}$  in Fig. 4.6(b). Since the number of users may be zero when  $R_a$  is very small for Monte Carlo simulations. However, non-zero data rate exists over an area with any size for the fluid modeling.

#### 4.5.3 EE variation vs cell network types

Considering the first scenario, Fig. 4.7 depicts the EE metric in macro ( $R = 1000m$ ), micro ( $R = 200m$ ) and femto ( $R = 50m$ ) cellular networks as a function of various  $R_a$  values, i.e., the radius of the cell over the serving BS, for  $\eta = 2.6$  and  $\eta = 2.8$ , respectively. These figures confirm that the proposed model is effective and match well with Monte Carlo results, whatever the types of the cellular networks. We observe a small difference between these curves, mainly at the network edge, due to the circular shaped form considered in fluid modeling. So, whatever the position of users in the inner circle, the average of the external power of all neighboring BSs is the same. However, in the hexagonal model, this assumption is no longer true, since we consider the real distance from neighboring BSs.

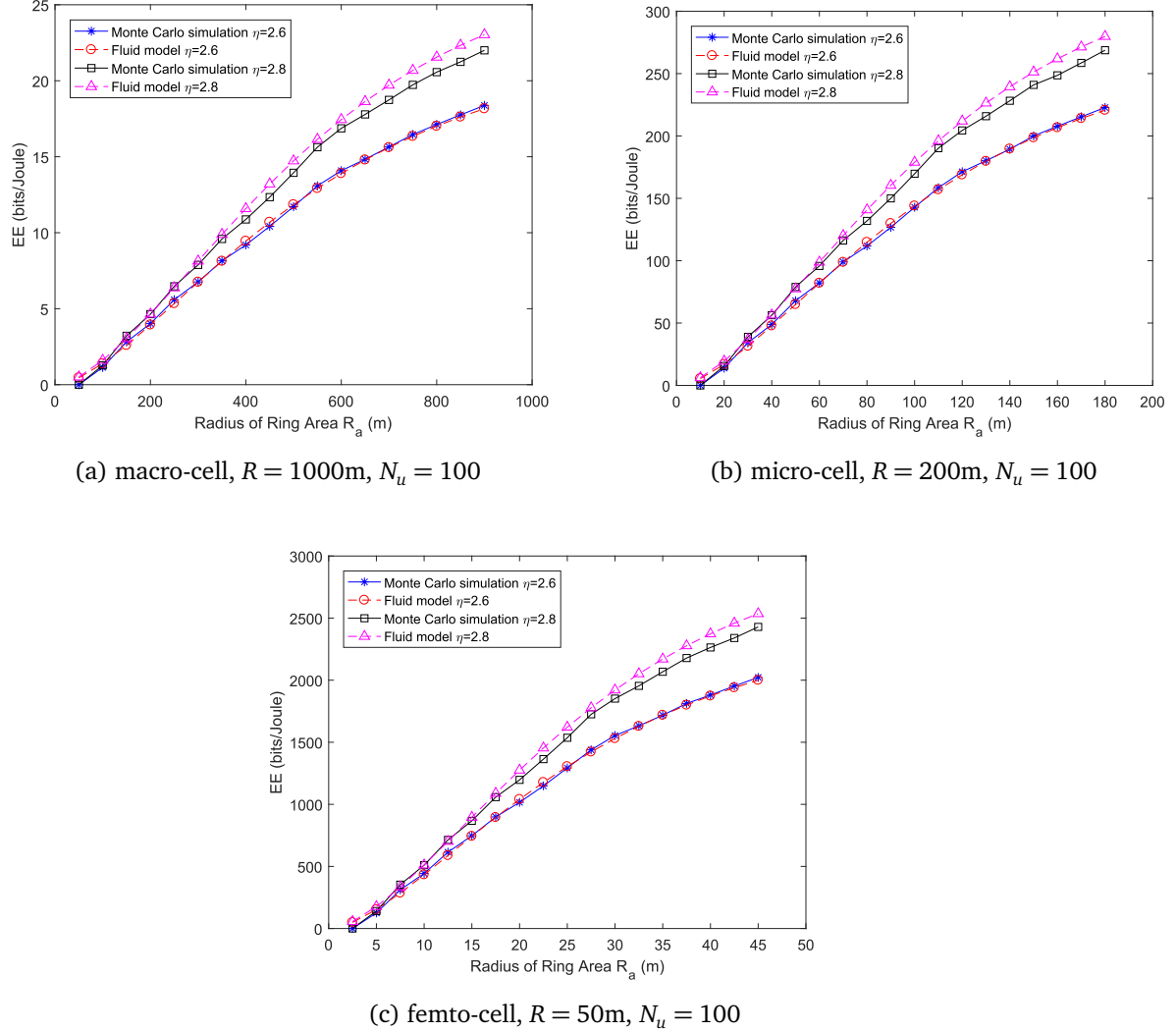


Fig. 4.7 EE variation vs network radius  $R_a$  for different network types.

Moreover, we observe that EE is improved with the increase of  $R_a$ . Surprisingly, EE is less effective closer to the BS, even though the SIR is high. Indeed, the total power consumption overall the network is much higher than the total data rate of a network with radius  $R_a$ . However, in this case, EE raises fast, due to the ratio between the cell area of radius  $R_a$  and the total network area of radius  $R_{nw}$ . For example, in Fig. 4.7(a), EE raises quickly for  $R_a \in [0, 600]$  and EE increases slightly for  $R_a \in [600, R_e]$ , since the SIR for a given user far from its serving BS is small in this case.

Furthermore, results show that EE is about  $24\text{bits/Joule}$  for the macro-cell network in Fig. 4.7(a) for  $\eta = 2.8$  and  $R_a = R_e$ . EE values are, respectively, near  $260\text{bits/Joule}$  for a micro-cell network in Fig. 4.7(b), and about  $2.5\text{Kbits/Joule}$  for a femto-cell network

in Fig. 4.7(c). However, the transmitting power per BS decreases from  $80W$  to  $0.25W$ . It means that small-cell networks can save a lot of energy during the transmission due to their lower energy dissipation and attenuation compared to the macro cellular networks. Therefore, the small-cell network is more efficient than a macro-cell one and a micro-cell one, which is consistent with findings in [82].

#### 4.5.4 Impacts of user's density on EE

Fig. 4.8 depicts the EE performance in a macro cellular network as a function of various  $R_a$  values, i.e., the size of the cell over the serving BS, with  $N_u = 500$ ,  $\eta = 2.6$  and  $\eta = 2.8$  respectively. In this case, the numerical values show the accuracy of the fluid modeling for EE evaluation. While comparing Fig. 4.8 and Fig. 4.7(a) with  $N_u = 500$ , we observe that the numerical values of EE are identical, for example, for  $R_a = R_e$  and  $\eta = 2.6$ , the energy efficiency is about  $EE = 18.16\text{ bits/Joule}$ , regardless the number of users  $N_u$ . Indeed, the data rate over the network area is not related to  $\rho_u$  and  $N_u$ , as defined in Eq. (4.3).

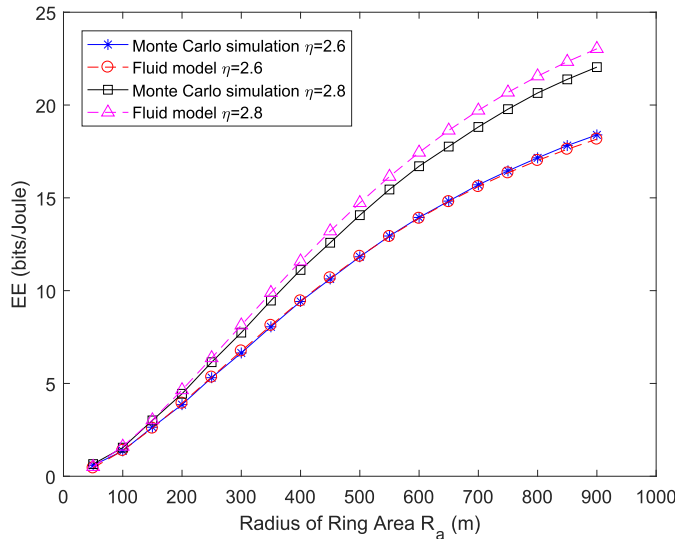


Fig. 4.8 EE variation vs network radius,  $R_a$ , with  $R = 1Km$ ,  $N_u = 500$

#### 4.5.5 EE vs path-loss exponent

While considering the thermal noise  $N_0 = -174\text{dBm/Hz}$  and  $N_u = 100$ , Fig. 4.9 shows the variation of EE over the cell ( $R_a = R_e$ ) depending on different path loss exponents  $\eta$  in case of macro and femto cellular networks, i.e.,  $R = 1000m$  and  $R = 50m$ , respectively. The results show that EE increases with the growth of  $\eta$  in both types of cellular networks.

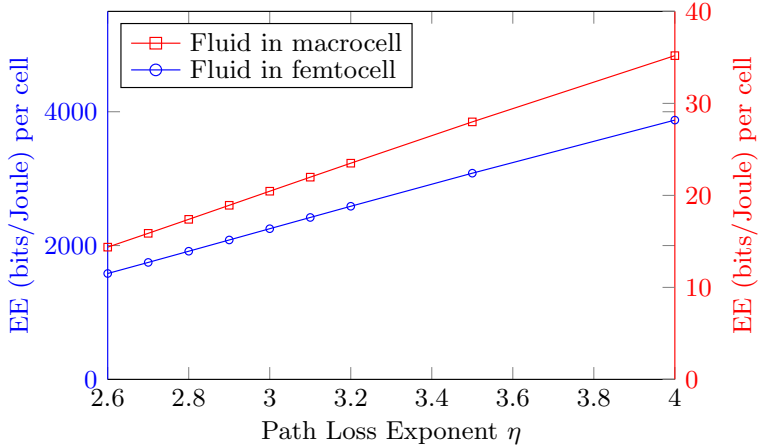


Fig. 4.9 EE vs path loss exponent in macro and femto cellular network

Interestingly, when  $\eta$  ranges from 2 to 3, i.e., from the free space to suburban environment, the dissipation of transmitting power becomes great. However, in this case the SIR for a fixed user increases leading to the EE improvement. Moreover, we observe that there is an obvious increase of EE in femto cellular one, owing to that the power expenditure for femto-BS is very small. Therefore, deployment of femto cells is more efficient to satisfy the 5G requirements.

#### 4.5.6 EE variation over a first ring

In a practical case, with the movement of UEs from the central cell to the adjacent cell, the data rate of UEs will change. As a result, the total data rate and the EE over a network area will be changed. Therefore, it is interesting to investigate the EE variation depending on the radius of the network area of interest  $R_a$ , in case of the second scenario,  $R_e < R_a \leq 2R_c$ , for different types of cellular networks. We observe that EE values increase fast when  $R_e < R_a \leq 2R_c$  w.r.t those of one cell, since the total data rate grows quickly for users close to their serving BS. Furthermore, results show that the EE is about 72 bits/Joule for the macro-cell network in Fig. 4.10(a) for  $\eta = 2.8$  and  $R_a = 2R_c$ , and it is about 7.9 Kbits/Joule for a femto-cell network in Fig. 4.10(c). It turns out that the small-cell network is more efficiency than a macro-cell one.

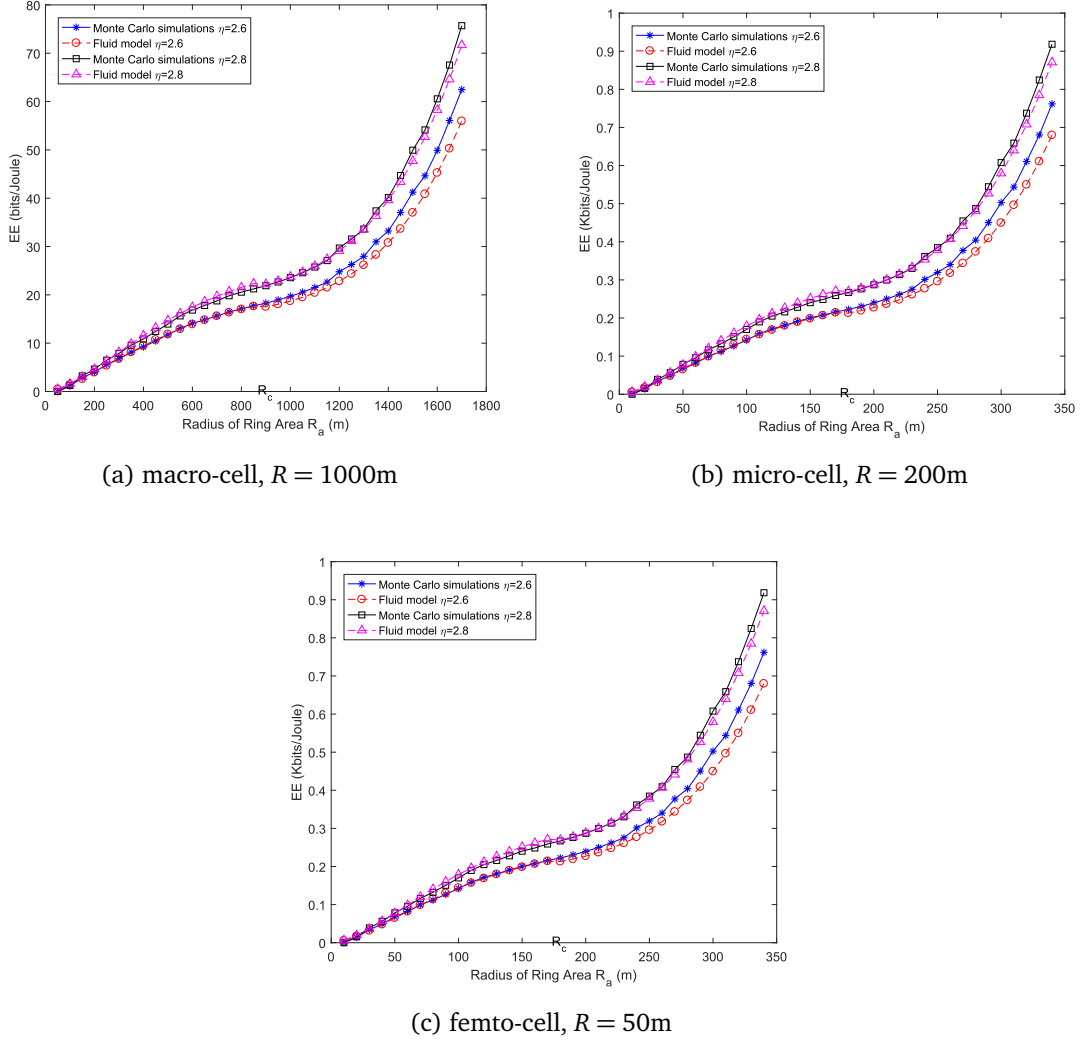
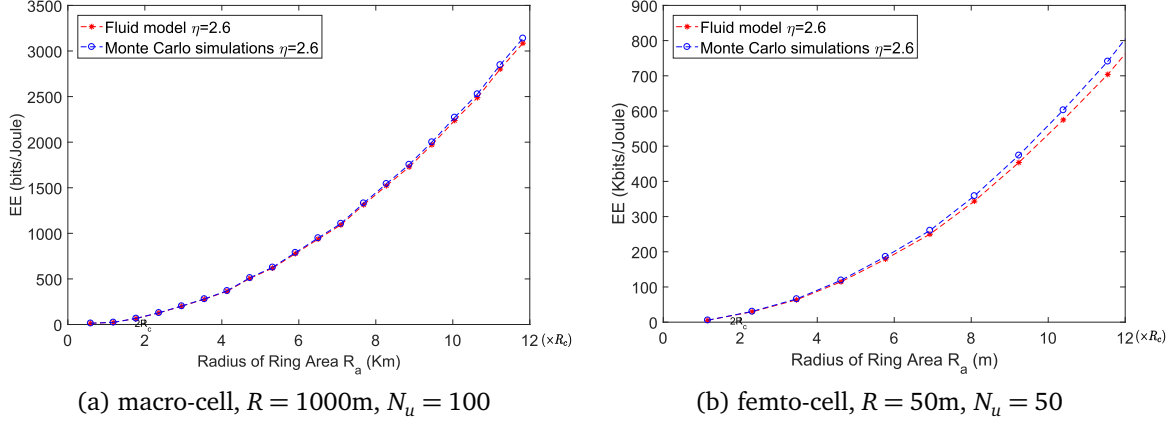


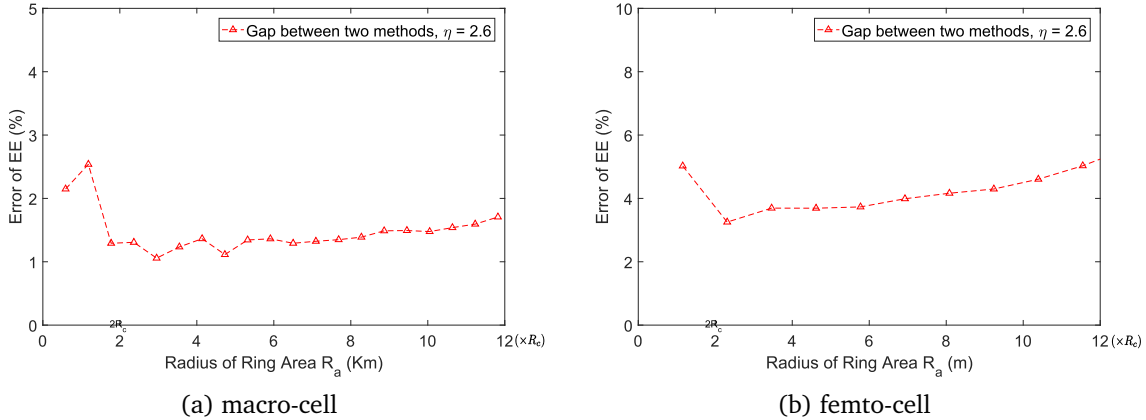
Fig. 4.10 EE variation vs network radius in a first ring

#### 4.5.7 EE variation over a large network

Finally, we assess the EE over a macro cellular network and a femto cellular network in case of the third scenario,  $0 < R_a \leq R_{nw}$ . Fig. 4.11 depicts the EE variation depending on the radius of the network area, with path-loss exponent  $\eta = 2.6$ , the number of users per cell  $N_u = 100$  and  $N_u = 50$ , respectively, in both types of cellular networks. We observe that the results obtained by the proposed model match well with the ones achieved by Monte Carlo simulations, which shows that the proposed model is accurate. This accuracy is further illustrated in Fig. 4.12, where the related relative error is given. The results show that all error values are below 2.5% in the macro cellular network and are below 5% in the

Fig. 4.11 EE vs network radius  $R_a$ 

femto cellular network. Thus, it illustrates that the proposed approach is an efficient and accurate tool to evaluate EE for any size of networks.

Fig. 4.12 EE error vs network radius  $R_a$ 

Using the tool of fluid modeling, we also compute the average EE over a macro cellular network and a femto cellular network, considering the same  $\eta = 2.6$ ,  $BW_n = 10\text{MHz}$ ,  $N_u = \{100, 50\}$ . The average EE, *Average EE*, is plotted in Fig. 4.13 and computed by

$$\text{Average EE} = \frac{D_{\text{area}}}{\rho_{\text{BS}} \times S_{\text{area}} \times P_{\text{exp}}} \quad (4.25)$$

where  $D_{\text{area}}$  is the total data rate over a network area with radius  $R_a$ ,  $S_{\text{area}}$  is the corresponding area of the network, and  $\rho_{\text{BS}}$  denotes the density of BSs over the entire network, respectively.

As seen from Fig. 4.13, we observe that the average EE values first decrease, then increase, and finally converge to a constant value, while varying  $R_a$ . Indeed, as the network is homogeneous, fluid modeling considers that the transmitting power over any subsurface area of the network is same, which causes the same power consumption over any subsurface area. Therefore, the average EE decreases, for  $R_c/2 < R_a \leq 1.3R_c$ , due to the slow increase of data rate  $D_{area}$  as well as the higher power cost. For  $1.3R_c/2 < R_a \leq 2R_c$ , the average EE values increase, since the data rate  $D_{area}$  contains more UEs, which are close to their serving BSs and have higher SIR. In particular, for  $R_a > 4R_c$ , we can observe that the average EE over a very large network, is the same as the average EE over one cell in both two figures. For example, for a macro cellular network, the average EE converges to  $13.3\text{Kbits/Joule}$  and for a femto cellular network, it converges to  $1.5\text{Mbits/Joule}$ . Since a large homogeneous network is actually composed of many identical cells and every cell has the same UEs distribution and same transmitting power. According to the convergence law of large numbers in probability theory, i.e., the average of the whole observed samples gets close to the average of an observed sample, the large network can be regarded as the sum of all cells, resulting the average EE over the entire network equals the individual average EE.

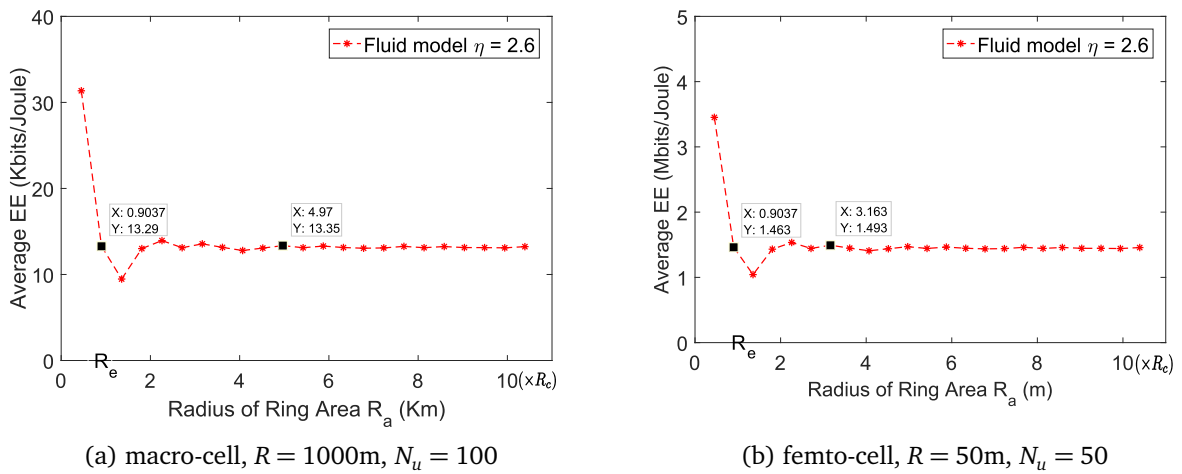


Fig. 4.13 Average EE vs network radius  $R_a$

## 4.6 Model evaluation: shadowing case

The aim of this section is threefold. First, we intend to show the relationship between the SINR threshold  $\Gamma_{th}$  and the UE's distance  $r$  in the case of a fixed coverage probability and

a known path-loss exponent. The closed-form expression is obtained through a polynomial curve fitting (PCF), and compared to the results obtained by the fluid modeling. Then, taking advantage of this above expression, we show the accuracy of the EE formula proposed by comparing the simulation results to those of Monte Carlo simulations over an equivalent hexagonal network while considering the impact of shadowing. Finally, we investigate the EE error between the fluid framework and Monte Carlo simulations, with the consideration of the same parameters values of path-loss exponent and standard deviation of shadowing.

#### 4.6.1 Simulation setup

The numerical results of fluid modeling are obtained by the simulations based on Eqs. (3.7), (4.17), and (4.23). We compute the coverage probability for every  $r_u$  according to Eqs. (4.16) and (4.21) in Monte Carlo simulations (sim.). The results of EE are obtained through averaging over 3000 independent iterations of Monte Carlo simulations. Here, we set  $\mathbb{P}_{cov}^r = \{0.7, 0.9\}$  since the  $\mathbb{P}_{cov}^r$  is required to be large enough to make sure good signal quality for all UEs [123]. According to Table 3.1 and Table 4.3, we set the other simulation parameters.

Table 4.3 Simulation Parameter Value

Parameters	Value
System bandwidth, $BW_n$	10MHz
UEs minimum distance to BS, $D_{min}$	10m
Half distance between BSs, $R_c$	{50, 1000}m
Cell radius, $R$	$2R_c/\sqrt{3}$
Range of network, $R_{nw}$	$15R_c$
Equivalent radius of one cell, $R_e$	$R_c\sqrt{2\sqrt{3}/\pi}$
Radius of interested area, $R_a$	[ $R/30$ $R_e$ ]
Number of antennas, $N_{ant}$	1
Number of users, $N_u$	{50, 100}
Path loss exponent, $\eta$	{2.6, 3}
Density of BSs, $\rho_{BS}$	$1/(2\sqrt{3}R_c^2)$
Density of users, $\rho_u$	$N_u/(2\sqrt{3}R_c^2)$
Shadowing standard deviation, $\sigma$	{3, 6, 8} dB
Coverage probability, $\mathbb{P}_{cov}^r$	{0.9, 0.7}

#### 4.6.2 Relationship between $\Gamma_{th}$ and $r$

As presented before, for the purpose to set up the relationship between  $\Gamma_{th}$  and  $r$ , we compare in Fig. 4.14, the coverage probability,  $\mathbb{P}_{cov}^r$ , obtained by fluid modeling framework to that obtained via Monte Carlo simulations (sim.) for the UEs located at the distance of  $r = R_c/3$ ,  $r = R_c/2$  and  $r = R_c$ , respectively, considering the lognormal shadowing deviation  $\sigma = 6\text{dB}$  and the path-loss exponent  $\eta = 3$ . The figure shows that the analytical fluid modeling gives results very close to those obtained by Monte Carlo simulations (sim.). Moreover, for a fixed coverage probability, the SIR threshold  $\Gamma_{th}$  varies depending on the UEs locations or distances to the serving BS, since we neglect the noise here. For example, we observe that for  $\mathbb{P}_{cov}^r = 90\%$ ,  $\Gamma_{th} = 11\text{dB}$ ,  $3.5\text{dB}$  and  $-8\text{dB}$  for  $r = R_c/3$ ,  $r = R_c/2$  and  $r = R_c$ , respectively, which due to the poor mean SIR for the cell-edge UEs. Obviously, a lower SIR threshold should be defined for UEs which are far from their serving BS in order that they can be covered.

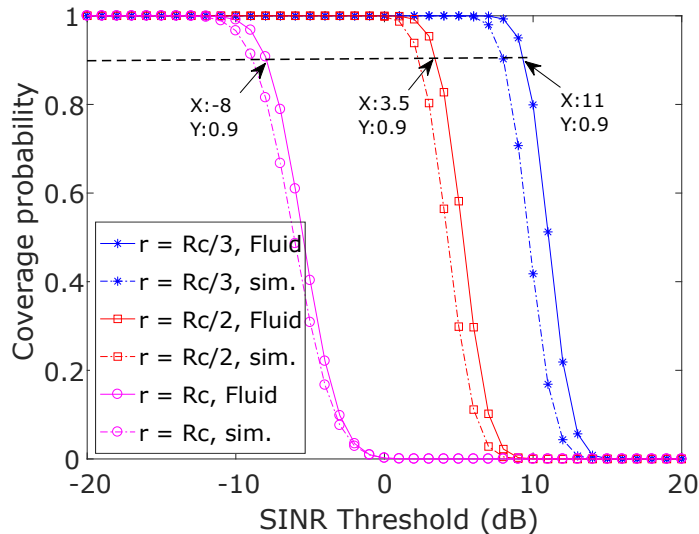


Fig. 4.14 Coverage probability vs SINR threshold for fixed UEs

Considering coverage probability  $\mathbb{P}_{cov}^r = 90\%$  and  $\mathbb{P}_{cov}^r = 70\%$  in the femto and macro cellular networks, Fig. 4.15 depicts the SINR threshold  $\Gamma_{th}$  as a function of the distance  $r$  of a UE to its serving BS while the shadowing standard deviation values  $\sigma$  are  $3\text{dB}$ ,  $6\text{dB}$  and  $8\text{dB}$ , respectively. In fact, we compare the results based on Eq. (4.21) using the fluid modeling to those derived from the Eq. (4.22) of the polynomial curve fitting (PCF) method. Fig. 4.15 shows that the obtained curves through the two methods all exhibit the same shape and match very well whatever the  $\sigma$  values, the  $\mathbb{P}_{cov}^r$  values and the types of cellular networks. Therefore, we can use the third degree polynomial of  $r$  to approximate the SIR

threshold  $\Gamma_{th}$  in both cases of  $\mathbb{P}_{cov}^r = 90\%$  and  $\mathbb{P}_{cov}^r = 70\%$ , which shows the effective and the accuracy of Eq. (4.22).

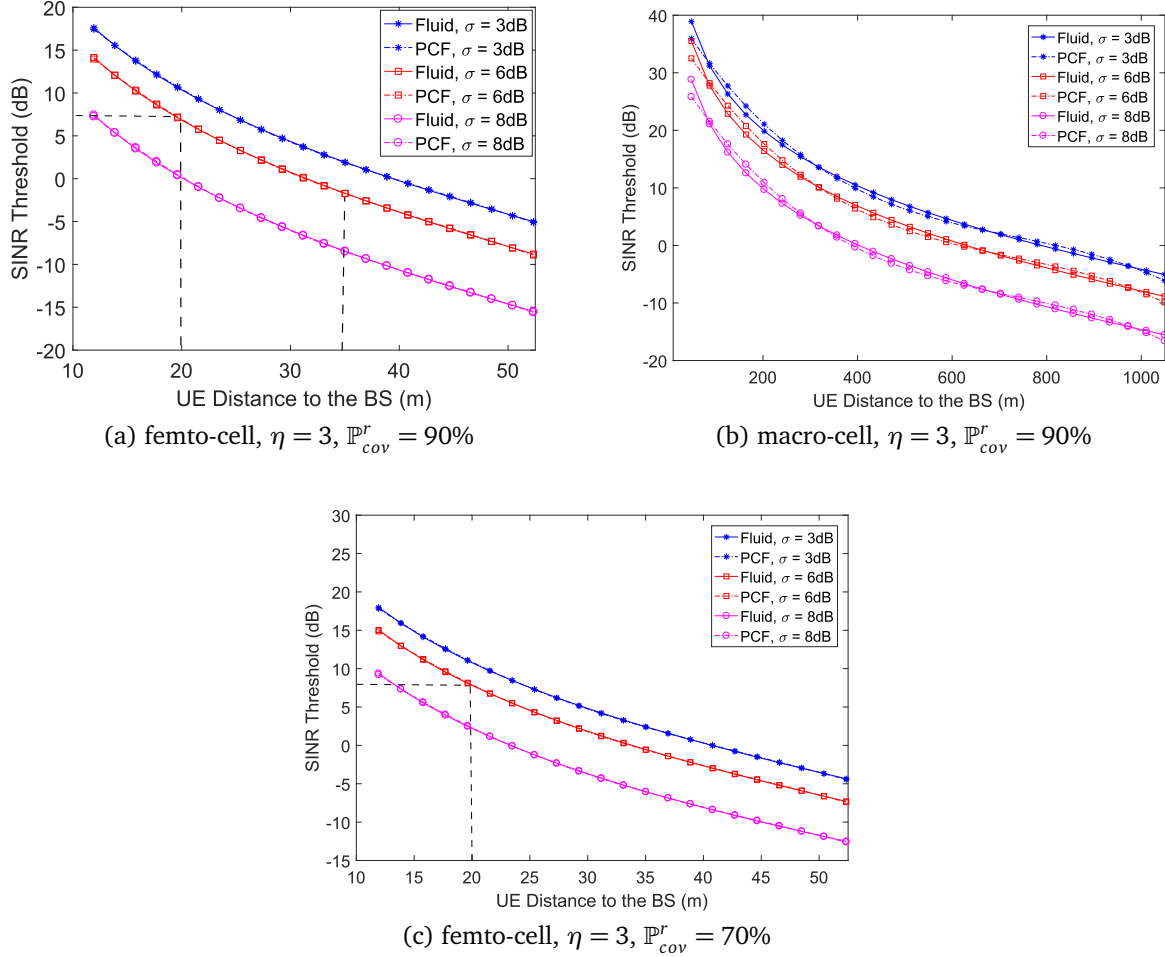


Fig. 4.15 SINR threshold  $\Gamma_{th}$  vs UE distance to the BS; Between fluid model and polynomial curve fitting (PCF)

Furthermore, comparing the numerical values in Fig. 4.15(a) and Fig. 4.15(c), we observe that the SINR threshold  $\Gamma_{th}$  in a femto cellular network increases with the decrease of  $\mathbb{P}_{cov}^r$ , for a fixed distance, a given  $\sigma$  and the same  $\eta$ . For example, for  $r = 20\text{m}$ ,  $\sigma = 6\text{dB}$  and  $\eta = 3$ , we find that  $\Gamma_{th} = 7\text{dB}$  for  $\mathbb{P}_{cov}^r = 90\%$  and  $\Gamma_{th} = 8\text{dB}$  for  $\mathbb{P}_{cov}^r = 70\%$ . Indeed, for a higher coverage probability, the SINR threshold is required to be lower in order to guarantee the good signal quality for UEs. Since the UEs may be not included in the coverage when SINR threshold is larger, which leads to a lower coverage probability.

Additionally, for a fixed distance and a given  $\mathbb{P}_{cov}^r$  and the same  $\eta$  in Fig. 4.15, the SINR threshold  $\Gamma_{th}$  decreases with the raise of  $\sigma$ . For example, for  $r = 35\text{m}$ ,  $\Gamma_{th} = 0\text{dB}$  for

$\sigma = 6\text{dB}$  and  $\Gamma_{th} = -6\text{dB}$  for  $\sigma = 8\text{dB}$  in Fig. 4.15(a). The reason is that the higher value of  $\sigma$  leads to more serious shadow fading and then a lower SINR at a certain distance. This observation has been already demonstrated in [113], that is the shadowing significantly impacts on the coverage performance especially when the SINR thresholds are small.

For further illustrating the accuracy of polynomial curve fitting (PCF) method, we compute the  $\Gamma_{th}$  fitting error as the difference between the fluid modeling and the PCF in a femto cellular network with  $\eta = 3$  and coverage probability  $\mathbb{P}_{cov}^r = 90\%$ , as shown numerically in Table 4.4. We observe that the error does not exceed 0.2, which validate the accuracy of PCF. Therefore, this method can be used to compute data rate and energy efficiency in the below part.

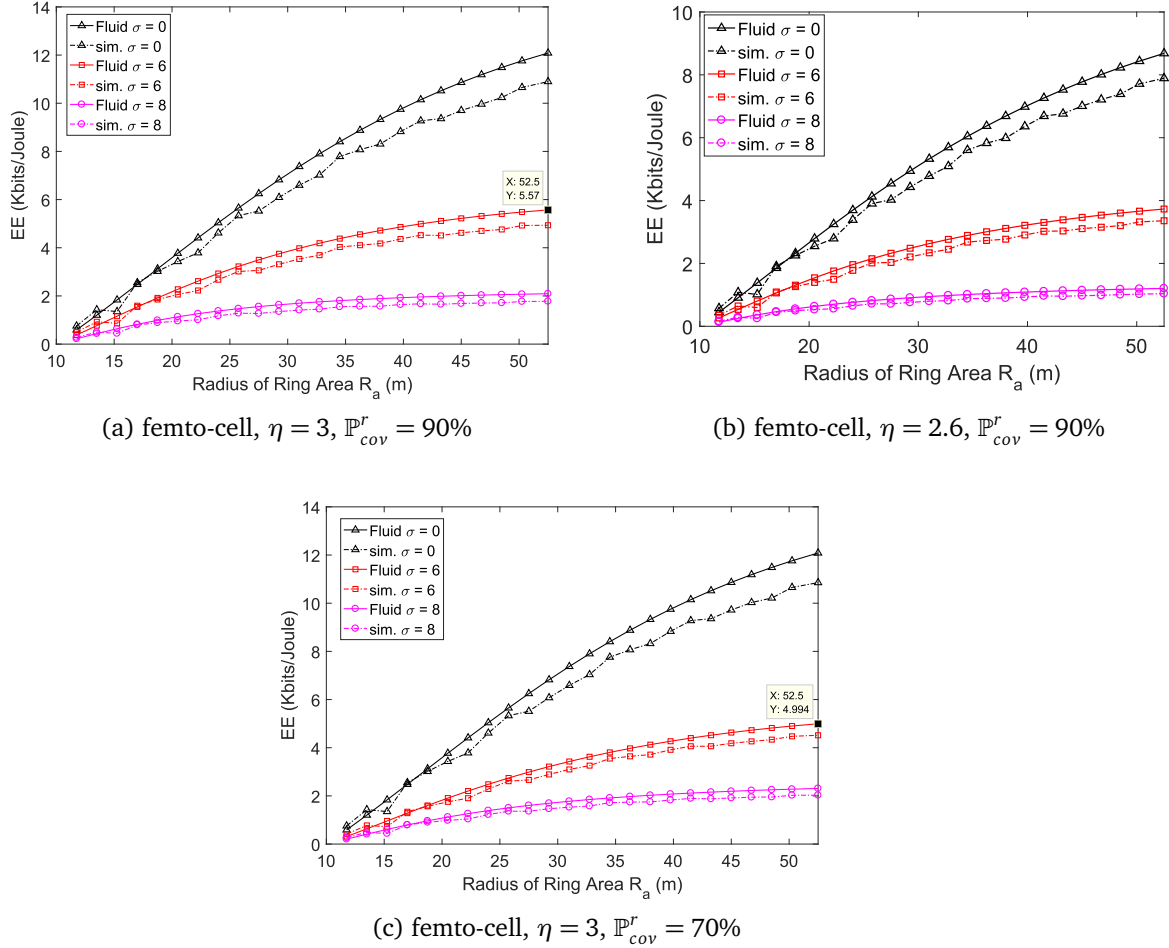
Table 4.4  $\Gamma_{th}$  fitting error between fluid and PCF with  $\mathbb{P}_{cov}^r = 90\%$ ,  $R = 50m$ ,  $\eta = 3$

	$r_u$ (m)									
	11.9	15.8	19.6	25.4	29.3	35	40.8	44.6	50.4	52.3=R <sub>e</sub>
<b><math>\sigma=3</math></b>	0.1802	0.1035	0.0902	0.0339	0.0764	0.0463	0.0404	0.0745	0.0154	0.1059
<b><math>\sigma=6</math></b>	0.1803	0.1036	0.0903	0.0339	0.0764	0.0465	0.0404	0.0746	0.0154	0.1062
<b><math>\sigma=8</math></b>	0.1814	0.104	0.0911	0.0339	0.077	0.0471	0.0406	0.0754	0.0154	0.1076

According to the polynomial expression of  $\Gamma_{th}$ , in the following part we will show some results of energy efficiency (EE) based on Eq. (3.1), when replacing the data rate  $D_{area}$  with Eq. (4.23).

#### 4.6.3 Energy efficiency discussion

Fig. 4.16 and Fig. 4.17 depict the EE variations in a femto cellular network and in a macro cellular network depending on  $R_a$ , i.e., the size of the ring over the serving BS. Both figures are obtained using the analytical model we proposed and Monte Carlo simulations (sim.) for three cases, depending on the standard deviation value  $\sigma = 0\text{dB}$  (without shadowing),  $\sigma = 6\text{dB}$  and  $\sigma = 8\text{dB}$ . The coverage probability is set  $\mathbb{P}_{cov}^r = 90\%$  or  $\mathbb{P}_{cov}^r = 70\%$ . Both of two figures confirm that the proposed model is effective and matches well with the Monte Carlo results, whatever the value of the path-loss exponent ( $\eta = 3$  or  $\eta = 2.6$ ). In addition, we observe a small difference between these curves due to the circular shape considered in the fluid modeling. Since in fluid modeling, the average interference factor  $y_f(r, \eta)$  without shadowing based on Eq. (3.7) is the same, resulting the same SINR threshold value

Fig. 4.16 EE variation vs network radius  $R_a$  in femto cellular network

according to Eq. (4.21). However, in the hexagonal modeling, the  $y_f(r, \eta)$  is calculated according to the real UEs' distances from neighboring BSs.

Furthermore, while comparing Fig. 4.16(a) and Fig. 4.16(c) with  $\mathbb{P}_{cov}^r = 90\%$  and  $\mathbb{P}_{cov}^r = 70\%$ , respectively, we observe that the numerical values of EE, obtained by fluid modeling, decrease with the reduction of  $\mathbb{P}_{cov}^r$  for same values of  $R_a$ ,  $\eta$  and  $\sigma$ . For example, the EE is about  $5.57\text{Kbits/Joule}$  for  $\eta = 3$ ,  $\sigma = 6\text{dB}$  and , at the cell edge ( $R_a = R_e$ ) and  $\mathbb{P}_{cov}^r = 90\%$ , whereas the EE is about  $4.99\text{Kbits/Joule}$  when  $\mathbb{P}_{cov}^r = 70\%$ . Since a higher coverage rate can lead to a larger data rate, and thus a larger EE can be obtained.

Moreover, focusing on Fig. 4.16(a), we observe that the values of EE decreases in a femto cellular network with the increase of  $\sigma$  for a fixed value of  $R_a$ . For example, in the case of  $R_a = 30\text{m}$ , EE is about  $3.85\text{Kbits/Joule}$  for  $\sigma = 6\text{dB}$ , and it is about  $1.65\text{Kbits/Joule}$

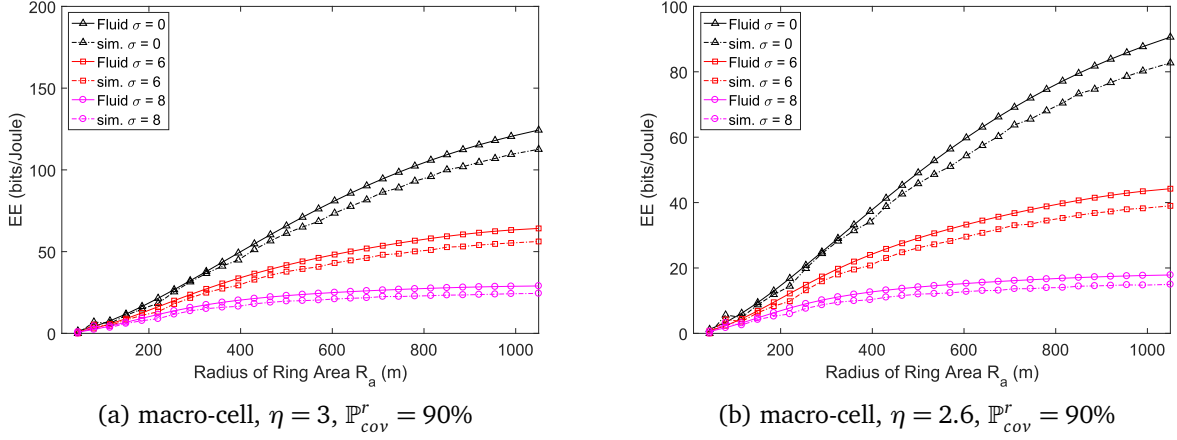


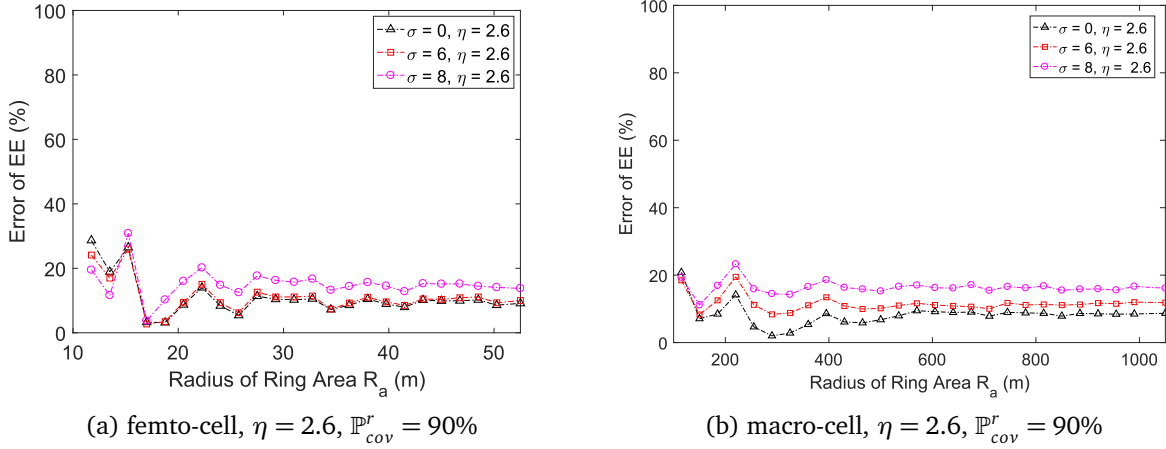
Fig. 4.17 EE variation vs network radius  $R_a$  in macro cellular network

for  $\sigma = 8$ dB. In fact, the larger the shadowing, the lower the achieved throughput of UEs. The similar conclusion can be found in other figures of Fig. 4.16 and in Fig. 4.17.

In addition, while comparing Fig. 4.16(a) and Fig. 4.16(b) in a femto cellular network with  $\mathbb{P}_{cov}^r = 90\%$ , we observe that the numerical values of EE, obtained by fluid modeling, decrease with the reduction of  $\eta$  for same values of  $R_a$  and  $\sigma$ . For example, the EE is about  $5.57K\text{bits}/\text{Joule}$  for  $\eta = 3$ , at the cell edge ( $R_a = R_e$ ) and  $\sigma = 6$ dB, whereas the EE is about  $3.73K\text{bits}/\text{Joule}$  when  $\eta = 2.6$ . When  $\eta$  ranges from 3 to 2, i.e., from the suburban environment to the free space, the dissipation of the transmission power reduces. However, in this case the SIR at a fixed distance decreases, which further leads to the EE decline. Therefore, EE decreases as  $\eta$  reduces. Comparing Fig. 4.17(a) and Fig. 4.17(b) in a macro cellular network with  $\mathbb{P}_{cov}^r = 90\%$ , we can find the same conclusion.

#### 4.6.4 EE model accuracy

For the accuracy purpose, in Fig. 4.18 we compute the EE error between the proposed fluid modeling and Monte Carlo simulations, depending on the network radius  $R_a$  of a femto cellular network and a macro cellular network, respectively, with  $\eta = 2.6$  and  $\mathbb{P}_{cov}^r = 90\%$ . In Fig. 4.18(a), we observe that the error is less than 20% for  $R_a > 17$ m in a femto cellular network, whatever the values of  $\sigma$ . Meanwhile, the results in Fig. 4.18(b) also show a error of less than 20% for  $R_a > 100$ m in a macro cellular network. Those numerical results illustrate the accuracy of fluid modeling as a tool for performance evaluation while considering the impact of shadowing. However, the EE error is less than 30% for  $10 < R_a < 17$ m in a femto cellular network, since the fitting error of  $\Gamma_{th}$  between fluid and PCF is larger for  $10 < R_a < 17$ m, as shown in Table 4.4.

Fig. 4.18 EE error vs network radius  $R_a$  in cellular networks

## 4.7 Conclusion

In this chapter, we propose a tractable expression of EE based on fluid modeling in an OFDMA cellular network. The model is proposed for a network area within the central cell and is extended to compute the EE for network area, with any size. The proposed EE model is assessed under the two conditions of non-shadowing and shadowing.

While neglecting the impact of shadowing, we assess the EE in three types of cellular networks including macro, micro and femto cellular networks. The model accuracy of the obtained EE model is shown through a comparison with Monte Carlo trials. Additionally, the results also exhibit that: 1) the density of users per cell has no impact on the EE, since the analysis is considered only in downlink transmissions, 2) EE is independent from the users' density but proportional to the path-loss exponent, 3) a femto cellular network is more efficient than the macro one, and 4) the proposed EE model over the network area with any size is accurate.

While taking the impact of shadowing and the path-loss exponent into account, we first developed a closed-form polynomial formula between UEs' location and the signal quality threshold using polynomial curve fitting (PCF) for a fixed coverage probability. Then taking advantage of this formula, we evaluated the energy efficiency (EE) based on the fluid modeling in an OFDMA femto and a macro cellular network. Finally, we shown the accuracy of the obtained EE models through a comparison with Monte Carlo trials. The results shown the effective of fluid modeling as a mathematical tool to evaluate the EE with the consideration of shadowing impact. The numerical results also illustrated the impact of

shadowing on EE, i.e., EE decreased with the raise of the lognormal shadowing standard deviation value of  $\sigma$ .

The results of this chapter provide adequate insights into that fluid modeling can be considered as an accuracy tool to evaluate the network EE with/without considering the effect of shadowing. Accordingly, in the following chapter, we derive an energy efficiency model for a cellular network based on the fluid modeling while using the joint transmission coordinated multipoint(JT-CoMP) scheme. Since the application of JT-CoMP brings the power consumption due to the more channel estimation operation, more overhead to deploy the coordinated cooperative base stations.

# Chapter 5

## EE analysis of JT-CoMP scheme in macro/femto cellular networks

### Contents

5.1	Introduction . . . . .	92
5.2	JT-CoMP scheme . . . . .	93
5.3	JT-CoMP performance evaluation . . . . .	94
5.4	System model . . . . .	96
5.4.1	Energy efficiency model with JT-CoMP scheme . . . . .	97
5.4.2	Power consumption model with JT-CoMP scheme . . . . .	97
5.4.3	SINR calculation: case of JT-CoMP . . . . .	98
5.5	Data rate computation . . . . .	100
5.5.1	Non-CoMP scenario . . . . .	102
5.5.2	AllUEs-CoMP scenario . . . . .	103
5.5.3	CoMP scenario . . . . .	103
5.6	Backhauling traffic computation: $C_{bh}$ . . . . .	104
5.7	Simulation and results . . . . .	104
5.7.1	Date rate vs the network radius . . . . .	105
5.7.2	EE vs radius $R_a$ in scenario AllUEs-CoMP . . . . .	107
5.7.3	Impact of distance threshold $d_{th}$ on cell EE $EE_{cell}$ in CoMP scenario .	111
5.7.4	EE gain vs BSs number . . . . .	112
5.7.5	Backhauling power cost vs BSs number . . . . .	114
5.8	Conclusion . . . . .	116

---

## 5.1 Introduction

5G wireless networks are expected to increase substantially data rates and quality-of-service (QoS) for users, at a similar or a lower power consumption as today's 4G networks. As discussed in chapter 1, Joint Transmission Coordinated Multipoint (JT-CoMP) transmission is a promising technology to improve the network energy efficiency (EE) and to fulfill upcoming communication demands [125], through turning the inter-cell interference into useful signals, especially for the cell-edge user equipments (UEs). Through taking advantage of the JT-CoMP technique, information is transmitted to a UE simultaneously from different coordinated BSs in order to improve the received signal quality and strength [47] as well as to enhance the spectral efficiency. However, this technology in practice also brings some additional energy consumption for transmitting the resource information, i.e., backhauling information. Additionally, while JT-CoMP approach is applied, the performance evaluation of energy efficiency (EE) becomes a hard task in terms of time expense to conduct simulations. Therefore, it is still an open issue to develop an accurate model for EE-evaluation while the JT-CoMP transmission is applied.

As illustrated in the results section of the previous chapter, fluid modeling can be considered as an effective and accuracy tool to evaluate EE for the cellular networks with/without taking the impact of shadowing into account. Since this modeling can reduce the analysis complexity and provide a macroscopic evaluation of the network performance. Therefore, spurred by the above advantages of fluid modeling, our objective in this chapter is to design a tractable model for evaluating EE based on the fluid modeling while JT-CoMP approach is considered in a network system.

In this chapter, we first introduce the concept of JT-CoMP in detail. Then, we discuss the JT-CoMP models and the numerical results in some literatures. Furthermore, combining our previous work in chapter 4, we derive a closed-form expression of EE based on the fluid modeling while the JT-CoMP approach is applied, which reduces the analysis complexity. Given that the definition of EE is related to the data rate and power consumption, we redefine a new power consumption model with considering the backhauling power consumption for the JT-CoMP system. Afterwards, depending on the JT-CoMP scheme, we consider three scenarios to compute the total data rate of the network area and the backhauling traffic. Finally, we discuss the simulation performance to prove the effectiveness and accuracy of our proposed model through a comparison between fluid modeling and Monte Carlo simulations.

## 5.2 JT-CoMP scheme

Before introducing the concept of JT-CoMP, we first recall the concept of CoMP since JT-CoMP is one of the main families coordination method of CoMP. As discussed in chapter 1, CoMP refers to a system where the transmission and/or reception at multiple, geographically separated antenna sites is dynamically coordinated in order to improve the coverage, cell-edge throughput and system efficiency. In a CoMP transmission system, several BSs are cooperated to transmit and receive data from multiple UEs based on the shared information between BSs so as to mitigate intercell interference and hence improve spectral efficiency. The set of several coordinated BSs is called as CoMP cooperative set, where the data is available at each BS. In the CoMP cooperative set, the BSs directly or indirectly participate in data transmission to UEs [126]. Hence, CoMP has been considered by 3GPP as a tool to provide a significant gain in terms of capacity and cell edge throughput.

Joint Transmission Coordinated Multipoint (JT-CoMP) is outlined by 3GPP [126], which is one of key strategies of CoMP. In JT-CoMP, data intended for a particular UE, comes jointly from multiple coordinated BSs (part of or entire CoMP cooperative set) at the same time and thus to improve the received signal quality as well as the spectral efficiency (SE) [75]. Fig. 5.1 illustrates the JT-CoMP scheme [40]. User 2 associates with BS 2 while user 1 associates with BS 1. Instead of serving their associated users independently, BSs 1 and 2 cooperatively transmit useful information to their users. For instance, if both BSs apply time-division multiple access (TDMA) in the first time slot, both BSs 1 and 2 transmit the same information to user 2. The user combines the signals from both BSs to decode the information. In the second time slot, the BSs cooperatively serve user 1. Due to JT, cell edge users experience higher receiving signal strength and lower interference, resulting the higher coverage and larger cell-edge throughput.

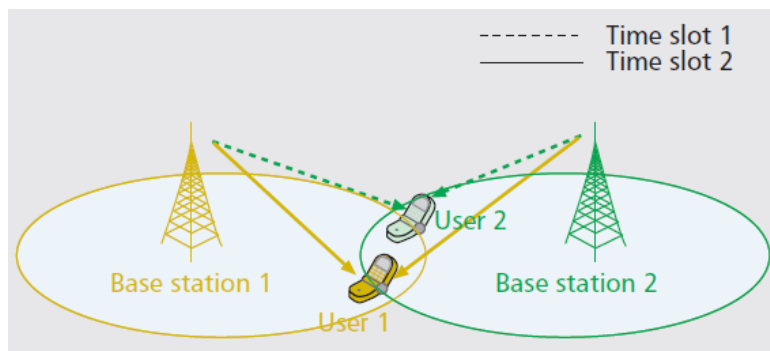


Fig. 5.1 JT-CoMP scheme [40]

According to the coordination way, JT-CoMP can be further classified into distance-based JT-CoMP technique and SINR-based one. In detail, in the former, several nearest BSs are intended to serve a UE, whereas in the SINR-based JT-CoMP technique, the best several BSs offering maximum SINR are selected to serve a UE.

### 5.3 JT-CoMP performance evaluation

EE evaluation is investigated in [75] for a downlink LTE-Advanced cellular system with using JT-CoMP scheme. Two JT-CoMP approaches are considered in that system, such as SINR-based JT-CoMP and distance-based JT-CoMP. Based on system-level simulations, simulation results illustrate that the SINR-based JT-CoMP scheme can achieve a superior EE performance compared to the distance-based JT-CoMP scheme.

In [91], authors investigate the problem of EE optimization in an OFDMA downlink heterogeneous network (HetNet) using a JT-CoMP transmission. The HetNet system is composed of several HetNet cells and they are coordinated via fiber backhauling, which can be called interbackhaul. Each of cell consists of one macro-BS, several low-power femto-BSs, and some uniformly distributed UEs. These femto-BSs are backhauled through fiber/microwave to the macro-BS in the one HetNet cell, which can be termed intrabackhaul. In particular, JT-CoMP is applied in the system when the received SINR at the UE is lower than 3dB. Using system-level simulations, simulation and analysis of results show that the EE first increases with respect to the SE and then decreases when the SE exceeds some value.

Additionally, the author in [125] investigated the outage probability and effective throughput of the system through taking advantage of the JT-CoMP technology. The JT-CoMP model is introduced as follows. A cellular network is considered, where each BS is located at the center of a hexagonal cell and all UEs are assumed to be distributed uniformly over a cell. Each cell is divided into the center zone, with a setting radius, and the edge zone. Accordingly, the distance-based JT-CoMP technique is only available for UEs, located at the edge zone over a downlink transmission so as to improve cell-edge performance. Based on this system model, analytical expressions of cumulative distribution function (CDF) of the SIR, outage probability and throughput are derived based on 2-dimensional Markov chain analysis, since the call arrival process is assumed to follow a Poisson process. The simulation results show that the system performance mainly depends on the center zone size and the offered load. Moreover, compared with the dynamic point selection scheme (one scheme dynamically switches the serving BS based on the UE's channel and the cell loading conditions), JT-CoMP scheme can achieve a lower outage probability.

Additionally, simulations in [41] show that JT-CoMP transmission and reception schemes have a significant effect in terms of improving the throughput of the cell-edge users based on the LTE-Advanced simulation conditions.

Moreover, a tractable model for Non-Coherent Joint-Transmission (NC-JT) cooperation is proposed in [127] while user-centric clustering and channel-dependent cooperation activation are taken into account. The user-centric clustering is defined such as, the cluster of cooperative BSs is formed around a typical user and the channel-dependent cooperation activation is defined such as, JT is adopted according to whether the channel to a cooperative BS is in deep fading. A single-tier OFDMA-based cellular system is considered, which is formed according to a stationary Poisson point process. The definitions of cooperative set and active cooperative set are introduced. The cooperative set is defined such as, if the received signal strength at a BS in the uplink is larger than a threshold, then this BS is grouped into the cooperative set. While, the active cooperative set is defined such as, if the signal received at the typical user is greater than a cooperation activation threshold, then this BS joins the cooperative transmission. The CDF of SINR of a typical user is characterized in the case of user-centric BS clustering. Simulation results show that when the NC-JT CoMP is used, increasing the BS density can improve the SINR, and that the average spectral efficiency is saturated at a cluster size of around 7 BSs with imperfect CSI at the receiver.

Until now, much leading work with JT-CoMP techniques is carried out either using system-level simulations or based on stochastic geometry. However, stochastic geometry framework yields to intractable models when non-Poisson point processes, eg., perturbed lattice,  $\beta$ -Ginibre point process, and Matérn point process, are considered to describe, in a more realistic way, the nodes' locations. In this case, either approximations or simulations are conducted to prove the model accuracy. In the other side, simulation-based models become resource-intensive when considering large networks, with a high number of base stations (BSs) and user equipments (UEs). As a result, an approximation-based is necessary to evaluate the network performance.

As mentioned before, spatial fluid modeling can be used to evaluate the network performance of cellular networks, such as SINR, outage probability, and energy efficiency through analytical expressions. In [99], the authors use this mathematical framework to study the SINR enhancement depending on the number of coordinated BSs and other network-related parameters in dense areas. The notation of the cooperation field is proposed to compute the power of coordinated BSs by integration. Depending on the number of coordinated BSs, three scenarios are considered. As a matter of fact, we use this tractable model to benchmark the EE variation depending on the network parameters, such as its size

and its type (macro, femto), the number of coordinated BSs, and the path-loss exponent as it reflects the network environment, while JT-CoMP is applied.

We combine here our previous work done in the last chapter to develop an EE model in the case of JT-CoMP. We first extend the fluid modeling with JT-CoMP to compute the total data rate over a network area. Then, we derive the closed-form expression of EE for the JT-CoMP downlink transmission, which is tractable and quite simple to compute. The effectiveness and the accuracy of the underlying model are shown for both types of cellular networks, macrocells and femtocells, by comparing the results to those of Monte Carlo (MC) simulations while considering several path-loss exponents and varying the number of cooperating BSs, in the case of a constant backhauling power cost. Furthermore, we investigate the EE improvement with the variation of the backhauling power cost, depending on some parameters, like the network area radius and the number of coordinated BSs. Actually, JT-CoMP is used to improve the signal quality of UEs far from their serving BS. Here, we define a distance threshold as well as the associated SIR threshold making JT-CoMP approach more efficient in terms of EE. We also discuss the impact of these thresholds in the case of variable backhauling power costs depending on the data rate requirement.

## 5.4 System model

To meet these objectives cited before, we consider the downlink channel of an OFDMA network with JT-CoMP approach, where the UE receives the useful signal from its serving BS and the cooperative BSs. Interference is only generated by the outer BSs, i.e., ones outside the cooperative set. The obtained model can be utilized as an efficient tool by an operator to benchmark the energy efficiency of its network even if some additional BSs are needed to boost the services.

Here, we describe the EE model when JT-CoMP is used through the network, mainly within the closest BSs, i.e., those belonging to the first ring as shown in Fig. 5.2. In the cellular system, only one BS is selected for data transmission to the UE. In contrast, when the coordination is used, multiple BSs in the coordination set send data together to the UE. Since interference mainly comes from neighbors in the first ring, we limit the coordination set of BSs on this ring, so that the total number of coordinated BSs,  $M_{co} = 2, \dots, 7$ . The system model presented here is quite similar to the one in chapter 3. It concerns an OFDMA cellular network, composed of  $N_{BS}$  base stations (BSs) and  $N_u$  user equipments (UEs) randomly distributed over the network.  $M_{co}$  BSs are able to jointly transmit data in order to improve the signal quality at the UE located at the distance  $r_u$  from its serving BS (central cell in Fig. 5.2). We assume that the radio resources of each BS are divided into many

parallel and orthogonal sub-carriers, only inter-cell interference is considered. The network is supposed homogeneous, such that the transmission power  $P_{tx}$  is the same for every BS.

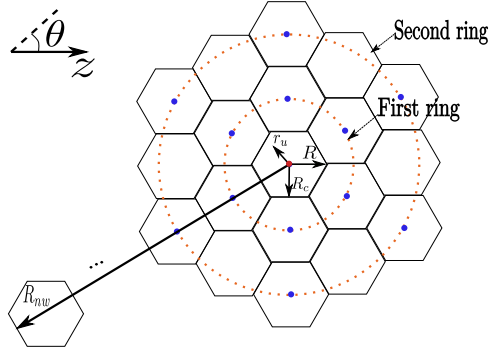


Fig. 5.2 Hexagonal network and main parameters.

Since we introduce the JT-CoMP scheme, the energy efficiency model is refined in this chapter and presented below.

### 5.4.1 Energy efficiency model with JT-CoMP scheme

In order to capture the energy-efficiency of that network with JT-CoMP we use the common Eq. (5.1) as in [37, 78]:

$$EE = \frac{D_{area}}{M_{co} \times P_{exp}^{CoMP} + (N_{BS} - M_{co}) \times P_{exp}}. \quad (5.1)$$

The EE is computed as the ratio of total data rate over a network area  $D_{area}$ , to the total power consumption. Here,  $P_{exp}^{CoMP}$  and  $P_{exp}$  are respectively the total energy expenditure per coordinated BS and per BS.

### 5.4.2 Power consumption model with JT-CoMP scheme

The power consumption of a coordinated BS,  $P_{exp}^{CoMP}$  in Eq. (5.2), is defined depending on the number of transmitting antennas  $N_{ant}$ , the transmitting power  $P_{tx}$  and the backhauling power cost  $K_{CoMP}$ . The fixed part,  $P_1$ , accounts for the direct current/alternating current (DC/AC) converters.  $\Delta_P$  and  $P_0$  denote some circuit power consumption.

$$P_{exp}^{CoMP} = N_{ant}(\Delta_P P_{tx} + P_0) + P_1 + K_{CoMP}. \quad (5.2)$$

Backhauling power consumption  $K_{CoMP}$  is the power cost due to the backhauling and data sharing for every BS. Fehske *et al.*, in [64] have investigated the impact of a microwave

backhauling in most cellular networks with a CoMP approach. They model the backhauling as a set of wireless micro wave links.  $K_{CoMP}$  can be a constant for simplification, or be calculated as in [64]:

$$K_{CoMP} = \frac{P_{bh}^0 C_{bh}}{C_{bh}^0} = \alpha_{bh} C_{bh}, \quad (5.3)$$

where  $P_{bh}^0$  denotes the power consumed by the backhaul equipment when supporting the maximum data rate  $C_{bh}^0$ ,  $\alpha_{bh} = P_{bh}^0/C_{bh}^0$  is the power coefficient of backhaul equipment, and  $C_{bh}$  is the backhauling traffic for every BS, i.e., the accumulated data rate of several UEs served by one cooperating BS [89]. Therefore,  $K_{CoMP}$  is linearly proportional to the backhauling requirement  $C_{bh}$ . The calculation of  $C_{bh}$  will be presented in the below sections.

In particular,  $\alpha_{bh} = 5 \times 10^{-7} \text{ Joules/bit}$  [64, 89] for a macro BS and  $\alpha_{bh} = 4 \times 10^{-8} \text{ Joules/bit}$  for a femto BS [89, 128, 129].

Obviously, the power consumption of a common BS, i.e., without coordination, also can be computed using the Eq. (5.2), without the  $K_{CoMP}$  part. In other words, in Non-CoMP mode,  $C_{bh}$  and  $K_{CoMP}$  are zero. Therefore, the total energy expenditure per BS with Non-CoMP is given by  $P_{exp} = N_{ant}(\Delta_p P_{Tx} + P_0) + P_1$  and the EE equation is reduced to  $EE = \frac{D_{area}}{N_{BS} \times P_{exp}}$ . The numerical values of each part in Eq. (5.2) are listed in Table 3.1, regarding the BSs types (macro, micro, femto).

Before presenting how to compute the total data rate  $D_{area}$ , we give the SINR calculation with fluid modeling in the case of JT-CoMP.

#### 5.4.3 SINR calculation: case of JT-CoMP

Basically, without any coordination and neglecting the noise, the SINR  $\Gamma_u$  at  $u$  in this basic case, as we denote it Non-CoMP mode, is displayed by

$$\Gamma_u = \frac{(\eta - 2)r_u^{-\eta}}{2\pi\rho_{BS}[(2R_c - r_u)^{2-\eta} - (R_{nw} - r_u)^{2-\eta}]} \quad (5.4)$$

The above equation is obtained by fluid framework, which can be seen more details in chapter 3.

Usually, BSs cooperate to transmit and receive data from multiple UEs in different cells to improve the coverage and especially, to enhance cell-edge throughput. As in [99], a UE  $u$  is served by the central BS  $b$ , and receives data from coordinated BSs as shown in Fig. 5.3. The UE experiences a SINR  $\Gamma_u^{CoMP}$  as

$$\Gamma_u^{CoMP} = \frac{p_{b,u} + p_{u,CoMP}}{p_{ext,u} - p_{u,CoMP}} \quad (5.5)$$

$p_{u,CoMP}$  denotes the received power at  $u$  from the BSs which are in the coordinated set together with the serving BS. It defines the received power improvement by means of the coordination.  $p_{b,u} = P_{tx}Kr_u^{-\eta}$  is the received power from its serving BS  $b$ ,  $p_{ext,u} = \frac{2\pi\rho_{BS}P_{tx}K}{\eta-2}[(2R_c - r_u)^{2-\eta} - (R_{nw} - r_u)^{2-\eta}]$  is the total external or interference power coming from others BSs without cooperation.

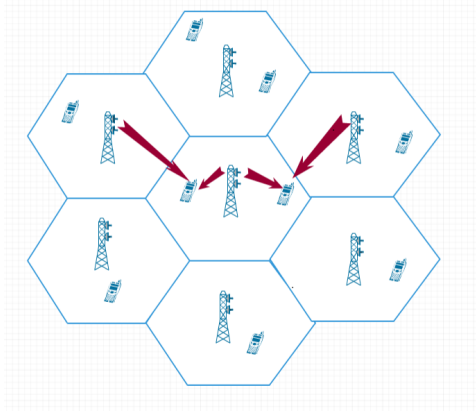


Fig. 5.3 JT-CoMP in hexagonal model

As the first ring is composed of six BSs around the serving BS, as shown in Fig. 5.3, the homogeneous network we consider is divided into six equal parts. Therefore, there are  $n$  BSs, such that  $n = \{1, \dots, 6\}$ , in the first ring to cooperatively transmit data with the central BS. Hence, the JT coordination area can be delimited over a ring of radii between  $[2R_c - r_u, 4R_c - r_u]$  and the angle of  $n\pi/6$  (see [99] for more details). For example, the red area in Fig. 5.4 is the cooperative region between serving BS and one coordinated BS ( $n = 1$ ).

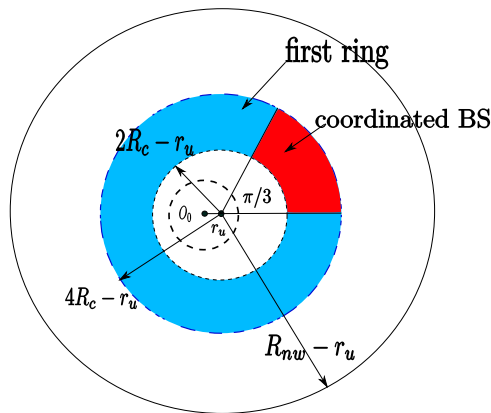


Fig. 5.4 JT-CoMP in fluid model with  $n(= 1)$  coordinated BSs

Therefore, for a given UE  $u$  with  $n$  ( $n = \{1, \dots, 6\}$ ) BSs in the coordinated set to jointly transmit data with its serving BS, the improvement of the received power or the coordinated power can be written as

$$\begin{aligned} p_{u,CoMP} &= \int_0^{\frac{n\pi}{3}} \int_{2R_c - r_u}^{4R_c - r_u} \rho_{BS} P_{tx} K z^{-\eta} dz d\theta \\ &= \frac{n\pi}{3} \frac{\rho_{BS} P_{tx} K}{\eta - 2} [(2R_c - r_u)^{2-\eta} - (4R_c - r_u)^{2-\eta}]. \end{aligned} \quad (5.6)$$

Consequently, we can compute the SINR  $\Gamma_u^{CoMP}$  in Eq. (5.5) at  $u$ , by replacing  $p_{b,u} = P_{tx} K r_u^{-\eta}$ ,  $p_{ext,u} = \frac{2\pi\rho_{BS}P_{tx}K}{\eta-2}[(2R_c - r_u)^{2-\eta} - (R_{nw} - r_u)^{2-\eta}]$  and  $p_{u,CoMP}$  as defined in Eq (5.6), displayed as

$$\Gamma_u^{CoMP} = \frac{3(\eta-2)r_u^{-\eta} + n\pi\rho_{BS}[(2R_c - r_u)^{2-\eta} - (4R_c - r_u)^{2-\eta}]}{6\pi\rho_{BS}[(2R_c - r_u)^{2-\eta} - (R_{nw} - r_u)^{2-\eta}] + n\pi\rho_{BS}[(2R_c - r_u)^{2-\eta} - (4R_c - r_u)^{2-\eta}]} \quad (5.7)$$

The analytically tractable expressions of  $\Gamma_u$  in Eq. (5.4) and  $\Gamma_u^{CoMP}$  in Eq. (5.7) can be easily exploited to compute data rate over a network area, since the two equations only depend on the density of BS,  $\rho_{BS}$ , the radius of the cell,  $R_c$ , the range of the network,  $R_{nw}$ , the path-loss exponent,  $\eta$ , the distance of a UE to its serving BS,  $r_u$ , and the number of coordinated BS,  $n$ , in the first ring.

Therefore, taking advantage of the expressions of  $\Gamma_u$  and  $\Gamma_u^{CoMP}$ , we will present the computation of data rate  $D_{area}$  in the following section.

## 5.5 Data rate computation

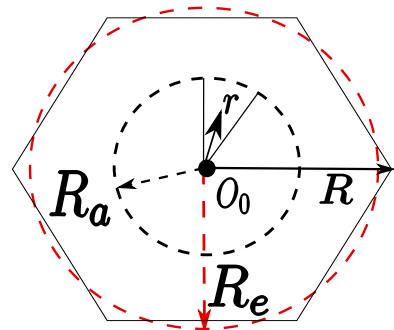


Fig. 5.5 Area of interest with various radius  $R_a$  ( $0 < R_a \leq R_e$ )

This section presents the evaluation of data rate over a network area of radius  $R_a$ , such that  $R_a$  varies in  $[0, R_e]$ , as shown in Fig. 5.5. Note that  $R_e$  is the radius of a disk with a surface equivalent to the hexagonal central cell, such that  $R_e = \sqrt{2\sqrt{3}/\pi}R_c$ .

We claim that JT-CoMP is not as much efficient for UEs with a greater  $\Gamma_u$ , and even can reduce EE performance of the network. To investigate this hypothesis, we consider the cell divided into two parts: inner region and outer region based on the signal quality  $\Gamma_u$  at UE  $u$ , as displayed in Fig. 5.6. Indeed, UEs located in the inner region, do not need the improvement of their SINR, since they are close to their serving BS. Hence, the inner region is regarded as Non-CoMP mode. In return, the outer region is defined as CoMP mode, due to the worst SINR experienced there. For example, a cell-edge UE  $u$  is in a CoMP mode since

$$\Gamma_u \leq \Gamma_{threshold}, \quad (5.8)$$

where  $\Gamma_{threshold}$  is a predefined threshold in dB, related to a distance, called the distance threshold  $d_{th}$ . Hence, we aim to define these thresholds in order to set up the network conditions ensuring a greatest JT-CoMP performance. Thus, we can further obtain the higher EE.

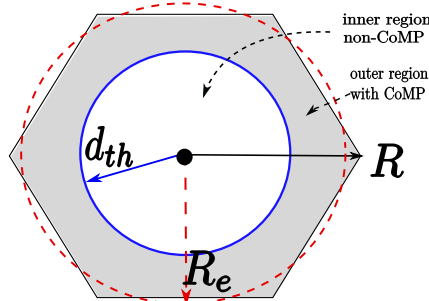


Fig. 5.6 JT-CoMP strategy defined by distance threshold  $d_{th}$

Depending on different values of  $d_{th}$ , we define three scenarios to resolve the problem.

- *Non-CoMP scenario* when  $d_{th} = R_e$ . Here, there is no need to use JT-CoMP, since the overall cell falls in the inner region. In other words, all UEs are in Non-CoMP mode, and their  $\Gamma_u$  can be calculated by Eq. (5.4). Although it is not realistic, this scenario serves as a baseline or a reference to evaluate and to compare the gain of EE when JT-CoMP is applied.
- *AllUEs-CoMP scenario* when  $d_{th} = 0$ . It is the worst case, where all UEs in the cell are in the outer region and choose JT-CoMP whatever their locations.  $\Gamma_u^{CoMP}$  can be computed by Eq. (5.7).

The results analysis of the latter scenario together with *Non-CoMP scenario* results, allow to define the  $d_{th}$  threshold and thereby define adequately the inner and the outer regions. Moreover, we can investigate the boundary of the EE using fluid approximation.

- *CoMP scenario* is the common and the more realistic scenario, since the cell is composed of two regions: inner region and outer region depending on the distance threshold  $d_{th}$ . In the inner, UEs do not use JT-CoMP scheme, whereas the UEs whose distances are larger than  $d_{th}$  choose JT-CoMP scheme. Using this scenario, we can evaluate the effectiveness of JT-CoMP depending on the coordinated BSs number, the distance threshold  $d_{th}$ , and the network size  $R_a$  such that  $0 < R_a \leq R_e$ .

Regarding the three scenarios described above, we detail how to compute the data rate in the following paragraphs.

### 5.5.1 Non-CoMP scenario

In this scenario, we aim at evaluating the data rate  $D_{area}$  over a network area with the condition of  $d_{th} = R_e$ . To do so, we focus on a network area with a radius  $R_a$ , such as  $(0 < R_a \leq R_e)$ , i.e., one part of the central cell, as depicted in Fig. 5.5. Since the UEs are uniformly distributed in space, the density  $\rho_u$  is constant. Therefore, the number of users  $N'_u$  over the area of interest, of radius  $R_a$ , is given as  $N'_u = (N_u R_a^2) / R_e^2$ , where  $N_u$  is the total number of UEs.

According to Shannon's formula, the spectral efficiency (SE), measured in bps/Hz, for a UE  $u$  located at the distance  $r$  depends on its signal quality  $\Gamma_u$  and is given as  $SE_u(r) = \log_2(1 + \Gamma_u(r))$ . The maximum theoretical achievable data rate  $D_u(r)$  of UE  $u$  can be computed as  $D_u(r) = B_u \times SE_u(r)$ , where  $B_u$  is the UE's bandwidth. Hence, the total data rate  $D_{area}$  over a network area of radius  $R_a$ , can be written by

$$D_{area} = \int_0^{2\pi} \int_0^{R_a} B_u \rho_u \log_2(1 + \Gamma_u(r)) r dr d\theta. \quad (5.9)$$

Considering an equal bandwidth sharing among UEs,  $B_u = BW_n / N_u$  where  $BW_n$  is the total bandwidth. Replacing  $\rho_u = N_u / (2\sqrt{3}R_c^2)$ , the total data rate is rewritten as

$$D_{area} = \frac{BW_n \pi}{\sqrt{3}R_c^2} \int_0^{R_a} r \log_2(1 + \Gamma_u(r)) dr. \quad (5.10)$$

A worthwhile observation is that Eq. (5.10) neither depends on the number of UEs deployed per cell, nor upon their density  $\rho_u$ . When  $R_a = R_e$ , the above equation is evolved to compute the total cell data rate,  $\tilde{D}$ .

### 5.5.2 AllUEs-CoMP scenario

In this scenario, whatever the location of UEs in the cell, all of them use JT-CoMP to receive signal from both the serving BS and the coordinated BSs deployed in the first ring. Therefore, in this case, the total data rate  $D_{area}$  over a network area with radius  $R_a$  can be expressed as

$$D_{area} = \frac{BW_n\pi}{\sqrt{3}R_c^2} \int_0^{R_a} r \log_2(1 + \Gamma_u^{CoMP}(r)) dr. \quad (5.11)$$

When  $R_a = R_e$ , the above equation is evolved to compute the total cell data rate,  $D_{cell}^{CoMP}$ .

### 5.5.3 CoMP scenario

CoMP Scheme is used for a fixed value of  $d_{th}$ , where only UEs with lower signal quality compared to  $\Gamma_{threshold}$  adopt JT-CoMP. The rest of UEs are in Non-CoMP mode. As same as the previous scenarios, the aim is to compute total data rate  $D_{area}$  over a network area with radius  $R_a$ . Therefore, depending on the network radius  $R_a$ , we can have two possibilities:

1. For  $R_a \leq d_{th}$ , the area of interest is one part of inner region and  $D_{area}$  can be computed with the same Eq. (5.10).
2. For  $d_{th} < R_a \leq R_e$ , the area of interest has two parts: inner region, i.e., a disk of radius  $d_{th}$ , and a ring part with inner radius  $d_{th}$  and outer radius  $R_a$ . The data rate over the inner region,  $D_{inner}$ , is computed by  $D_{inner} = \frac{BW_n\pi}{\sqrt{3}R_c^2} \int_0^{d_{th}} r \log_2(1 + \Gamma_u(r)) dr$ . The data rate over the ring between inner radius  $d_{th}$  and outer radius  $R_a$ ,  $D_{outer}$  is computed as  $D_{outer} = \frac{BW_n\pi}{\sqrt{3}R_c^2} \int_{d_{th}}^{R_a} r \log_2(1 + \Gamma_u^{CoMP}(r)) dr$ .

Therefore, the data rate  $D_{area}$  in *CoMP scenario* can be expressed as

$$D_{area} = \begin{cases} \frac{BW_n\pi}{\sqrt{3}R_c^2} \int_0^{R_a} r \log_2(1 + \Gamma_u(r)) dr, & R_a \leq d_{th} \\ D_{inner} + D_{outer}, & d_{th} < R_a \leq R_e \end{cases} \quad (5.12)$$

According to the above definition of data rate, we find that  $D_{area}$  is mainly related to the distance threshold  $d_{th}$  and the radius  $R_a$ . The accuracy of Eqs. (5.10), (5.11) and (5.12) is verified in the simulation section through a comparison with Monte Carlo simulations.

The bit-per-joule capacity indicates the amount of energy consumed for transmitting information. In fact, the last parameter to define for the EE model concerns the power consumption which must take into account not only the power consumed at each BS, but also the relative backhauling power used to share data between cooperative BSs. In the subsequent section we introduce the definition of energy efficiency expression depending on these powers and the total data rate formulated above.

## 5.6 Backhauling traffic computation: $C_{bh}$

Regarding the last section, when JT-CoMP is applied, we suppose that  $K_{CoMP}$  is related to total data rate over the shaded region with CoMP as shown in Fig. 5.6. So we consider different equations of  $C_{bh}$  depending on the scenarios of CoMP approach, for example,

- AllUEs-CoMP:  $C_{bh} = D_{cell}^{CoMP}$ ,
- CoMP scenario:  $C_{bh} = D_{shade}^{CoMP}$ ,

where  $D_{shade}^{CoMP} = \frac{BW_n\pi}{\sqrt{3}R_c^2} \int_{d_{th}}^{R_e} r \log_2(1 + \Gamma_u^{CoMP}(r)) dr$ . Meanwhile, in Non-CoMP mode,  $C_{bh}$  and  $K_{CoMP}$  are zero.

## 5.7 Simulation and results

In this section, we evaluate the proposed EE models through simulations and several purposes are exposed as follows. First, we show some numerical results of the data rate  $D_{area}$  over both macro cellular networks (denoted MCN) and femto cellular networks (denoted FCN). Then, we present the accuracy of the EE expressions proposed in the last section by comparing the simulation results to those of Monte Carlo (MC) simulations of a hexagonal network. Additionally, we investigate the suitable value of SIR threshold,  $\Gamma_{threshold}$  and its corresponding distance threshold  $d_{th}$  in order to define the inner and outer regions. Finally, we show the impact of the number of coordinated BSs,  $n$ , variable path-loss exponent,  $\eta$ , on the energy efficiency improvement and investigate the variation of the backhauling power consumption, as mentioned in chapter 2. Simulations are carried out on MATLAB.

For MC simulations, we consider 7 rings of hexagonal cells around a central hexagon such that  $R_{nw} = 15R_c$ .  $N_u$  UEs are generated uniformly in the central hexagon and we assume that they are attached to the BS located at the center of a hexagon. We compute the  $\Gamma_u$  (without JT-CoMP case),  $\Gamma_u^{CoMP}$  (in case of JT-CoMP), for each UE in the area and

Table 5.1 Simulation Parameter Value

Parameters	Value
System bandwidth B	10MHz
Cell radius $R$ : macro, femto, resp.	{1000, 50}m
Half distance between BSs, $R_c$	$R\sqrt{3}/2$
Range of network $R_{nw}$	$15R_c$
Radius of interested area $R_a$	$[R/20 \ R_e]$
Equivalent radius of one cell, $R_e$	$R_c\sqrt{2\sqrt{3}/\pi}$
Number of antennas $N_{ant}$	1
Number of users $N_u$ : macro, femto, resp.	{300, 100}
Power coefficient of backhaul equipment	$\{5 \times 10^{-7} Joules/bit,$
$\alpha_{bh}$ : macro, femto, resp.	$4 \times 10^{-8} Joules/bit\}$
Path loss exponent $\eta$	{2.6, 3, 3.5, 4}
Density of BSs $\rho_{BS}$	$1/(2\sqrt{3}R_c^2)$
Density of users $\rho_u$	$N_u/(2\sqrt{3}R_c^2)$

then sum the achievable data rate for all UEs depending on  $D_u = B_u \times \log_2(1 + \Gamma_u)$  or  $D_u = B_u \times \log_2(1 + \Gamma_u^{CoMP})$ , related to two cases above respectively. Finally, we obtain the total data rate  $D_{area}$  in the area. We use the Eq. (5.1) to plot the EE variation. The results presented here are obtained by averaging over 5000 independent iterations of MC simulations. The other simulation parameters are set up according to Table 3.1 for the power consumption model, and Table 5.1 for the other network parameters.

### 5.7.1 Date rate vs the network radius

Fig. 5.7 and Fig. 5.8 depict the data rate  $D_{area}$  as a function of the network radius  $R_a$  for two path-loss exponent  $\eta = 2.6$  or  $\eta = 3.5$  in the MCN and FCN, respectively. The results confirm that the proposed model is effective and match well with MC results for the case of JT-CoMP, whatever the type of the cellular network and the values of  $\eta$ . Moreover, the results in both figures show that the theoretical  $D_{area}$  increases with the size of the network area  $R_a$  when the JT-CoMP is applied. Indeed, the data rate over the network area is related to  $R_a$ , as defined in Eq. (5.11). Alternatively, while comparing Fig. 5.7 and Fig. 5.8, we observe that the numerical values of  $D_{area}$  are identical. For example, for  $R_a = R_e$  (the whole cell) and  $\eta = 2.6$ , the data rate is constant  $D_{area} = 17.85 Mbps$ . Therefore, the data rate enhancement is the same, regardless of the type of cellular networks. In fact, if we introduce the normalized distance  $x = r_u/R_c$ , and considering  $R_{nw} = 15R_c$ ,  $\Gamma_u^{CoMP}(r_u)$  can be rewritten as Eq. (5.13).

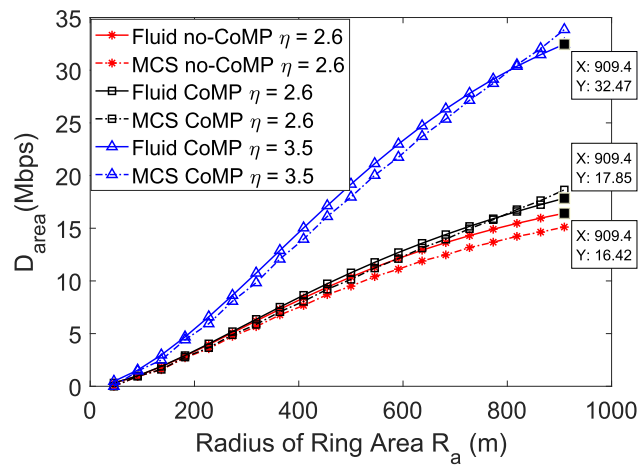


Fig. 5.7  $D_{area}$  vs radius of the MCN,  $R = 1000m$ ,  $K_{CoMP} = 50W$ ,  $n = 1$ , **AllUEs-CoMP scenario**

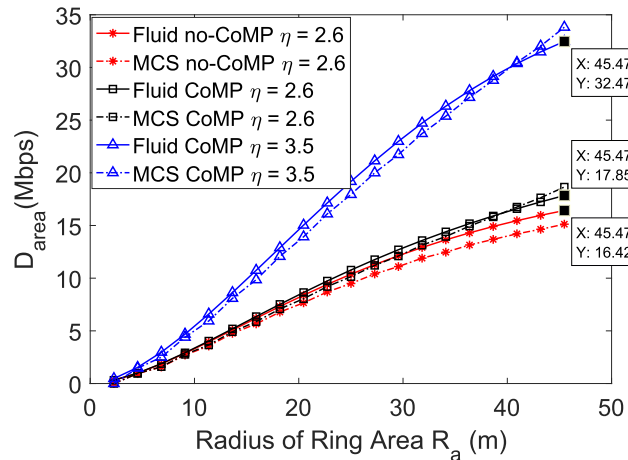


Fig. 5.8  $D_{area}$  vs radius of the FCN,  $R = 50m$ ,  $K_{CoMP} = 30mW$ ,  $n = 1$ , **AllUEs-CoMP scenario**

$$\Gamma_u^{CoMP}(x) = \frac{x^{-\eta} + \frac{n\pi}{6\sqrt{3}(\eta-2)}[(2-x)^{2-\eta} - (4-x)^{2-\eta}]}{\frac{\pi}{\sqrt{3}(\eta-2)}[(2-x)^{2-\eta} - (15-x)^{2-\eta}] + \frac{n\pi}{6\sqrt{3}(\eta-2)}[(2-x)^{2-\eta} - (4-x)^{2-\eta}]} \quad (5.13)$$

With  $R_a = kR_c$ , then the total data rate  $D_{area}$  over a network area of radius of  $R_a$  can be rewritten as:

$$\begin{aligned} D_{area} &= \frac{BW_n\pi}{\sqrt{3}R_c^2} \int_0^{R_a} r \log_2(1 + \Gamma_u^{CoMP}(r)) dr \\ &= \frac{BW_n\pi}{\sqrt{3}} \int_0^k x \log_2(1 + \Gamma_u^{CoMP}(x)) dx \end{aligned} \quad (5.14)$$

As a result,  $D_{area}$  does not depend on  $R_c$  and  $R_{nw}$ , but is related to the ratios of  $R_a/R_c$ ,  $R_{nw}/R_c$  and  $\eta$ . In other words, we can obtain same data rate in the MCN and the FCN, if the same path-loss exponent and the same bandwidth are set together with the same distance ratios of  $R_a/R_c$  and  $R_{nw}/R_c$ .

### 5.7.2 EE vs radius $R_a$ in scenario AllUEs-CoMP

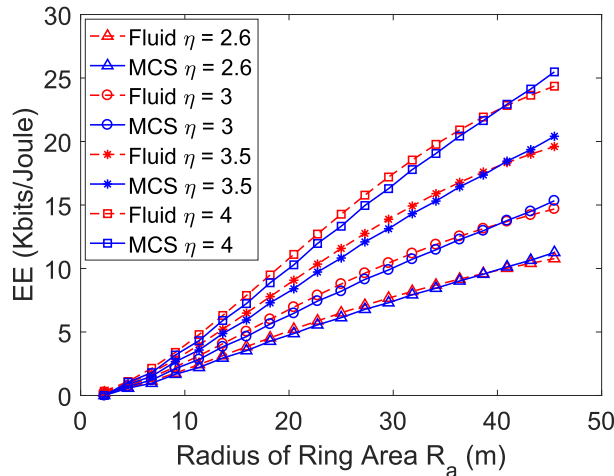


Fig. 5.9 EE vs radius of the network area in a FCN,  $K_{CoMP} = 30mW$ , **AllUEs-CoMP scenario**,  $n = 1$

The simulation results of energy efficiency for a FCN obtained through fluid model and MCS are shown in Figs. 5.9 and 5.10 along with various  $R_a$ , and considering different network parameters, such as the path-loss exponent  $\eta$  and the number of cooperative BSs  $n$ . Figs. 5.11 and 5.12 depict the EE performance as a function of  $R_a$  values in a MCN. The results in the four figures are obtained for the *AllUEs-CoMP scenario*. Here, we consider the number of coordinated BSs,  $n = \{1, 3\}$ . Additionally, we set the backhauling power cost  $K_{CoMP}$  as a constant, i.e.,  $K_{CoMP} = 50W$  for a MCN and  $K_{CoMP} = 30mW$  for a FCN as in [90].

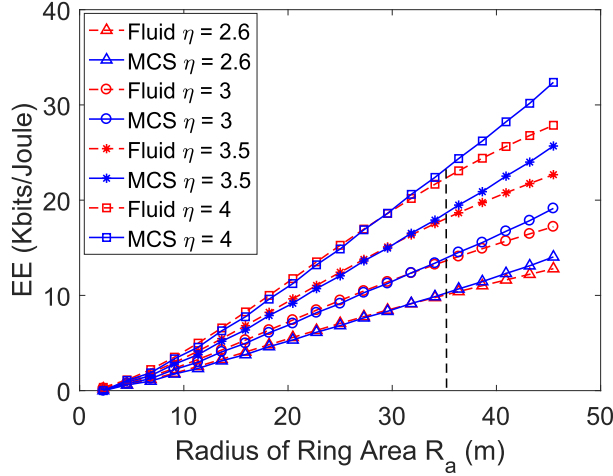


Fig. 5.10 EE vs radius of the network area in a FCN,  $K_{CoMP} = 30mW$ , **AllUEs-CoMP scenario**,  $n = 3$

Fig. 5.9 describes EE along with various  $R_a$  for 4 different values of  $\eta$  and one coordinated BS,  $n = 1$ . Fig. 5.10 depicts the EE along with various  $R_a$  for 3 coordinated BSs,  $n = 3$ . In both cases, we observe that EE values increase with the growth of  $\eta$  for a fixed  $R_a$ , whatever the value of  $n$ , which is due to the improvement of SIR for a fixed UE along with the raise of  $\eta$ . We conclude that EE gain in suburban area ( $\eta \in \{3.5, 4\}$ ) is more attractive than the one in the urban area ( $\eta \in \{2, 6, 3\}$ ). However, BSs coordination is still more important in such environment than in the suburban area.

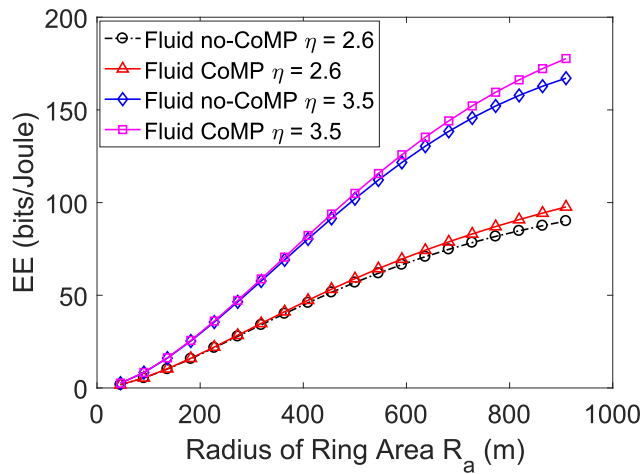


Fig. 5.11 EE vs radius of the network area in a MCN,  $R = 1000m$ ,  $K_{CoMP} = 50W$ , **AllUEs-CoMP scenario**,  $n = 1$

Moreover, the numerical values in Figs. 5.9 and 5.10 show that the analytical results match well with Monte Carlo ones, whatever the values of  $\eta$ , as in [130], which reveals the proposed model is effective and accurate, despite the small gap we observe in Fig. 5.10 when  $35m < R_a < R_e$ . Indeed, as the network is homogeneous, the approximated fluid modeling considers that the impact of the 6 cooperative BSs located in the first ring on the UE is same, which causes the same SIR improvement for the cell-edge UEs whatever its position to the coordinated BSs. However, this assumption is no longer true in hexagonal model, since the real distances from a UE to its serving BS, and to the coordinated BSs are considered, which leads to a higher SIR and a greater EE for cell-edge UEs than the analytical fluid results.

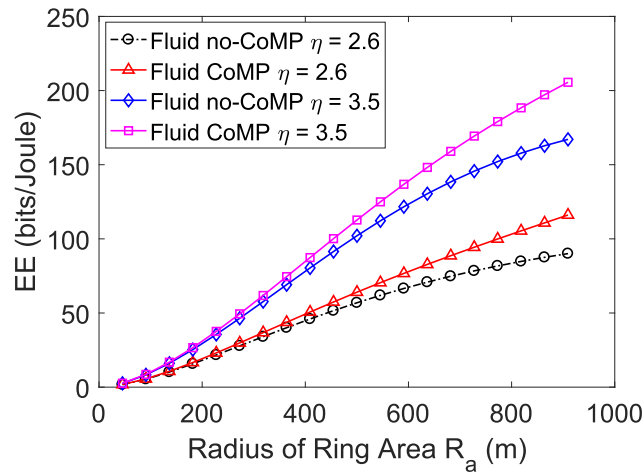


Fig. 5.12 EE vs radius of the network area in a MCN,  $R = 1000m$ ,  $K_{CoMP} = 50W$ , **AllUEs-CoMP scenario,  $n = 3$**

Figs. 5.11 and 5.12 depict the EE performance as a function of various  $R_a$  values in a MCN. We observe that the numerical results of EE are improved with JT-CoMP scheme compared to those without JT-CoMP in both two figures. Especially, while comparing the numerical values in Figs. 5.11 and 5.12 for  $\eta = 3.5$ , we observe that the EE improvement is more important when 3 coordinated BSs are used than the case where only one BS is considered ( $n = 1$ ). Hence, increasing the number of cooperating BSs improves the data rate over the network area in the case of fixed backhauling power consumption.

In addition, for convenient presentation purpose, the EE numerical values of a FCN based on fluid modeling are presented in Table 5.2 for two scenarios: *Non-CoMP* and *AllUEs-CoMP*, while considering a constant backhauling power cost  $K_{CoMP} = 30mW$ , cooperation with 1 and 3 BSs  $n = \{1, 3\}$  and various path loss exponent  $\eta = \{2.6, 3, 4\}$ . We observe that EE is improved when the number of coordinated BSs increases. Moreover, compared

to the baseline case of Non-CoMP where no coordination is considered, the EE gain varies within the interval of  $[0.12 \text{ } 2.89] K\text{bits}/\text{Joule}$  in the urban area, whereas it changes within the interval of  $[0.21 \text{ } 4.84] K\text{bits}/\text{Joule}$  in the suburban area, depending on the distance to the serving BS.

Table 5.2 EE results ( $K\text{bits}/\text{Joule}$ ) of a FCN in different scenarios: **Non-CoMP** and **AllUEs-CoMP**.  $K_{CoMP} = 30mW$ ,  $n = [1, 3]$ ,  $\eta = [2.6, 3, 4]$  and  $R_a = [10, 15, 20, 25, 30, 35, 40, R_e] (m)$

		$R_a (\text{m})$							
		10	15	20	25	30	35	40	45.5=R_e
$\eta=2.6$	<b>Non-CoMP</b>	1.99	3.47	4.93	6.26	7.42	8.4	9.2	9.91
	<b>AllUEs-CoMP (<math>n = 1</math>)</b>	2.03	3.56	5.08	6.5	7.77	8.88	9.85	10.77
	<b>AllUEs-CoMP (<math>n = 3</math>)</b>	2.11	3.75	5.43	7.06	8.59	10.03	11.38	12.8
$\eta=3$	<b>Non-CoMP</b>	2.55	4.55	6.58	8.49	10.16	11.56	12.7	13.66
	<b>AllUEs-CoMP (<math>n = 1</math>)</b>	2.59	4.65	6.76	8.77	10.58	12.15	13.48	14.69
	<b>AllUEs-CoMP (<math>n = 3</math>)</b>	2.7	4.89	7.2	9.47	11.6	13.57	15.38	17.21
$\eta=4$	<b>Non-CoMP</b>	3.88	7.1	10.54	13.89	16.92	19.47	21.47	23.02
	<b>AllUEs-CoMP (<math>n = 1</math>)</b>	3.94	7.24	10.78	14.27	17.47	20.24	22.48	24.35
	<b>AllUEs-CoMP (<math>n = 3</math>)</b>	4.09	7.58	11.4	15.25	18.92	22.24	25.14	27.86

Furthermore, we observe that the EE gain exceeds  $3K\text{bits}/\text{Joule}$  for  $R_a \geq 25m$  when 3 BSs jointly transmit the signal to the UE, which shows that the coordination is enough important. However, the EE improvement is not as expected for  $R_a < 25m$ . In fact, it is not very interesting to coordinated transmission for UEs with a great signal quality, i.e., those UEs close to the serving BS. Coordination for closer UEs does not bring any improvement on their SIR, quite the opposite, it increases the backhauling cost and impacts the energy efficiency. Therefore, in the following, we present some results to analyze the EE gain depending on the number of coordinated BSs,  $n$ , mainly when  $R_a > 25m$ . But, prior to that, we need to fix the distance threshold  $d_{th}$ , even so we can suppose it equal to  $25m$  as observed in the last result.

Since the CoMP approach has slight impact on UEs, in particular those far from their serving BS in the case of a constant  $K_{CoMP}$  about  $30mW$ . Therefore, it is necessary in the following part, to show the impact of distance threshold  $d_{th}$  on  $EE_{cell}$ , considering the CoMP scenario with variable  $K_{CoMP}$ , depending on data rate requirement  $C_{bh}$ .

### 5.7.3 Impact of distance threshold $d_{th}$ on cell EE $EE_{cell}$ in CoMP scenario

Considering the slight effect of coordinated BSs on the UEs close to their serving BS, we aim to define the distance threshold  $d_{th}$ , and investigate its impact on the cell EE,  $EE_{cell}$ . To do so, we consider the third scenario, the realistic one as detailed earlier in section 5.5, i.e., CoMP scenario ( $0 < d_{th} < R_e$ ). By varying  $d_{th}$ , we evaluate the EE gain in a FCN with variable  $K_{CoMP}$  depending on  $C_{bh}$ , the backhauling requirement as in Eq. (5.3). By this experiment we capture the network parameters/environment together with the backhauling constraints.

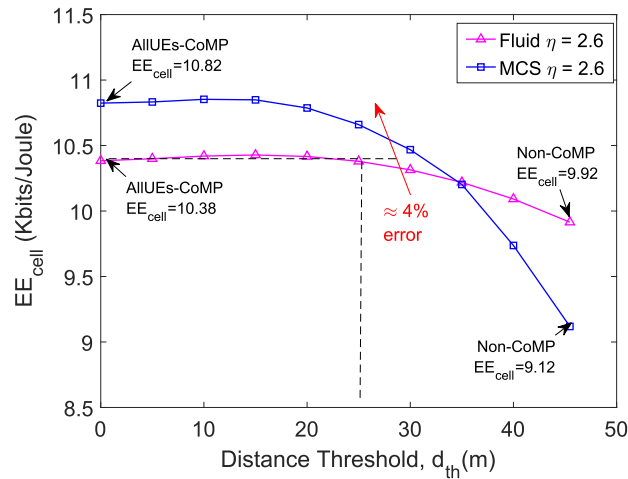


Fig. 5.13 EE per cell vs  $d_{th}$ , various  $K_{CoMP}$ ,  $\eta = 2.6$  and  $n = 1$  in a FCN

Fig. 5.13 shows the obtained result and compares the  $EE_{cell}$  of a FCN between the proposed framework and Monte Carlo simulations taking into account  $\eta = 2.6$  and  $n = 1$ . Once again, Fig. 5.13 shows a slight error, below 4%, when compared with Monte Carlo results, which validate the accuracy of the proposed model for evaluating EE. Furthermore, we can clearly see from this figure, that the distance threshold  $d_{th}$  makes a significant impact on  $EE_{cell}$ . If we focus on fluid modeling result (the red curve), we observe that the  $EE_{cell}$  values are almost constant for  $d_{th} < 25m$ , and decrease when beyond. Indeed, in this scenario, the outer region becomes smaller with the raise of  $d_{th}$ , which leads to lower data rate as well as higher power cost for backhauling brought by CoMP technique. Interestingly, we can observe the analytical value of  $EE_{cell}$  (the red line) in scenario AllUEs-CoMP is the same with the one for  $d_{th} = 25m$ , i.e.,  $EE_{cell} = 10.38Kbits/Joule$ . In other words, unnecessary use of CoMP for inner-region UEs with  $r_u < 25m$  can cause high energy consumption and low inefficiency, due to excess signaling transmission for cooperative BSs.

Therefore, the distance threshold  $d_{th}$  can be set as  $25m$ , which is reasonable in our work. Moreover, regarding the Fig. 5.14, where we plot quite simply the SIR depending on UE's distance to the serving BS in Non-CoMP mode, we observe that the UEs located beyond  $25m$  experience a  $SIR \leq 3dB$ . We emphasize that  $3dB$  is considered as a standard reference threshold beyond which a cell-edge UE makes use of joint transmission to increase signal strength as set up previously in several references, as in [74, 92, 131].

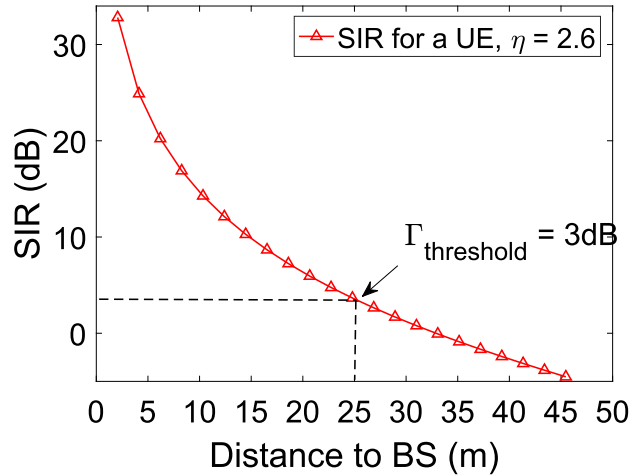


Fig. 5.14 SIR versus distance to the BS in *Non-CoMP* mode, simulated by fluid model with  $\eta = 2.6$  in a FCN

To further analyze the impact of  $n$  on EE when  $R_a > 25m$ , we present some numerical results of EE in case of two scenarios, *AllUEs-CoMP* and *CoMP*, considering both constant  $K_{CoMP}$  and varying  $K_{CoMP}$  as defined in Eq. (5.3). Here, constant  $K_{CoMP}$  is set as  $30mW$  rather than computed by Eq. (5.3). Since adding a new BS in the coordination set produces a slight change in the backhauling power cost  $K_{CoMP}$ , which will be shown in the following parts.

#### 5.7.4 EE gain vs BSs number

Figs. 5.15 and 5.16 show the numerical values of EE for various number of coordinated BSs  $n$  and  $\eta = 2.6$  for  $R/2 < R_a < R_e$ , in a MCN and a FCN, respectively. In both two figures, we observe that EE is improved as the growth of  $n$  for a fixed  $R_a$ . In fact, for a fixed  $R_a$ , the data rate  $D_{area}$  increases with the raise of coordinated BSs number  $n$ , regarding the fixed backhauling power cost. In the MCN, the EE enhancement reaches  $66bits/Joule$  when 6 BSs are used to jointly transmit data, against  $26bits/Joule$  in case of 3 BSs. The

EE improvement is more substantial in a FCN, since it is about  $2.9\text{Kbits/Joule}$  when 3 BSs are considered and reaches  $7.3\text{Kbits/Joule}$  in case of 6 coordinated BSs.

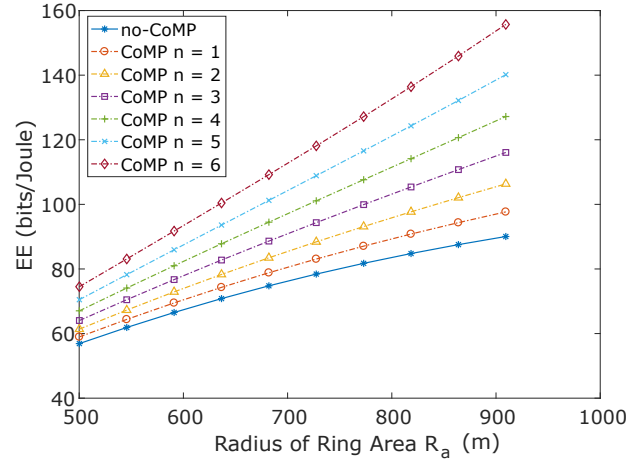


Fig. 5.15 EE improvement in a MCN,  $R = 1000\text{m}$ ,  $\eta = 2.6$ ,  $K_{CoMP} = 50\text{W}$  for **AllUEs-CoMP scenario**

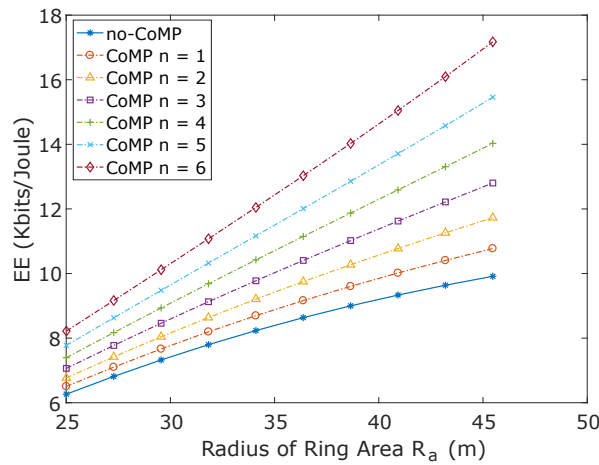


Fig. 5.16 EE improvement in a FCN,  $R = 50\text{m}$ ,  $\eta = 2.6$ ,  $K_{CoMP} = 30\text{mW}$  for **AllUEs-CoMP scenario**

For convenient presentation purpose, the fluid-based numerical values of EE per cell (denoted as  $EE_{cell}$  for  $R_a = R_e$ ) and EE (denoted as  $EE_{25}$  for  $R_a = 25\text{m}$ ) in Fig. 5.16 are presented respectively in Table 5.3 while considering constant backhauling power cost  $K_{CoMP} = 30\text{mW}$ . We observe that the  $EE_{25}$  gain is less than  $2\text{Kbits/Joule}$  whatever the value of  $n$ . Once again, it demonstrates that the EE improvement is not very important for

$R_a < 25m$ , as in Table 5.2. Therefore, the numerical results of EE in Fig. 5.16 is presented only for  $25m < R_a < 50m$ .

Table 5.3 Numerical results of  $EE_{cell}$  and  $EE_{25}$  measured by  $K\text{bits}/\text{Joule}$  in Fig. 5.16 when  $\eta = 2.6$  for  $R_a = R_e$ ,  $R_a = 25$ , respectively, in a FCN

	Non-CoMP	CoMP Mode					
		$n = 1$	$n = 2$	$n = 3$	$n = 4$	$n = 5$	$n = 6$
$EE_{cell}$	9.91	10.77	11.73	12.8	14.03	15.46	17.17
$EE_{25}$	6.26	6.5	6.77	7.06	7.4	7.77	8.22

Additionally, comparing Figs. 5.10 and 5.12 for  $\eta = 3.5$  and  $n = 3$ , we observe that EE is improved about  $38\text{bits}/\text{Joule}$  at the edge of a MCN, whereas it is about  $4.3\text{Kbits}/\text{Joule}$  in a FCN. This means that the JT-CoMP is more effective and brings higher improvement in small cellular networks. Although the same data rate  $D_{area}$  is observed in the MCN and the FCN, the EE improvement is higher in the FCN than in MCN, thanks to the smaller fixed backhauling power cost in the FCN.

### 5.7.5 Backhauling power cost vs BSs number

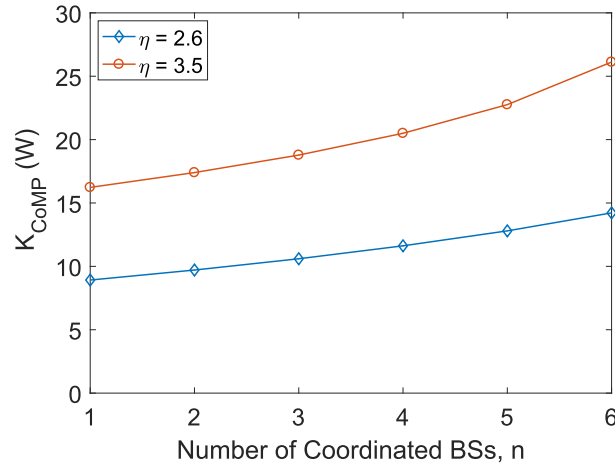
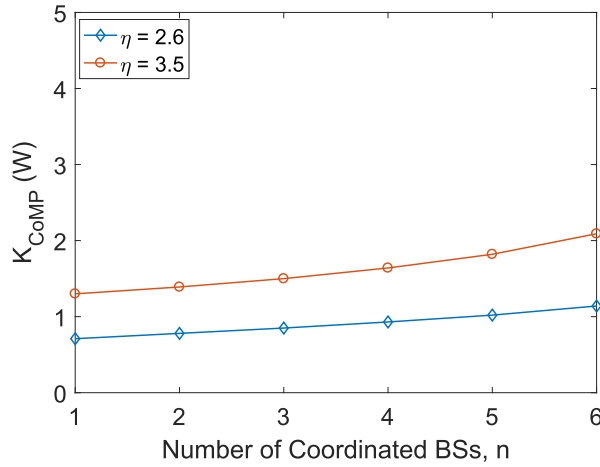


Fig. 5.17  $K_{CoMP}$  vs the number of coordinated BSs  $n$  in a MCN, *AllUEs-CoMP scenario*

When a new cooperative BS is added in the system, some additional energy is needed due to the additional power consumption for transmitting the backhauling traffic. Therefore, based on Eq. (5.3), Figs. 5.17 and 5.18 show some numerical results of the backhauling power consumption,  $K_{CoMP}$ , along with the various number of coordinated BSs  $n$  in a MCN and a FCN, for  $\eta = 2.6$  and 3.5. We observe that the values of  $K_{CoMP}$  in a FCN increases

Fig. 5.18  $K_{CoMP}$  vs the number of coordinated BSs  $n$  in a FCN, *AllUEs-CoMP scenario*

slightly with the raise of  $n$  whatever the values of  $\eta$ . Regarding the macrocell case, the additional energy cost for transmitting the backhauling capacity between BSs while adding the new coordinated BS is more significant. Specially, the results show that  $K_{CoMP}$  is about 26W for  $\eta = 3.5$  and  $n = 6$  in a MCN, as shown in Fig. 5.17 , and it is about 2W for a FCN in Fig. 5.18. For  $\eta = 3.5$  and  $n = 3$ ,  $K_{CoMP} = 18.8W$  in a MCN and  $K_{CoMP} = 1.5W$  in a FCN. Since the FCN has lower power dissipation compared to the MCN, which causes the smaller  $K_{CoMP}$  in FCN.

Table 5.4 Numerical Results of  $EE_{cell}$  measured by  $K\text{bits}/\text{Joule}$  in the FCN for fixed  $K_{CoMP}$  and various  $K_{CoMP}$  with  $\eta = 2.6$ 

	Non-CoMP	CoMP Mode					
		$n = 1$	$n = 2$	$n = 3$	$n = 4$	$n = 5$	$n = 6$
$EE_{cell}$ (Fixed $K_{CoMP}$ )	9.91	10.77	11.73	12.8	14.03	15.46	17.17
$EE_{cell}$ (Various $K_{CoMP}$ )	9.91	10.74	11.69	12.76	13.98	15.4	17.1

Table 5.5 Numerical Results of  $EE_{cell}$  measured by  $\text{bits}/\text{Joule}$  in the MCN for fixed  $K_{CoMP}$  and various  $K_{CoMP}$  with  $\eta = 2.6$ 

	no-CoMP	CoMP Mode					
		$n = 1$	$n = 2$	$n = 3$	$n = 4$	$n = 5$	$n = 6$
$EE_{cell}$ (Fixed $K_{CoMP}$ )	90.05	97.68	106.34	116.07	127.19	140.15	155.71
$EE_{cell}$ (Various $K_{CoMP}$ )	90.05	97.83	106.5	116.25	127.38	140.35	155.92

For a convenient presentation purpose, we compare in Table. 5.4, the numerical values of EE per cell (denoted as  $EE_{cell}$  when  $R_a = R_e$ ) obtained from fluid model in a FCN regarding of the two cases: a constant backhauling power cost  $K_{CoMP} = 30mW$  and variable  $K_{CoMP}$ , calculated by Eq. (5.3). As presented previously, we observe that  $EE_{cell}$  increases with the growth of  $n$  in the two cases, which is due to the higher data rate improvement brought by JT-CoMP. Moreover, the results show that  $EE_{cell}$  gain is about  $1.8K\text{bits/Joule}$  when there are 2 coordinated BSs in the first ring.  $EE_{cell}$  gain is around  $2.8K\text{bits/Joule}$  when 3 coordinated BSs are utilized regardless of the cases of  $K_{CoMP}$ . Moreover, it is to emphasize that  $EE_{cell}$  are quite similar in both two cases. Therefore, considering  $K_{CoMP} = 30mW$  is reasonable choice, it does not compromise the first results presented above. The same observations are verified in case of a MCN with  $K_{CoMP} = 50W$ , as shown in Table. 5.5.

In conclusion, the obtained results emphasize the JT-CoMP scheme in small cells as opposed to macrocells. It is a very interesting result that matches very well with the 5G scenario characterized by high density and more short-range communication such as Internet-of-Things (IoT).

## 5.8 Conclusion

In this chapter, we proposed a tractable expression of the energy efficiency (EE) performance based on fluid modeling for the downlink transmission system while considering the JT-CoMP approach. The expression of EE is a function of the total received data rate and the total power consumption. Regarding the power consumption while JT-CoMP is applied in the system, we consider the backhauling power cost in two cases: i) a constant backhauling power cost, and ii) variable backhauling power cost depending on the data rate requirement. Then, we investigate the impact of the path-loss exponent, the number of coordinated BSs, and the radius of interest on the EE metric in both types of cellular networks: macro (MCN) and femto (FCN) and its gain for three scenarios, which are divided according to the different values of distance threshold  $d_{th}$ . The numerical results show the model accuracy of EE through a comparison with Monte Carlo trials. Moreover, the results exhibit that the data rate is the same for both types of cellular networks, whereas the energy efficiency in a FCN is larger than the one in a MCN. In both networks, the EE is improved with the raise of the number of coordinated BSs  $n$  for the two cases: fixed backhauling power cost  $K_{CoMP}$  and variable  $K_{CoMP}$ , since the total data rate of the area increases when  $n$  increases. For various  $K_{CoMP}$  values, we observe that  $d_{th}$  set as  $25m$ , is reasonable, which is corresponding to the  $3dB$  threshold value as defined in most of papers. The backhauling power cost also increases with the growth of  $n$ , due to the additional energy cost for transmitting the

additional backhauling capacity between macro BSs. However, in the FCN, adding a new BS in the coordination set, produces a slight change in the backhauling power cost  $K_{CoMP}$ . Consequently, the proposed EE model with JT-CoMP is tractable and allow the study of network energy efficiency through the main parameters of the network, which may provide some insights on the design of future network.



# Chapter 6

## Conclusion and Perspective

### Contents

6.1 Conclusion . . . . .	119
6.2 Future work . . . . .	121
6.2.1 Other bandwidth scheduling approach . . . . .	122
6.2.2 EE in heterogeneous networks . . . . .	122
6.2.3 EE-evaluation for uplink system . . . . .	123
6.2.4 EE mobility model . . . . .	123

---

In this chapter, the main results obtained in this thesis will be first summarized. Then we will give some possible and interesting ideas for the further work that may extend these results.

### 6.1 Conclusion

The advent of the fifth generation of wireless networks requires an incredible increase in throughput, simultaneous connections number and, low latency to provide the full set of capabilities. However, this unprecedented increase in capacity are expected not leading to an energy crunch. Therefore, 5G requirements specify it must be achieved at similar or lower power consumption as todays' networks. The energy efficiency (EE) becomes one of the key performance indicators in 5G wireless communication network. To evaluate the performance of large representative cellular networks, investigate the impact of the environmental parameters on EE, and capture the significant factors involved in the energy consumption process, representative and accurate models are needed.

Furthermore, the advanced technology of Joint Transmission Coordinated MultiPoint (JT-CoMP) is a promising scheme to enhance throughput and increase the capacity by reducing the interference, especially for cell-edge users. Nevertheless, some additional energy for hardware circuit and resource information is consumed by this technology. Hence, a tractable model for the performance evaluation of EE in dense networks with JT-CoMP approach is needed in terms of time expense to conduct simulations.

Fluid modeling is an approximation approach for the network evaluation, assuming that a given finite number of transmitters are regarded as an equivalent continuum of transmitters with a certain density. Then, the total interference power over the continuous field can be easily calculated by integrating. Unlike other network models, SINR, outage probability and data rate can be calculated easily based on this fluid modeling. Hence, fluid modeling has the potential to be used for the energy efficiency evaluation, since it reduces the analysis complexity and provides a macroscopic evaluation of the network performance.

The objective of this thesis is to design and model the dense cellular network based on a tractable and efficient fluid modeling in order to evaluate the network EE and to investigate the impact of shadowing and JT-CoMP scheme on EE. With these objectives, we summarize the key findings of our chapters.

Taking advantage of the proposed system model in chapter 3, chapter 4 evaluated the network EE without and with considering the impact of shadowing on EE.

In the non-shadowing case, a tractable and efficient model based on spatial fluid modeling has been developed for the investigation of network EE, whatever its size. Furthermore, the effectiveness and accuracy of the proposed model have been verified in both macro- and femto-cellular networks, through a comparison of the results obtained by Monte Carlo simulations. Moreover, the EE variation has also been analyzed while considering different network parameters, such as network size, network types, users' density and the path-loss exponent. The simulation results have shown that the proposed EE model over the network area with any size is accurate and that the femto-cellular network is more efficient than the macro-cellular one due to the lower energy dissipation and attenuation in the femto-cellular network. More interestingly, the simulation results have also exhibited that the users' density has no effect on EE and that EE increases as the path-loss exponent increases.

In the case of shadowing, we have studied the joint impact of shadowing and path-loss exponent on EE for both the macro- and femto-cellular networks, based on the tractable fluid modeling. Using a polynomial curve fitting method, we first developed a closed-form expression of SINR threshold, which is related to the users' location. Based on the above

expression and the spatial fluid modeling, we then established a tractable and efficient EE model for both macro- and femto- cellular networks while considering the network parameter of coverage probability. In addition, the effectiveness and accuracy of the proposed model have been validated through a comparison with the results obtained by Monte Carlo simulations. The simulation results have exhibited that EE increases as the path-loss exponent and coverage probability increase and that EE decreases as the standard deviation values of lognormal shadowing increases.

While the JT-CoMP approach is applied, in chapter 5 we proposed a tractable expression of EE performance based on fluid modeling for a downlink transmission system. We considered two cases of backhauling power cost, a constant backhauling power cost, and variable backhauling power cost depending on the data rate requirement. We first defined three scenarios according to the application of JT-CoMP. For example, in the first one, we computed the EE expression without considering the coordination between BSs. The second scenario is the worst case, where joint transmission is applied whatever the positions of UEs in the cell. The third scenario is the realistic one, such that the coordination is applied when necessary, at the cell edge or more precisely at a certain distance from the serving BS. Regarding the three scenarios, we confirmed the accuracy of the proposed EE model for both macro- (MCN) and femto- (FCN) cellular networks through comparing the simulation results with the ones obtained by Monte Carlo trials. The simulation results have been exhibited that the data rate is same in both types of cellular networks, whereas the EE in a FCN was larger than the one in a MCN. The simulation results have also shown that EE increases with the raise of the network area, path-loss exponent and the coordinated BSs number in both cases of a constant backhauling power cost and variable backhauling power cost. More interestingly, the simulation results have also demonstrated that SINR threshold of 3dB is reasonable for the JT-CoMP system in the scenario of variable backhauling power cost. Additionally, the simulation results have also pointed out that adding a new coordinated BS in the FCN, compared with the MCN, produces a slighter change to the backhauling power cost, illustrating that JT-CoMP is more efficient in the small cellular network due to the short range transmissions.

## 6.2 Future work

This thesis concentrates on how to design and model the energy efficiency metrics based on the spatial fluid modeling and the proposed model shows the effective and accuracy of the fluid modeling, as a mathematical tool to benchmark the energy efficiency for the cellular networks. However, there are other scenarios and test cases which could be reflected on as

future work. Some of the potential extensions of our work done in this thesis are listed in the below subsections.

### 6.2.1 Other bandwidth scheduling approach

For the investigation of EE based on the bandwidth scheduling approach, all the results in this thesis have been obtained based on the equal bandwidth scheduling scheme, which represents all users are assigned the same bandwidth whatever the spectral efficiency is available to them. However, the user at the cell-edge experiences a lower signal-to-interference-plus-noise ratio (SINR) due to the long distance and fast attenuation. If we assign the same bandwidth to the cell-edge user, it has difficulties to get enough resource for the communication and the requirement of quality of services can not be guaranteed. Therefore, a resource allocation scheme is necessary to balance the bandwidth among users in order to meet the users' demand and improve the network performance. Thus, the EE-evaluation through a new bandwidth scheduling scheme can be considered as a further work of this thesis.

### 6.2.2 EE in heterogeneous networks

For the sake of simplicity, we have made some assumptions in this thesis that all the studied cellular networks are homogeneous, i.e., the transmitting power of each base station is the same. However, in most practical applications, the networks are heterogeneous to meet the network flexibility and the increasing data rate requirements. Thus, heterogeneous network deployment has been an advanced technology to improve the network coverage and enhance the network energy efficiency in the view of operators, as cited in the first chapter. The dense deployment of multi-tier small cells will incur a tremendous escalation of energy consumption, which is one of the significant concerns faced by cellular networks. And some work on EE has been done mainly depending on simulation analysis. However, it needs massive computation and is not tractable. Additionally, the work in [97] demonstrated that the spatial fluid modeling can be utilized to evaluate the signal-to-interference-plus-noise ratio (SINR) of users in a heterogeneous cellular network, composed of macro- and femto-cells. Therefore, it would be worthwhile to investigate the EE model, based on the fluid modeling, for a 2-tier heterogeneous cellular network, which is composed by macro and femto cells.

### 6.2.3 EE-evaluation for uplink system

Due to the fact that limitations of downlink transmission speed are currently considered the more important bottleneck of cellular communications, the work in this thesis only focuses on evaluating the energy efficiency for the downlink system, from the operators' view. However, from the users' perspective, energy-efficient wireless communication is also crucial. Since the high energy expenditure of wireless access networks has facilitated quickly economic concerns and quality-of-experience (QoE) considerations for mobile users. Additionally, the slow advances in battery technologies, as mentioned in chapter 1, also set a limitation of energy demand for mobile multimedia services. For battery-constrained mobile terminals, uplink power consumption dominates the power budget for data transmission. Therefore, it is also interesting to evaluate the energy efficiency in the uplink scenario.

Additionally, the authors in [132] have already studied the effect of interference factor based on the spatial fluid modeling for an uplink system, where the given fixed finite number of mobile users are regarded as an equivalent continuum of mobile users distributed at a certain density. That work illustrated that the fluid modeling also can be used for the uplink system. But so far, there is no work on EE evaluation for the uplink system through taking advantage of the spatial fluid modeling. Hence, following an analogue way as the downlink one, how to model and design an effective and tractable EE model for the uplink system, based on the spatial fluid modeling, is still an open issue.

### 6.2.4 EE mobility model

Our model is proposed without considering the constraints of quality of service for users and under the assumption that the users are stationary during the transmission process. However, for a given deployment scenario of wireless network, we know the average daily traffic at a certain time of one day is changing with the hours of a day. For example, the traffic demand during the evening is very low, since not all users are always active, which leads to low energy consumption. However, the traffic demand increases as raise of the number of active subscribers between busy and off-peak hours, as shown in Fig. 1.8. Therefore, it is important to identify the spatial and temporal variation of EE in the wireless network with the consideration of various traffic demand. Alternatively, when we consider a deployed system where has many fixed users transmitting the signals, one user may move from one cell to another as time passes. In this case, the network energy efficiency may change. In addition, new users may appear on the deployed wireless cellular networks as time passes and they request to communicate and allocate new channels. This leads to changes in channel access and network energy efficiency. Therefore, in such scenarios, how

to model the spatial-temporal change of EE becomes a critical issue in the wireless cellular networks.

# Appendix A

## Computation of data rate in remaining part

### A.1 Basic functions and application on example 1

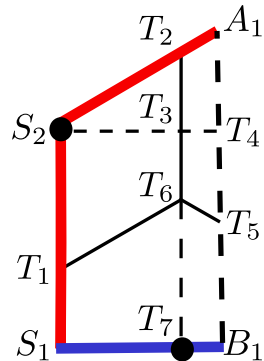


Fig. A.1 Decomposition of the remaining region for example 1.

This appendix illustrates the computation approach of the data rate of the remaining part in Chapter 4. The illustration is based on the example 1, the remaining part of which is shown in Fig. A.1. The corresponding data rate can be decomposed as data rate of subregions as

$$D_{re} = D_{S_1 T_1 T_6 T_7} + D_{T_1 S_2 T_3 T_6} + D_{S_2 T_2 T_3} + D_{T_3 T_2 A_1 T_4} + D_{T_6 T_3 T_4 T_5} + D_{T_7 T_6 T_5 B_1}, \quad (\text{A.1})$$

where the subscript of the summand denotes the vertices of the decomposed subregions. Since the data rate is only related with the relative distance between the serving base station (BS) and the user, it is no hard to conclude that  $D_{S_1 T_1 T_6 T_7}, D_{T_1 S_2 T_3 T_6} = D_{cell}/4$ ,  $D_{S_2 T_2 T_3} =$

$D_{cell}/12$  and  $D_{T_3 T_2 A_1 T_4} = D_{T_6 T_3 T_4 T_5}$ ,  $D_{cell}$  being the date rate for one cell. Thus, Eq. (A.1) is rewritten as

$$D_{re} = 7D_{cell}/12 + 2D_{T_3 T_2 A_1 T_4} + D_{T_7 T_6 T_5 B_1}. \quad (\text{A.2})$$

The solution to  $D_{T_3 T_2 A_1 T_4}$  and  $D_{T_7 T_6 T_5 B_1}$  is obtained based on the introduced basic functions.

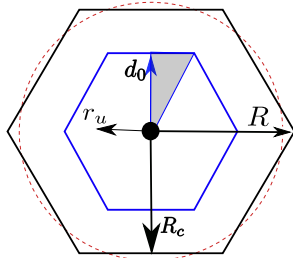


Fig. A.2 Fluid model: small integral triangular region (shaded area) and main parameters

Two basic functions are used to compute the data rate of the decomposed subregions. The first is the function  $\Gamma_t^{in}$  computing the data rate over a small triangular shaded region, as shown in Fig. A.2. For a user  $u$  having the distance  $r$  to its serving base station, the data rate  $= B_u \log_2(1 + \gamma_u(r))$ , where  $\gamma_u(r)$  denotes the signal-to-interference-plus-noise ratio (SINR) and computed with Eq. (3.8). When the user density  $\rho_u$  is known, the number of users in an infinitesimal area equals  $\rho_u r dr d\theta$  and the data rate  $\Gamma_t^{in}$  over the shaded area is computed by the integration

$$\Gamma_t^{in}(d_0) = \int_0^{\frac{\pi}{6}} \int_0^{\frac{d_0}{\cos \theta}} B_u \log_2(1 + \gamma_u(r)) \rho_u r dr d\theta, \quad (\text{A.3})$$

where  $0 < d_0 \leq R_c$ . In particular, when  $d_0 = R_c$ ,

$$\Gamma_t^{in}(R_c) = D_{cell}/12. \quad (\text{A.4})$$

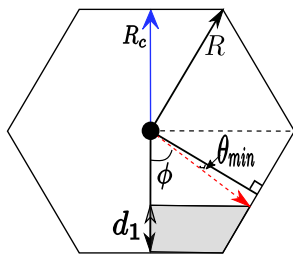


Fig. A.3 Fluid model: integral basin region (shaded area) and main parameters

The second basic function  $\Gamma_{bas}$  computes the data rate over a trapezoid region, which is shown as the shaded area in Fig. A.3. With the value of  $d_1$ ,  $0 < d_1 \leq R_c$ , the involved angle  $\phi = \arctan \frac{R_c + d_1}{\sqrt{3}(R_c - d_1)}$  and  $\theta_{min} = \frac{\pi}{3} - \phi$ . Then, the total data rate over the shaded region follows the integration

$$\Gamma_{bas}(d_1) = \frac{D_{cell}}{6} - \int_0^{\phi} \int_0^{\frac{R_c - d_1}{\cos \theta}} B_u \log_2(1 + \gamma_u(r)) \rho_u r dr d\theta - \int_0^{\theta_{min}} \int_0^{\frac{R_c}{\cos \theta}} B_u \log_2(1 + \gamma_u(r)) \rho_u r dr d\theta \quad (\text{A.5})$$

The solution to  $D_{T_3 T_2 A_1 T_4}$  and  $D_{T_7 T_6 T_5 B_1}$  can be expressed according to  $\Gamma_{bas}$  as  $D_{T_3 T_2 A_1 T_4} = \Gamma_{bas}(R_a/a - 4R_c)$ ,  $D_{T_7 T_6 T_5 B_1} = D_{cell}/4 - \Gamma_{bas}(5R_c - R_a/a)$ .

## A.2 Data rate for the remaining part for a disc area with any size

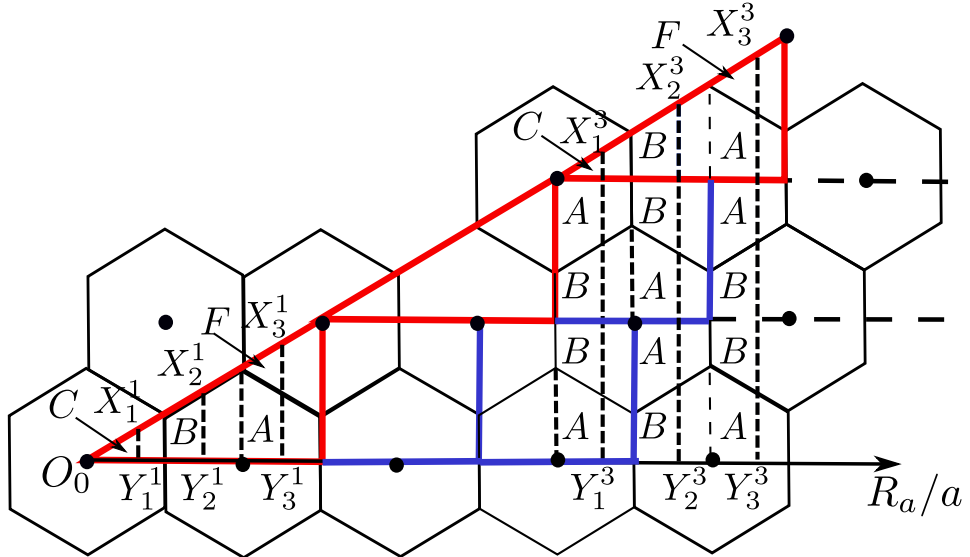


Fig. A.4 Decomposition of the interested area with any size for the computation of data rate.

As described in Chapter 4, with the decomposition of the interested space into repeated  $D_\Delta$ ,  $D_\square$ , and the remaining region, the total data rate is computed by

$$D_{hex}^{tri} = n_t D_\Delta + k D_\square + D_{re}, \quad (\text{A.6})$$

with  $D_{\Delta} = 3D_{cell}/4$ ,  $D_{\square} = D_{cell}$ ,  $n_t = \left[ \frac{R_a}{a}, 3R_c \right]$ ,  $k = \sum_{n=1}^{n_t} \max \left\{ 0, \left[ \frac{R_a}{a} - 3nR_c, 2R_c \right] \right\}$ ,  $[\cdot, \cdot]$  being the quotient operator. The computation of  $D_{re}$  needs further decomposition of the remaining region, as sketched in Fig. A.4.

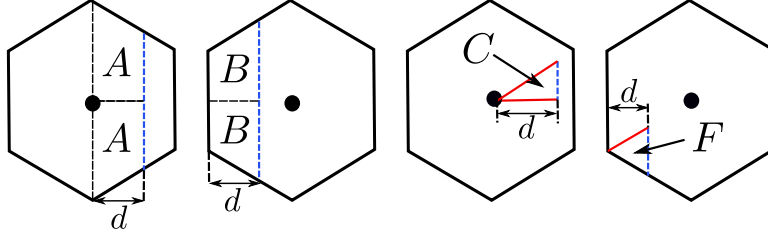


Fig. A.5 Four types of subregions in the decomposition of interested area.

When  $0 < R_a/a \leq 3R_c$ , three cases need to be considered as shown by the line segments  $X_1^1Y_1^1$ ,  $X_2^1Y_2^1$ ,  $X_3^1Y_3^1$ , which stand for the case of  $0 < R_a/a \leq R_c$ ,  $R_c < R_a/a \leq 2R_c$ ,  $2R_c < R_a/a \leq 3R_c$ , respectively. One summarizes that four types of subregions shown in Fig. A.5 are the basic units of the decomposition. Defining  $D_A$ ,  $D_B$ ,  $D_C$ ,  $D_F$  as the data rate for the corresponding region with the parameter  $d$ , we have

$$D_{hex}^{tri} = \begin{cases} D_C(R_a/a) & , 0 < R_a/a \leq R_c \\ D_{cell}/12 + D_B(R_a/a - R_c) & , R_c < R_a/a \leq 2R_c \\ D_{cell}/3 + D_A(R_a/a - 2R_c) + D_F(R_a/a - 2R_c) & , 2R_c < R_a/a \leq 3R_c \end{cases} \quad (\text{A.7})$$

The solution to  $D_A$ ,  $D_B$ ,  $D_C$ ,  $D_F$  as a function of  $d$  is not hard to be represented based on the function  $\Gamma_t^{in}$  and  $\Gamma_{bas}$  as  $D_A(d) = D_{cell}/4 - \Gamma_{bas}(R_c - d)$ ,  $D_B(d) = \Gamma_{bas}(d)$ ,  $D_C(d) = \Gamma_t^{in}(d)$ ,  $D_F(d) = \Gamma_{bas}(d) - (D_{cell}/12 - \Gamma_t^{in}(R_c - d))$ . To simply the illustration below, new notations are defined as  $D_1(d) = D_C(d)$ ,  $D_2(d) = D_{cell}/12 + D_B(d)$ ,  $D_3(d) = D_{cell}/3 + D_A(d) + D_F(d)$ . The parameter  $d$  equals  $(R_a/a) \bmod R_c$ .

When  $6R_c \leq R_a/a < 9R_c$ ,  $n_t = 2$ , mod being the reminder operator. When  $6R_c \leq R_a/a < 7R_c$  (corresponding with the line segment  $X_1^3Y_1^3$ ),  $D_{re} = D_1(d) + D_{cell}/2 + 2(D_A(d) + D_B(d))$ , where  $D_{cell}/2$  is due to  $[R_a/a - 3R_c - 2R_c, R_c] = 1$  for the bottom layer of decomposition in Fig. A.4. The multiplied number 2 for  $(D_A(d) + D_B(d))$  equals  $n_t$ . Following similar analysis, when  $7R_c \leq R_a/a < 8R_c$  (corresponding with the line segment  $X_2^3Y_2^3$ ), since  $[R_a/a - 3R_c - 2R_c, R_c] = 0$  for the bottom layer and  $[R_a/a - 2 \times 3R_c - 0 \times 2R_c, R_c] = 1$  for the second layer,  $D_{re} = D_2(d) + D_{cell}/2 + 2(D_A(d) + D_B(d))$ . For the line segment  $X_3^3Y_3^3$ ,  $D_{re} = D_3(d) + D_{cell}/2 + 2(D_A(d) + D_B(d))$ , where the summand  $D_{cell}/2$  is due to that  $[R_a/a - 3R_c - 2 \times 2R_c, R_c] = 1$  for the bottom layer.

From the above analysis, the formula to compute  $D_{re}$  for any value of  $R_a/a$  is written as

$$D_{re}(R_a) = D_{1,2,\text{or}3}(d) + \nu D_{cell}/2 + n_t(D_A(d) + D_B(d)), \quad (\text{A.8})$$

where

$$\nu = \sum_{n=1}^{n_t} (R_a/a - 3nR_c - 2k_n R_c) \bmod R_c \quad (\text{A.9})$$

and

$$k_n = \max \left\{ 0, \left[ \frac{R_a}{a} - 3nR_c, 2R_c \right] \right\}. \quad (\text{A.10})$$



# References

- [1] L. Deng, Y. Rui, P. Cheng, J. Zhang, Q. Zhang, and M. Li, “A unified energy efficiency and spectral efficiency tradeoff metric in wireless networks,” *IEEE Communications Letters*, vol. 17, no. 1, pp. 55–58, 2012.
- [2] G. Auer, V. Giannini, C. Dessel, I. Godor, P. Skillermark, M. Olsson, M. A. Imran, D. Sabella, M. J. Gonzalez, O. Blume, *et al.*, “How much energy is needed to run a wireless network?,” *IEEE Wireless Communications*, vol. 18, no. 5, 2011.
- [3] H. Q. Ngo, E. G. Larsson, and T. L. Marzetta, “Energy and spectral efficiency of very large multiuser MIMO systems,” *IEEE Transactions on Communications*, vol. 61, no. 4, pp. 1436–1449, 2013.
- [4] A. Fehske, G. Fettweis, J. Malmodin, and G. Biczok, “The global footprint of mobile communications: The ecological and economic perspective,” *IEEE Communications Magazine*, vol. 49, no. 8, 2011.
- [5] M. A. Matin, *Handbook of Research on Progressive Trends in Wireless Communications and Networking*. IGI Global, 2014.
- [6] G. Y. Li, Z. Xu, C. Xiong, C. Yang, S. Zhang, Y. Chen, and S. Xu, “Energy-efficient wireless communications: tutorial, survey, and open issues,” *IEEE Wireless Communications*, vol. 18, no. 6, 2011.
- [7] “Why the EU is betting big on 5G,” *Res. EU Focus Mag*, vol. 15, no. 1977-4036, 2015.
- [8] E. W. Paper, “More than 50 billion connected devices,” *Ericsson, Tech. Rep.*, pp. 284 353–354 Uen, Feb. 2011.
- [9] S. Buzzi, I. Chih-Lin, T. E. Klein, H. V. Poor, C. Yang, and A. Zappone, “A survey of energy-efficient techniques for 5G networks and challenges ahead,” *IEEE Journal on Selected Areas in Communications*, vol. 34, no. 4, pp. 697–709, 2016.

- [10] I. Vision, “Framework and overall objectives of the future development of IMT for 2020 and beyond,” *International Telecommunication Union (ITU), Document, Radiocommunication Study Groups*, 2015.
- [11] T. Chen, Y. Yang, H. Zhang, H. Kim, and K. Horneman, “Network energy saving technologies for green wireless access networks,” *IEEE Wireless Communications*, vol. 18, no. 5, 2011.
- [12] C. Han, T. Harrold, S. Armour, I. Krikidis, S. Videv, P. M. Grant, H. Haas, J. S. Thompson, I. Ku, C.-X. Wang, *et al.*, “Green radio: radio techniques to enable energy-efficient wireless networks,” *IEEE communications magazine*, vol. 49, no. 6, 2011.
- [13] Y. Chen, S. Zhang, S. Xu, and G. Y. Li, “Fundamental trade-offs on green wireless networks,” *IEEE Communications Magazine*, vol. 49, no. 6, 2011.
- [14] H. Bogucka and A. Conti, “Degrees of freedom for energy savings in practical adaptive wireless systems,” *IEEE Communications Magazine*, vol. 49, no. 6, 2011.
- [15] E. Oh, B. Krishnamachari, X. Liu, and Z. Niu, “Toward dynamic energy-efficient operation of cellular network infrastructure,” *IEEE Communications Magazine*, vol. 49, no. 6, 2011.
- [16] Y. S. Soh, T. Q. Quek, M. Kountouris, and H. Shin, “Energy efficient heterogeneous cellular networks,” *IEEE Journal on Selected Areas in Communications*, vol. 31, no. 5, pp. 840–850, 2013.
- [17] I. Humar, X. Ge, L. Xiang, M. Jo, M. Chen, and J. Zhang, “Rethinking energy efficiency models of cellular networks with embodied energy,” *IEEE Network*, vol. 25, no. 2, 2011.
- [18] D. Feng, C. Jiang, G. Lim, L. J. Cimini, G. Feng, and G. Y. Li, “A survey of energy-efficient wireless communications,” *IEEE Communications Surveys & Tutorials*, vol. 15, no. 1, pp. 167–178, 2013.
- [19] M. Ismail, W. Zhuang, E. Serpedin, and K. Qaraqe, “A survey on green mobile networking: From the perspectives of network operators and mobile users,” *IEEE Communications Surveys & Tutorials*, vol. 17, no. 3, pp. 1535–1556, 2015.
- [20] S. Tombaz, A. Vastberg, and J. Zander, “Energy-and cost-efficient ultra-high-capacity wireless access,” *IEEE wireless Communications*, vol. 18, no. 5, 2011.

- [21] L. M. Correia, D. Zeller, O. Blume, D. Ferling, Y. Jading, I. Gódor, G. Auer, and L. Van Der Perre, “Challenges and enabling technologies for energy aware mobile radio networks,” *IEEE Communications Magazine*, vol. 48, no. 11, 2010.
- [22] S. McLaughlin, P. M. Grant, J. S. Thompson, H. Haas, D. I. Laurenson, C. Khirallah, Y. Hou, and R. Wang, “Techniques for improving cellular radio base station energy efficiency,” *IEEE Wireless Communications*, vol. 18, no. 5, 2011.
- [23] “2010 wireless smartphone customer satisfaction study,” *J.D. Power and Associates*, 2010.
- [24] “2010 China nokia mobile phone user research report,” 2010.
- [25] X. Ma, M. Sheng, Y. Zhang, and X. Wang, “Concurrent transmission for energy efficiency in heterogeneous wireless networks,” *IEEE Transaction on Wireless Communications*.
- [26] M. Ismail, W. Zhuang, and S. Elhedhli, “Energy and content aware multi-homing video transmission in heterogeneous networks,” *IEEE Transactions on Wireless Communications*, vol. 12, no. 7, pp. 3600–3610, 2013.
- [27] G. Miao, N. Himayat, Y. G. Li, and A. Swami, “Cross-layer optimization for energy-efficient wireless communications: a survey,” *Wireless Communications and Mobile Computing*, vol. 9, no. 4, pp. 529–542, 2009.
- [28] R. Mahapatra, Y. Nijsure, G. Kaddoum, N. U. Hassan, and C. Yuen, “Energy efficiency tradeoff mechanism towards wireless green communication: A survey,” *IEEE Communications Surveys and Tutorials*, vol. 18, no. 1, pp. 686–705, 2016.
- [29] T. Chen, H. Kim, and Y. Yang, “Energy efficiency metrics for green wireless communications,” *2010 International Conference on Wireless Communications & Signal Processing (WCSP)*, pp. 1–6, 2010.
- [30] H. Kwon and T. Birdsall, “Channel capacity in bits per joule,” *IEEE Journal of Oceanic Engineering*, vol. 11, no. 1, pp. 97–99, 1986.
- [31] V. Rodoplu and T. H. Meng, “Bits-per-joule capacity of energy-limited wireless networks,” *IEEE Transactions on Wireless Communications*, vol. 6, no. 3, pp. 857–865, 2007.
- [32] S. Verdú, “Spectral efficiency in the wideband regime,” *IEEE Transactions on Information Theory*, vol. 48, no. 6, pp. 1319–1343, 2002.

- [33] A. Lozano, A. M. Tulino, and S. Verdú, “Multiple-antenna capacity in the low-power regime,” *IEEE Transactions on Information Theory*, vol. 49, no. 10, pp. 2527–2544, 2003.
- [34] O. Oyman and A. J. Paulraj, “Spectral efficiency of relay networks in the power limited regime,” *2004 IEEE 42th Annual Allerton Conference on Communication, Control and Computing, Allerton, USA*, 2004.
- [35] J. Gómez-Vilardebó, A. I. Pérez-Neira, and M. Nájar, “Energy efficient communications over the awgn relay channel,” *IEEE Transactions on Wireless Communications*, vol. 9, no. 1, pp. 32–37, 2010.
- [36] C. Bae and W. E. Stark, “Energy and bandwidth efficiency in wireless networks,” *2006 International Conference on Communications, Circuits and Systems*, vol. 2, pp. 1297–1302, 2006.
- [37] K. N. R. S. V. Prasad, E. Hossain, and V. K. Bhargava, “Energy efficiency in massive mimo-based 5g networks: Opportunities and challenges,” *IEEE Wireless Communications*, vol. 24, no. 3, pp. 86–94, 2017.
- [38] E. Björnson, L. Sanguinetti, J. Hoydis, and M. Debbah, “Optimal design of energy-efficient multi-user MIMO systems: Is massive MIMO the answer?,” *IEEE Transactions on Wireless Communications*, vol. 14, no. 6, pp. 3059–3075, 2015.
- [39] R. Irmer, H. Droste, P. Marsch, M. Grieger, G. Fettweis, S. Brueck, H.-P. Mayer, L. Thiele, and V. Jungnickel, “Coordinated multipoint: Concepts, performance, and field trial results,” *IEEE Communications Magazine*, vol. 49, no. 2, pp. 102–111, 2011.
- [40] T. Han and N. Ansari, “On greening cellular networks via multicell cooperation,” *IEEE Wireless Communications*, vol. 20, no. 1, pp. 82–89, 2013.
- [41] S. Singh, A. Kumar, S. S. Khurmi, and T. Singh, “Coordinated multipoint (CoMP) reception and transmission for LTE-Advanced/4G 1,” 2012.
- [42] M. O. E. H. Mauro Renato Boldi, Antti Tölli, “Coordinated multipoint (CoMP) systems,” *Mobile and Wireless Communications for IMT-Advanced and Beyond*, pp. 121–155, 2011.
- [43] 3GPP TR 36.814, LTE, “Technical specification group radio access network; evolved universal terrestrial radio access (e-utra); further advancements for e-utra physical layer aspects (release 9),” 3GPP Tech. Rep., 9.0.0, 3 2010.

- [44] J. Wu, S. Jin, L. Jiang, and G. Wang, "Dynamic switching off algorithms for pico base stations in heterogeneous cellular networks," *EURASIP Journal on Wireless Communications and Networking*, vol. 2015, no. 1, p. 117, 2015.
- [45] A. Ghosh, N. Mangalvedhe, R. Ratasuk, B. Mondal, M. Cudak, E. Visotsky, T. Thomas, J. Andrews, P. Xia, H.-S. Jo, H. Dhillon, and T. Novlan, "Heterogeneous cellular networks: From theory to practice," *IEEE Communications Magazine*, vol. 50, pp. 54–64, 06 2012.
- [46] Hu, Rose Qingyang and Qian, Yi, "An energy efficient and spectrum efficient wireless heterogeneous network framework for 5G systems," *IEEE Communications Magazine*, vol. 52, no. 5, pp. 94–101, 2014.
- [47] Z. Hasan, H. Boostanimehr, and V. K. Bhargava, "Green cellular networks: A survey, some research issues and challenges," *IEEE Communications surveys & tutorials*, vol. 13, no. 4, pp. 524–540, 2011.
- [48] Y. Yang, H. Hu, J. Xu, and G. Mao, "Relay technologies for WiMAX and LTE-advanced mobile systems," *IEEE Communications Magazine*, vol. 47, no. 10, pp. 100–105, 2009.
- [49] S. ULC, "Sandvine global internet phenomena report-1h2012," tech. rep., Technical report, 2012.
- [50] A. Checko, H. L. Christiansen, Y. Yan, L. Scolari, G. Kardaras, M. S. Berger, and L. Dittmann, "Cloud RAN for mobile networks-a technology overview," *IEEE Communications surveys & tutorials*, vol. 17, no. 1, pp. 405–426, 2014.
- [51] "C-RAN: the road towards green ran, ver. 3.0," *White Paper, China Mobile*, Dec. 2013.
- [52] B. Dai and W. Yu, "Energy efficiency of downlink transmission strategies for cloud radio access networks," *IEEE Journal on Selected Areas in Communications*, vol. 34, no. 4, pp. 1037–1050, 2016.
- [53] D. Pompili, A. Hajisami, and T. X. Tran, "Elastic resource utilization framework for high capacity and energy efficiency in cloud RAN," *IEEE Communications Magazine*, vol. 54, no. 1, pp. 26–32, 2016.
- [54] M. Sinaie, A. Zappone, E. A. Jorswieck, and P. Azmi, "5G green networking: Enabling technologies, potentials, and challenges," *2016 IEEE 17th Annual Conference on Wireless and Microwave Technology (WAMICON)*, pp. 1–6, 2016.

- [55] A. Mämmelä, “Energy efficiency in 5G mobile networks,” *2015 IEEE 14th IFIP Networking Conference, Toulouse, France*, 2015.
- [56] R. L. Cavalcante, S. Stanczak, M. Schubert, A. Eisenblätter, and U. Türke, “Toward energy-efficient 5G wireless communications technologies: Tools for decoupling the scaling of networks from the growth of operating power,” *IEEE Signal Processing Magazine*, vol. 31, no. 6, pp. 24–34, 2014.
- [57] A. A. Ibrahim, K. P. Kpochi, and E. J. Smith, “Energy consumption assessment of mobile cellular networks,” *American Journal of Engineering Research (AJER)*, vol. 7, pp. 96–101, 2018.
- [58] F. Richter, A. J. Fehske, and G. P. Fettweis, “Energy efficiency aspects of base station deployment strategies for cellular networks,” *2009 IEEE 70th Vehicular Technology Conference Fall (VTC 2009-Fall)*, pp. 1–5, 2009.
- [59] G. Auer, O. Blume, V. Giannini, I. Godor, M. Imran, Y. Jading, E. Katranaras, M. Olsson, D. Sabella, P. Skillermack, *et al.*, “D2. 3: Energy efficiency analysis of the reference systems, areas of improvements and target breakdown,” *INFSO-ICT-247733 EARTH*, pp. 1–69, 2012.
- [60] E. Björnson, L. Sanguinetti, and M. Kountouris, “Deploying dense networks for maximal energy efficiency: Small cells meet massive MIMO,” *IEEE Journal on Selected Areas in Communications*, vol. 34, no. 4, pp. 832–847, 2016.
- [61] I. Ashraf, F. Boccardi, and L. Ho, “Sleep mode techniques for small cell deployments,” *IEEE Communications Magazine*, vol. 49, no. 8, pp. 72–79, 2011.
- [62] K. Son, H. Kim, Y. Yi, and B. Krishnamachari, “Base station operation and user association mechanisms for energy-delay tradeoffs in green cellular networks,” *IEEE journal on selected areas in communications*, vol. 29, no. 8, pp. 1525–1536, 2011.
- [63] W. Cheng, X. Zhang, and H. Zhang, “Joint spectrum and power efficiencies optimization for statistical QoS provisionings over SISO/MIMO wireless networks,” *IEEE Journal on Selected Areas in Communications*, vol. 31, no. 5, pp. 903–915, 2013.
- [64] A. J. Fehske, P. Marsch, and G. P. Fettweis, “Bit per joule efficiency of cooperating base stations in cellular networks,” *2010 IEEE Globecom Workshops (GCWkshps '10)*, pp. 1406–1411, 2010.

- [65] O. Arnold, F. Richter, G. Fettweis, and O. Blume, “Power consumption modeling of different base station types in heterogeneous cellular networks,” *2010 Future Network Mobile Summit*, pp. 1–8, 2010.
- [66] M. Sinaie, A. Zappone, E. A. Jorswieck, and P. Azmi, “A novel power consumption model for effective energy efficiency in wireless networks,” *IEEE Wireless Communications Letters*, vol. 5, no. 2, pp. 152–155, 2016.
- [67] C. Li, J. Zhang, and K. B. Letaief, “Throughput and energy efficiency analysis of small cell networks with multi-antenna base stations,” *IEEE Transactions on Wireless Communications*, vol. 13, no. 5, pp. 2505–2517, 2014.
- [68] F. Héliot, M. A. Imran, and R. Tafazolli, “On the energy efficiency-spectral efficiency trade-off over the MIMO rayleigh fading channel,” *IEEE Transactions on Communications*, vol. 60, no. 5, pp. 1345–1356, 2012.
- [69] D. Gesbert, S. Hanly, H. Huang, S. S. Shitz, O. Simeone, and W. Yu, “Multi-cell MIMO cooperative networks: A new look at interference,” *IEEE Journal on Selected Areas in Communications*, vol. 28, pp. 1380–1408, dec 2010.
- [70] G. Miao, “Energy-efficient uplink multi-user MIMO,” *IEEE Transactions on wireless communications*, vol. 12, no. 5, pp. 2302–2313, 2013.
- [71] G. Miao, N. Himayat, and G. Y. Li, “Energy-efficient link adaptation in frequency-selective channels,” *IEEE Transactions on communications*, vol. 58, no. 2, 2010.
- [72] Y. Rui, Q. Zhang, L. Deng, P. Cheng, and M. Li, “Mode selection and power optimization for energy efficiency in uplink virtual MIMO systems,” *IEEE Journal on Selected Areas in Communications*, vol. 31, no. 5, pp. 926–936, 2013.
- [73] F. Héliot, M. A. Imran, and R. Tafazolli, “Energy efficiency analysis of idealized coordinated multi-point communication system,” pp. 1–5, IEEE, 2011.
- [74] G. Cili, H. Yanikomeroglu, and F. R. Yu, “Cell switch off technique combined with coordinated multi-point (CoMP) transmission for energy efficiency in beyond-LTE cellular networks,” *2012 IEEE International Conference on Communications (ICC)*, pp. 5931–5935, 2012.
- [75] A. Jahid, A. B. Shams, and M. F. Hossain, “Energy efficiency of JT-CoMP based green powered LTE-A cellular networks,” *2017 International Conference on Wireless*

- Communications, Signal Processing and Networking (WiSPNET)*, pp. 1739–1745, 2017.
- [76] H. Klessig, A. J. Fehske, and G. P. Fettweis, “Energy efficiency gains in interference-limited heterogeneous cellular mobile radio networks with random micro site deployment,” *2011 IEEE 34th Sarnoff Symposium*, pp. 1–6, 2011.
  - [77] S. Rizvi, A. Aziz, M. T. Jilani, N. Armi, G. Muhammad, and S. H. Butt, “An investigation of energy efficiency in 5G wireless networks,” *2017 International Conference on Circuits, System and Simulation (ICCSS)*, pp. 142–145, 2017.
  - [78] T. Zhang, J. Zhao, L. An, and D. Liu, “Energy efficiency of base station deployment in ultra dense HetNets: A stochastic geometry analysis,” *IEEE Wireless Communications Letters*, vol. 5, no. 2, pp. 184–187, 2016.
  - [79] R. Fantini, D. Sabella, and M. Caretti, “Energy efficiency in LTE-advanced networks with relay nodes,” *2011 IEEE 73rd Vehicular Technology Conference (VTC Spring)*, pp. 1–5, 2011.
  - [80] O. Onireti, F. Héliot, and M. A. Imran, “On the energy efficiency-spectral efficiency trade-off in the uplink of comp system,” *IEEE Transactions on Wireless Communications*, vol. 11, no. 2, pp. 556–561, 2012.
  - [81] J. Peng, P. Hong, and K. Xue, “Energy-aware cellular deployment strategy under coverage performance constraints,” *IEEE Transactions on Wireless Communications*, vol. 14, no. 1, pp. 69–80, 2014.
  - [82] A. Shojaeifard, K.-K. Wong, K. A. Hamdi, E. Alsusa, D. K. So, and J. Tang, “Stochastic geometric analysis of energy-efficient dense cellular networks,” *IEEE Access*, vol. 5, pp. 455–469, 2017.
  - [83] M. W. Kang and Y. W. Chung, “An efficient energy saving scheme for base stations in 5G networks with separated data and control planes using particle swarm optimization,” *Energies*, vol. 10, no. 9, p. 1417, 2017.
  - [84] E. Bjornson, M. Kountouris, and M. Debbah, “Massive MIMO and small cells: Improving energy efficiency by optimal soft-cell coordination,” pp. 1–5, 2013.
  - [85] P.-H. Huang, S.-S. Sun, and W. Liao, “GreenCoMP: energy-aware cooperation for green cellular networks,” *IEEE Transactions on Mobile Computing*, vol. 16, no. 1, pp. 143–157, 2017.

- [86] S. He, Y. Huang, S. Jin, and L. Yang, “Coordinated beamforming for energy efficient transmission in multicell multiuser systems,” *IEEE Transactions on Communications*, vol. 61, no. 12, pp. 4961–4971, 2013.
- [87] A. Zappone, L. Sanguinetti, G. Bacci, E. Jorswieck, and M. Debbah, “Energy-efficient power control: A look at 5G wireless technologies,” *IEEE Transactions on Signal Processing*, vol. 64, no. 7, pp. 1668–1683, 2016.
- [88] Y. Zhang, Q. Cui, and N. Wang, “Energy efficiency maximization for CoMP joint transmission with non-ideal power amplifiers,” *2017 IEEE 28th Annual International Symposium on Personal, Indoor, and Mobile Radio Communications (PIMRC)*, pp. 1–6, 2017.
- [89] D. Liu and C. Yang, “Energy efficiency of downlink networks with caching at base stations,” *IEEE Journal on Selected Areas in Communications*, vol. 34, no. 4, pp. 907–922, 2016.
- [90] B. Du, C. Pan, W. Zhang, and M. Chen, “Distributed energy-efficient power optimization for CoMP systems with max-min fairness,” *IEEE Communications Letters*, vol. 18, no. 6, pp. 999–1002, 2014.
- [91] K. M. S. Huq, S. Mumtaz, J. Bachmatiuk, J. Rodriguez, X. Wang, and R. L. Aguiar, “Green HetNet CoMP: Energy efficiency analysis and optimization,” *IEEE Transactions on vehicular technology*, vol. 64, no. 10, pp. 4670–4683, 2015.
- [92] K. M. S. Huq, S. Mumtaz, and J. Rodriguez, “QoS aware energy-efficient resource scheduling for HetNet CoMP,” *2015 IEEE International Conference on Communications (ICC)*, pp. 5954–5960, 2015.
- [93] Z. Xu, C. Yang, G. Y. Li, Y. Liu, and S. Xu, “Energy-efficient CoMP precoding in heterogeneous networks,” *IEEE Transactions on Signal Processing*, vol. 62, no. 4, pp. 1005–1017, 2014.
- [94] G. Zhao, S. Chen, L. Zhao, and L. Hanzo, “Joint energy-spectral-efficiency optimization of COMP and BS deployment in dense large-scale cellular networks,” *IEEE Transactions on Wireless Communications*, vol. 16, no. 7, pp. 4832–4847, 2017.
- [95] C. Liu, B. Natarajan, and H. Xia, “Small cell base station sleep strategies for energy efficiency,” *IEEE Transactions on Vehicular Technology*, vol. 65, no. 3, pp. 1652–1661, 2016.

- [96] J.-M. Kelif, M. Coupechoux, and P. Godlewski, “A fluid model for performance analysis in cellular networks,” *EURASIP Journal on Wireless Communications and Networking*, vol. 2010, no. 1, p. 435189, 2010.
- [97] J.-M. Kelif, W. Diego, and S. Senecal, “Impact of transmitting power on femto cells performance and coverage in heterogeneous wireless networks,” *2012 IEEE Wireless Communications and Networking Conference (WCNC)*, pp. 2996–3001, 2012.
- [98] J.-M. Kelif, S. Senecal, C. Bridon, and M. Coupechoux, “Quality of service and performance evaluation: A fluid approach for poisson wireless networks,” *2014 IEEE International Conference and Workshop on the Network of Future (NOF)*, pp. 1–5, 2014.
- [99] L. Zitoune, S. Cerovic, D. Cerovic, V. Vèque, and J.-M. Kelif, “Performance evaluation of JT CoMP approach: Tractable model using spatial fluid modeling,” *2016 IEEE IFIP Networking Conference*, pp. 198–206, 2016.
- [100] M. Maqbool, P. Godlewski, M. Coupechoux, and J.-M. Kélfif, “Analytical performance evaluation of various frequency reuse and scheduling schemes in cellular OFDMA networks,” *Performance Evaluation*, vol. 67, no. 4, pp. 318–337, 2010.
- [101] Alliance, “5G white paper,” *Next generation mobile networks (NGMN), White Paper*, February 2015.
- [102] S. C. V. N. Index., “Global mobile data traffic forecast update,” *White Paper*, pp. 2015–2020, February 2016.
- [103] D. D. EARTH, “Energy efficiency analysis of the reference systems, areas of improvements and target breakdown,” *version 2.0*, January 2012.
- [104] “Final trend workshop,” *Brussels*, October 2013.
- [105] A. Osseiran, F. Boccardi, V. Braun, K. Kusume, P. Marsch, M. Maternia, O. Queseth, M. Schellmann, H. Schotten, H. Taoka, *et al.*, “Scenarios for 5G mobile and wireless communications: the vision of the metis project,” *IEEE Communications Magazine*, vol. 52, no. 5, pp. 26–35, 2014.
- [106] “<https://green-touch.org/>,”
- [107] G. V. 5G PPP, “The 5G infrastructure public private partnership, the next generation of communication networks and services,” *IEEE Wireless Communications Letters*, February 2015.

- [108] H. Wei, N. Deng, W. Zhou, and M. Haenggi, "Approximate SIR analysis in general heterogeneous cellular networks," *IEEE Transactions on Communications*, vol. 64, no. 3, pp. 1259–1273, 2016.
- [109] R. Hekmat and P. Van Mieghem, "Connectivity in wireless ad-hoc networks with a log-normal radio model," *Mobile networks and applications*, vol. 11, no. 3, pp. 351–360, 2006.
- [110] Y. Tian, Y. Ou, G. You, and Z. Wang, "A coverage configuration scheme of wireless sensor networks base on collaborative sensing in shadow fading," *2017 IEEE 29th Chinese Control And Decision Conference (CCDC)*, pp. 5993–5997, 2017.
- [111] D. B. Cheikh, J.-M. Kelif, M. Coupechoux, and P. Godlewski, "SIR distribution analysis in cellular networks considering the joint impact of path-loss, shadowing and fast fading," *EURASIP Journal on Wireless Communications and Networking*, vol. 2011, no. 1, p. 137, 2011.
- [112] J.-M. Kelif and M. Coupechoux, "Impact of topology and shadowing on the outage probability of cellular networks," *2009 IEEE International Conference on Communications(ICC)*, pp. 1–6, 2009.
- [113] J. Chen, L.-C. Wang, and C.-H. Liu, "Coverage probability of small cell networks with composite fading and shadowing," *2014 IEEE 25th Annual International Symposium on Personal, Indoor, and Mobile Radio Communication (PIMRC)*, pp. 1965–1969, 2014.
- [114] Y. Zhuang, Y. Luo, L. Cai, and J. Pan, "A geometric probability model for capacity analysis and interference estimation in wireless mobile cellular systems," *2011 IEEE Global Telecommunications Conference - GLOBECOM 2011*, pp. 1–6, 2011.
- [115] Z. Lei, D. Goodman, and N. Mandayam, "Location-dependent other-cell interference and its effect on the uplink capacity of a cellular cdma system," *IEEE VTS 50th on Vehicular Technology*, vol. 3, pp. 2164 – 2168, August 1999.
- [116] M. Jansen and R. Prasad, "Capacity, throughput, and delay analysis of a cellular ds cdma system with imperfect power control and imperfect sectorization," *IEEE Transactions on Vehicular Technology*, vol. 44, pp. 67 – 75, march 1995.
- [117] G. L. Stüber, *Principles of mobile communication*, vol. 2. Springer, 1996.

- [118] L. Fenton, “The sum of log-normal probability distributions in scatter transmission systems,” *IRE Transactions on Communications Systems*, vol. 8, no. 1, pp. 57–67, 1960.
- [119] J.-M. Kelif, S. Senecal, M. Coupechoux, and C. Bridon, “Analytical performance model for Poisson wireless networks with pathloss and shadowing propagation,” *2014 IEEE Globecom Workshops (GC Wkshps)*, pp. 1528–1532, 2014.
- [120] Y. Gu and S. Aissa, “RF-based energy harvesting in decode-and-forward relaying systems: Ergodic and outage capacities,” *IEEE Transactions on Wireless Communications*, vol. 14, no. 11, pp. 6425–6434, 2015.
- [121] J. G. Andrews, F. Baccelli, and R. K. Ganti, “A tractable approach to coverage and rate in cellular networks,” *IEEE Transactions on communications*, vol. 59, no. 11, pp. 3122–3134, 2011.
- [122] R. F. Guiazon, K.-K. Wong, and M. Fitch, “Coverage probability of cellular networks using interference alignment under imperfect CSI,” *Digital Communications and Networks*, vol. 2, no. 4, pp. 162–166, 2016.
- [123] G. Koutitas, “Green network planning of single frequency networks,” *IEEE transactions on broadcasting*, vol. 56, no. 4, pp. 541–550, 2010.
- [124] V. Erceg, L. J. Greenstein, S. Y. Tjandra, S. R. Parkoff, A. Gupta, B. Kulic, A. A. Julius, and R. Bianchi, “An empirically based path loss model for wireless channels in suburban environments,” *IEEE Journal on selected areas in communications*, vol. 17, no. 7, pp. 1205–1211, 1999.
- [125] S.-Y. Kim and C.-H. Cho, “Call blocking probability and effective throughput for call admission control of CoMP joint transmission,” *IEEE Transactions on Vehicular Technology*, vol. 66, no. 1, pp. 622–634, 2017.
- [126] 3GPP TR 36.913, LTE, “Requirements for further advancements for evolved universal terrestrial radio access (E-UTRA)(LTE-advanced)(release 10),” evolved universal terrestrial radio access (E-UTRA), 3GPP Tech. Rep., version 10.0.0, 2011.
- [127] R. Tanbourgi, S. Singh, J. G. Andrews, and F. K. Jondral, “A tractable model for noncoherent joint-transmission base station cooperation,” *IEEE Transactions on Wireless Communications*, vol. 13, no. 9, pp. 4959–4973, 2014.

- [128] Y. Xu, Y. Li, Z. Wang, T. Lin, G. Zhang, and S. Ci, “Coordinated caching model for minimizing energy consumption in radio access network,” pp. 2406–2411, 2014.
- [129] N. Choi, K. Guan, D. C. Kilper, and G. Atkinson, “In-network caching effect on optimal energy consumption in content-centric networking,” pp. 2889–2894, 2012.
- [130] Y. Hou, L. Zitoune, and V. Vèque, “Fluid modeling of energy efficiency in large cellular networks,” *2018 IEEE 29th Annual International Symposium on Personal, Indoor and Mobile Radio Communications (PIMRC)*, pp. 1–5, 2018.
- [131] M. Sawahashi, Y. Kishiyama, A. Morimoto, D. Nishikawa, and M. Tanno, “Coordinated multipoint transmission/reception techniques for LTE-advanced [Coordinated and Distributed MIMO],” *IEEE Wireless Communications*, vol. 17, no. 3, 2010.
- [132] J.-M. Kelif, “Admission control on fluid cdma networks,” *2006 IEEE 4th International Symposium on Modeling and Optimization in Mobile, Ad Hoc and Wireless Networks*, pp. 1–7, 2006.



# **Publications**

## **JOURNAL PAPERS**

---

### **Published**

Y. Hou, L. Zitoune, and V. Vèque, “Fluid-based Energy Efficiency Analysis of JT-CoMP Scheme in Femto Cellular Networks”, *IEEE Transactions on Green Communications and Networking*, pp. 1-1, 2020. doi: 10.1109/TGCN.2020.3036903.

## **CONFERENCE PAPERS**

---

### **Published**

Y. Hou, L. Zitoune, and V. Vèque, “Analysis of the energy efficiency of JT-CoMP in macro/femto cellular networks”, *Francophone Meetings on Protocol Design, Performance Assessment and Experimentation of Communication Networks (CORES2020)*, Lyon, France, 2020.

Y. Hou, L. Zitoune, and V. Vèque, “Energy Efficiency Analysis of JT-CoMP Scheme in Macro/Femto Cellular Networks”, *2019 IEEE Global Communications Conference (GLOBECOM)*, Waikoloa, HI, USA, pp. 1-6, 2019. doi: 10.1109/GLOBECOM38437.2019.9013282.

Y. Hou, L. Zitoune, and V. Vèque, “Effect of Shadowing on Energy Efficiency in Small Cellular Networks”, *2019 IEEE 27th International Symposium on Modeling, Analysis, and Simulation of Computer and Telecommunication Systems (MASCOTS)*, Rennes, FR, pp. 221-227, 2019.

doi: 10.1109/MASCOTS.2019.00031.

Y. Hou, L. Zitoune, and V. Vèque, “Fluid modeling of energy efficiency in large cellular networks”, *2018 IEEE 29th Annual International Symposium on Personal, Indoor and Mobile Radio Communications (PIMRC)*, Bologna, pp. 1-5, 2018. doi: 10.1109/PIMRC.2018.8580879.

## Poster Presentations

Y. Hou, L. Zitoune, and V. Vèque, “Journée Des Doctorants”, *Laboratoire des Signaux et Systèmes (L2S), CentraleSupélec*, Paris, 27 June 2018.

Y. Hou, L. Zitoune, and V. Vèque, “Journée Doctorants ESIEE”, *École Supérieure d'Ingénieurs en Électrotechnique et Électronique (ESIEE)*, Paris, 21 June 2018.

Y. Hou, L. Zitoune, and V. Vèque, “Journées Non-thématiques DU GDR RSD”, *École nationale supérieure d'électrotechnique, d'électronique, d'informatique, d'hydraulique et des télécommunications (ENSEEIHT)*, Toulouse, 18-19 Jan. 2018.

Y. Hou, L. Zitoune, and V. Vèque, “Seminar in the Research Team”, *Laboratoire des Signaux et Systèmes (L2S), CentraleSupélec*, Paris, 11 July 2017.

**Titre :** Évaluation de l'efficacité énergétique dans les réseaux cellulaires mobiles à l'aide de la modélisation fluide

**Mots clés :** efficacité énergétique, réseaux mobiles, JT-CoMP, évaluation des performances, modélisation fluide

**Résumé :** La conception des systèmes de communication dits 5G cible une efficacité énergétique ambitieuse, au moins 1000 fois supérieure à celle du système 4G actuellement disponible, tout en offrant un débit de transmission de données supérieur et un temps de latence très faible. Il est donc nécessaire de développer des modèles représentatifs et précis des grands réseaux cellulaires afin d'évaluer leur performance et d'identifier les principaux facteurs impliqués dans la consommation d'énergie comme l'atténuation de signal, le type et la qualité de la couverture cellulaire radio.

Nous avons utilisé la modélisation fluide spatiale pour développer des modèles représentatifs et calculables afin de calculer la métrique d'efficacité énergétique. Notre modèle considère un réseau composé de plusieurs cellules opérant en OFDMA sur les liens descendants, et de multiples équipements utilisateurs répartis aléatoirement. Une expression analytique de l'efficacité énergétique a été dérivée pour prendre en compte les principaux facteurs liés à la communication : coefficient d'atténuation de signal, probabilité de couverture, type du réseau. Des simulations numériques ont permis de comparer les résultats avec ceux obtenus par les simulations Monte Carlo et ainsi, montrer l'efficacité et la

précision de la modélisation fluide pour de grands réseaux cellulaires. Les résultats numériques montrent que l'efficacité énergétique est indépendante de la densité des équipements utilisateurs. Par ailleurs, l'efficacité énergétique est plus importante dans les environnements suburbains que dans les milieux urbains où l'effet de shadowing est grand et ce, quel que soit le type de réseaux (macro, micro ou femto). Cependant, et d'une façon plus générale, le déploiement de petits réseaux (small cells) offre une meilleure efficacité énergétique comparée au réseau macro classique. En outre, nous avons évalué l'effet de la technique de transmission conjointe multipoint (JT-CoMP) sur l'efficacité énergétique, qui est considérablement améliorée lorsque le nombre de stations de base coordonnées augmente. En revanche, la coordination entre les stations de base n'est efficace que pour les équipements utilisateurs éloignés de leur station de base. En résumé, nos résultats numériques mettent en évidence l'efficacité et la précision de la modélisation fluide qui peut être considérée comme un outil mathématique par les opérateurs pour évaluer l'efficacité énergétique des réseaux cellulaires.

**Title :** Evaluation of energy efficiency in mobile cellular networks using a fluid modeling framework

**Keywords :** energy efficiency, mobile networks, JT-CoMP, performance evaluation, fluid modeling

**Abstract :** The design target of energy efficiency for 5G networks is at least 1000-fold than the currently available 4G system, while offering higher data transmission rate and very low latency. To evaluate the performance of large representative cellular networks and capture the main factors involved in the energy consumption process, representative and accurate models must be developed.

To develop tractable and efficient models, we use the spatial fluid modeling framework and compute the energy efficiency metric. Our model consists of a downlink transmission of an OFDMA cellular network, composed of several base stations and multiple user equipments randomly distributed over the area. An analytical expression of energy efficiency is then derived to study the impact of the major factors involved in the energy consumption process such as fading and shadowing attenuation, cellular coverage type and quality. Extensive numerical simulations were run to compare the results obtained by Monte Carlo simulations and demonstrate the effectiveness and accuracy of the fluid modeling for

large cellular networks. The numerical results indicate that user density does not affect energy efficiency. Besides, energy efficiency is more important in suburban environments than in urban environments where the shadowing effect is great, regardless of the cellular coverage type. However, and more generally, micro-cellular networks' deployment offers better energy efficiency than the conventional macro-cellular ones.

Besides, we evaluated the effect of the promising Joint Transmission Coordinated MultiPoint (JT-CoMP) technique on energy efficiency, which is significantly improved as the number of coordinated BSs increases. On the other hand, coordination between base stations is only effective for user equipment that is remote from their base station.

To resume, our numerical results illustrate the effectiveness and accuracy of fluid modeling, which can be considered as a mathematical tool by operators to benchmark cellular networks' energy efficiency.